UNIVERSITY OF MILAN-BICOCCA

Faculty of Medicine and Surgery

Department of Neuroscience and Biomedical Technologies

Ph.D. Program in Neuroscience

CYTOGENETIC, GENOMIC, EPIGENOMIC AND DRUG SENSITIVITY LANDSCAPES TO UNRAVEL THE COMPLEXITY OF GLIOMA STEM CELL LINES: A MULTI-LEVEL APPROACH

Coordinator: Professor Guido CAVALETTI

Tutor: Professor Leda DALPRÀ

Doctoral thesis of

Simona BARONCHELLI

058765

Academic year 2010-2011

ABSTRACT

BACKGROUND. Glioblastoma multiforme (GBM) is the most common and malignant type of glioma and it is characterized by extensive heterogeneity, both at the cellular and molecular level. The poor prognosis and the lack of an effective treatment are due to the presence of a small sub-population of cells with stem-like properties, termed glioma stem cells (GSCs). At the genomic level, heterogeneity is characterized by multiple levels of alterations, including cytogenetic, genomic and epigenomic alterations. Drug sensitivity is an additional level of GSC complexity and heterogeneity and the identification of an effective treatment for GBM depends on the depletion of the GSC pool. Valproic acid (VPA) is a histone deacetylase inhibitor and so it can be used for an epigenetic therapy for cancer. Besides, a differentiation inducing ability of VPA on cancer cells was demonstrated. Paclitaxel (PTX) is a conventional chemotherapeutic agent and in the last years it was shown to be a potential therapeutic drug for gliomas.

AIMS AND PROJECT DESIGN. Six GSC lines were studied, as they represent a valuable tool for the investigation of cytogenomic and epigenomic landscapes of GBM, in order to unravel specific molecular pathways, involved in the stem-like counterpart. Drug sensitivity profiles were assessed, evaluating cell viability and cytomorphological parameters (mitotic index, ploidy and polymorphic nuclei), after VPA and PTX administration. The reliability of differentiation and epigenetic therapy through the use of VPA was further investigated by morphological and molecular epigenomic analysis, investigating the DNA methylation status.

RESULTS AND DISCUSSION. Several shared cytogenetic and genomic alterations linked to GBM pathogenesis were found among the GSC lines. Specifically, polysomy of chromosome 7, loss of chromosome 10, CDKN2A and CDKN2B deletions are aberrations related to highly relevant pathways in GBM tumorigenesis. Moreover, a minimal deleted region at 1p36.31 was common among the six GSC lines, including *CAMTA1* gene, a putative tumor suppressor gene, specific for cancer stem-like cells. Disregulated cytogenenomic pathways in GSCs were preferentially linked to the control of stem cell proliferation, invasion, cellular development and differentiation. The evaluation of the methylation profiles of GSC lines revealed aberrant methylation of developmental genes, which are targeted by Polycomb Repressive Complex 2 in

embryonic stem cells and involved in cellular development and nervous system differentiation, evidencing a specific impairment of these processes in cancer stem-like cells. VPA is able to begin a differentiation process in GSCs, as demonstrated by the study of methylation changes caused by VPA, through the methylation of pathways which are involved in self-renewal maintenance, such as Wnt/β-catenin, and several cancer-related mechanisms. Anyway, terminal differentiation was impaired, due to an intrinsic characteristic of cancer cells endowed with stem like properties. GSCs viability was severely affected by dual drug treatment, combining VPA and PTX: VPA caused an initial differentiation, enabling PTX to induce cell death of downstream cells in tumor hierarchy. Thus, a dual approach with drugs affecting different features of malignancy could be a successful approach to GBM treatment.

CONCLUSIONS. A multi-level study for the evaluation of cytogenomic and epigenomic landscapes of GSCs is an effective approach for the identification of molecular pathways, specifically de-regulated in stem-like cells, giving an outstanding contribution in the identification of key mechanisms sustaining self-renewal. GSC lines are a valuable tool to evaluate the potentiality of new therapeutical approaches, which should be able to overwhelm the stem-like related counterpart. VPA and PTX combined treatment was found to fulfill the therapeutical potential of VPA and might be a successful approach to unlock the self-renewal loop, typical of GSCs and affect their growth.

“Read the directions and directly you

will be directed in the right direction”

Alice's Adventures in Wonderland

by Lewis Carroll

ACKNOWLEDGEMENTS

I would like to gratefully acknowledge my doctoral tutor Professor Leda Dalprà, for her advices, support and guidance during these years. Another special thanks goes to Dr. Angela Bentivegna for her help with experimental setup, general advices and stimulating discussion, but foremost, for her friendship. I am grateful to all my present and past lab mates: Donatella, Elena, Gabriele, Laura, Serena and Valentina, who were always ready to offer a helping hand and for all the time we spent together. I want to acknowledge Dr. Antonio Daga, Dr. Ida Biunno and Biorep Srl., who kindly provided the cell lines used in this study. I sincerely want to thank all my university mates, for the never-ending scientific discussions, for the research engagements and future working dreams that we share, but above all, because wherever we are, or whenever we see each other, friendship remains. I will be forever grateful to my relatives and friends for their love and continuous encouragements.

The most important thanks goes to my mother, who unfortunately will not be with me in this significant moment of my life, but I still feel her beside me; to my father and my aunt Piera, who gave me the strength to overcome this difficult moment and who encouraged me to fulfill my dreams.

Finally, I want to really thank all the people who will read this thesis.

TABLE OF CONTENTS

BACKGROUND

GLIOBLASTOMA MULTIFORME

Primary brain tumors are relatively common in the United States and account for 2% of all cancers, with an incidence of 14.8 per 100˙000 person-years (Jemal et al., 2007). Central nervous system (CNS) tumors are categorized based on the predominant cell type and can be divided in gliomas and neuronal tumors. Tumors arising from neurons are rare, whereas gliomas are the most common intracranial neoplasm of adults (78% of all CNS malignant tumors) and include tumors that are composed mainly of astrocytes (astrocytomas), oligodendrocytes (oligodendriomas) and ependymal cells (ependymomas) (Buckner et al., 2007; Louis et al., 2007). Most malignant gliomas are sporadic, but approximately 5% of patients have a familial history of glioma and they may occasionally be associated with rare genetic syndromes, such as neurofibromatosis type 1 and 2, Li-Fraumeni syndrome and Turcot's syndrome (Farrell and Plotkin, 2007). Malignant gliomas have no underling causes, only exposure to ionizing radiation has been identified as established risk factor (Fisher et al., 2007). Astrocytomas, which are tumors comprised predominantly of neoplastic astrocytes, amount to 60-85% of primary brain tumors (Nakada et al., 2007; Wen and Kesari, 2008) and are characterized by a heterogeneous morphology, biologic behavior and clinical course. World Health Organization (WHO) grading (I-IV) provides a scale of malignancy, based on specific histopathological criteria, such as mitotic activity, nuclear atypia, endothelial hyperplasia and necrosis (Louis et al., 2007). Pilocytic astrocytomas (WHO grade I) are lesions with low proliferative potential and generally does not tend to evolve into higher-grade tumors. Diffuse astrocytoma (WHO grade II) is a well-differentiated, slowly growing tumor, but it is also generally infiltrative and may tend to progress to higher grade of malignancy, such as anaplastic astrocytoma (grade III). Anaplastic astrocytoma is characterized by focal or diffuse anaplasia, increased cellularity, nuclear atypia and mitotic activity. WHO grade IV astrocytoma, also referred as glioblastoma multiforme (GBM), is the most frequent (60-70%) (Central Brain Tumor Registry of the United States, CBTRUS, www.cbtrus.org) and malignant type of glioma, with a median age of patients at the time of diagnosis of 64 years (Fisher et al., 2007). Microscopically, GBM is a highly anaplastic

tumor, which may be composed by cells with various morphologies, including astrocyte-like cells, fusiform cells and pleomorphic multinuclear giant cells. High mitotic activity, neovascularization and necrosis are all features linked to a very aggressive, invasive and destructive malignancy (DeAngelis, 2001; Louis et al., 2007; Reifenberger and Collins, 2004; Wen and Kesari, 2008). The onset of symptoms is most commonly related to mass effect and focal neurologic symptoms. Patients have partial or generalized seizures and vasogenic oedema, due to the raised intracranial pressure, that produces leakage of the blood-tumor barrier. Moreover, patients develop headache, nausea, vomiting, drowsiness and visual abnormalities (Behin et al., 2003). Males have a slight preponderance over females, with a male-to-female ratio of 3:2 (Ohgaki and Kleihues, 2005). Primary GBMs, also termed *de novo* GBMs, account for the vast majority of cases (95%) and tend to occur in older patients (mean age 55 years). They develop rapidly with no clinical, radiological or histopathological evidences of lower-grade malignancy. Secondary GBMs (5% of cases) typically occur in younger adults (45 years of age or less) and arise through malignant progression from less malignant astrocytoma (Furnari et al., 2007; Kleihues and Ohgaki, 1999; Ohgaki and Kleihues, 2005). Even if primary and secondary GBMs constitute distinct disease entities and develop through different genetic pathways, morphologically, they cannot be distinguished and the prognosis seems to be equally poor, when adjusted for patient age (Dropcho and Soong, 1996; Ohgaki and Kleihues, 2007). Uncommon GBM variants are listed in the WHO classification. Giant cell GBM is histologically characterized by highly pleomorphic, multinucleated giant cells and usually shows a well-circumscribed growth, which may contribute to a better prognosis. Gliosarcoma comprise a biphasic tissue pattern, with areas displaying phenotypic features of gliomas and sarcomas. Furthermore, glioblastoma with oligodendroglial component is a GBM which contains areas associated with oligodendroglial differentiation (Louis et al., 2007; Miller and Perry, 2007; Reifenberger and Collins, 2004). Despite aggressive treatment strategies, the outcome of patients with GBM remains extremely poor: median survival rate is approximately 9-12 months from the initial diagnosis (Maher et al., 2001; Stupp et al., 2005) and only 2-3% of patients survive for 5 years or more (Steinbach et al., 2006). The fundamental problem is linked

to the highly infiltrative nature of GBM and its extreme resistance to conventional treatments. Standard therapy typically consists of debulking surgical resection of the lesion, whenever possible. Unfortunately, malignant gliomas cannot be completely eliminated surgically, due to the aggressive invasion of GBM cancer cells into the normal brain tissue, preventing complete tumor removal. Surgical resection usually is followed by radiotherapy and chemotherapy, but despite multimodal treatments, nearly all malignant gliomas eventually recur, generally after 6.9 months (Stupp et al., 2005). Thus, the development of new therapies for GBM is urgently needed, but to achieve this target a deeper insight into the properties of malignant glioma cells is essential.

CANCER STEM CELL HYPOTHESIS AND GLIOMA STEM CELLS

The therapeutic challenge and the tumor heterogeneity in GBM have been the driving force in the identification of specific sub-populations of cells, within the tumor mass, that possess distinct tumorigenic capabilities, respond differentially to therapies and may be responsible for tumor initiation and progression. Such cells are called cancer stem cells (CSCs), cancer stem-like cells or tumor-initiating cells (TICs), all terms used to describe tumor cells with stem-like properties (Hadjipanayis and Van Meir, 2009; Reya et al., 2001). CSCs are believed to mimic the normal adult stem cells, which are undifferentiated cells, endowed with extensive self-renewal ability and which can give rise to differentiated cells. Thus, if these properties are altered, the mechanism of stem cell maintenance might shift to a transformation process and contribute to tumorigenesis (Piccirillo et al., 2009a; Reya et al., 2001). CSCs represents only a small percentage of cells in the whole tumor, but have tumorigenic potential, not shared by the bulk population of cancer cells, which are considered non-tumorigenic (Clarke et al., 2006; Ishii et al., 2008). The morphological heterogeneity of cancer tissue might be explained by a functional hierarchy in terms of proliferation and tumor initiation capacity, within the pool of cells that make up a tumor. Thus, tumors are organized as a cellular hierarchy based on a subpopulation of tumor cells (Dirks, 2008). The hierarchical model implies that the tumor is a result of developmental diversity among cancer cells, with a small subset of cancer stem cells

(at the top of the hierarchical pyramid) and a large population of bulk cells. CSCs, with the capability of asymmetric cell division, give rise to daughter transient amplifying cells, that proliferate and differentiate into partially or terminally differentiated cancer cells, with limited proliferative capacity (Bonnet and Dick, 1997; Dalerba et al., 2007; Tabatabai and Weller, 2011). The hierarchy in the tumor mass parallels normal tissue and recent studies also suggest that tumors can be considered as a distortion of normal development (Dirks, 2008). The actual cell of origin of CSCs has not yet been determined: the term "cancer stem cell" does not imply that these tumor cells are derived from the direct transformation of normal tissue stem cells. The origin of CSCs is controversial, with three main theories: i) de-differentiatiation of mature cells; ii) restricted progenitors acquire mutations that endow them with stem-like properties; iii) adult tissue stem cells are hit by mutations that influence their division and proliferation properties, achieving a tumorigenic potential (Pardal et al., 2003; Passegué et al., 2003; Zaidi et al., 2009).

The first experimental evidence for the actual existence of CSCs arose from studies on acute myeloid leukemia (AML) by John Dick's group in 1994 (Bonnet and Dick, 1997; Lapidot et al., 1994). The knowledge of the cell surface markers for hematopoietic stem cells (HSCs) allowed the isolation of tumor initiating cells in AML, using a tumor xenograft model. Dick and colleagues purified a population of $CD34^{+}CD38^{-}$ leukemic stem cells (LSCs) by fluorescence-activated cell sorting (FACS) from human AML: these cells were able to engraft human leukemia in nonobese diabetic severe combined deficiency (NOD/SCID) mice, compared with the $CD34^{+}CD38^{+}$ and $CD34^{-}$ fractions (Bonnet and Dick, 1997; Lapidot et al., 1994). Such insights contributed to the idea that the CSCs hypothesis might be extended to solid tumors: CSCs have been isolated from breast, prostate, ovary, colon, skin, bladder and brain cancers, including GBM (Bentivegna et al., 2010; Lobo et al., 2007). CSCs from glioblastoma are termed brain tumor stem cells (BTSCs) or glioma stem cells (GSCs) and are defined by three different properties: i) the capacity to generate clusters of clonally derived-cells, called neurospheres, a clue of self-renewal; ii) multipotency, that is the ability to differentiate into cells with neural phenotype; iii) tumor initiation and propagation upon serial orthotopic implantations

in immunocompromised mice (Singh et al., 2004; Vescovi et al., 2006). GSCs were firstly isolated by Ignatova and co-workers in 2002, exploiting the characteristic of normal neural stem cells (NSCs). GSCs were identified through the selection of cells expressing the NSC marker CD133, also known as prominin-1, from post surgery specimen of human GBM (Ignatova et al., 2002). The enriched GSC population showed clonogenic neurosphere-forming capability, the first evidence of stem-like characteristic. GSCs, like NSCs, posses the ability to proliferate and generate clones, that grow as floating spheroids in a specific serum-free medium, supplemented with mitogens, such as epidermal growth factor (EGF) and basic fibroblast growth factor (bFGF). After dissociation into single-cell suspension and re-plating in the same culture conditions, GSCs are able to form secondary neurospheres. This process, referred as neurosphere assay, can be replicated for unlimited culture passages and is the evidence for the extensive self-renewal capability of GSCs (Ignatova et al., 2002; Singh et al., 2003; Vescovi et al., 2006). In serum-free conditions GSCs express cellular markers typical of NSCs, such as CD133 and Nestin, a protein belonging to class IV intermediate filaments, expressed in stem/progenitor cells in human central nervous system (CNS) (Galli et al., 2004; Sanai et al., 2005; Singh et al., 2004). Mitogen withdrawal and plating in serum-supplemented medium may induce GSCs to differentiate into all neural lineages, expressing the markers of mature neurons (i.e. β-III tubulin), astrocytes (i.e. Glial acidic fibrillary protein, GFAP) and oligodendrocytes (i.e. GalC) (Fan et al., 2007; Galli et al., 2004; Hemmati et al., 2003; Suslov et al., 2002). The differentiation ability of GSCs suggests that cellular tumor hierarchy parallels normal developmental process (Dirks, 2008; Gürsel et al., 2011b). However, GSCs display aberrant growth and differentiation capacity compared to normal NSCs: indeed, GSCs commonly express multiple-lineage markers in one differentiated cells or retain the expression of stemness markers (Denysenko et al., 2010; Huang et al., 2010; Ignatova et al., 2002). In 2003, Singh and colleagues demonstrated that $CD133^+$ cells from human GBM, posses enhanced tumorigenicity *in vivo*. When transplanted in NOD/SCID mice, as few as 100 uncultured $CD133^+$ cells were able to produce a phenocopy of the original primary tumor, whereas $CD133^-$ cells (10^5 cells) engrafted, but failed to form tumors, even when injected in higher quantities (Singh et al.,

2003). Subsequently, the same capability was identified for sphere-forming GBM cells (Galli et al., 2004; Yuan et al., 2004).

Originally, CD133 surface antigen was discovered as target of the monoclonal antibody, AC133, that was employed to bind $CD34^+$ HSC subpopulation (Yin et al., 1997). C133 is a transmembran glycoprotein normally expressed in HSCs, endothelial precursor cells and NSCs and down-regulated during differentiation (Salven et al., 2003; Uchida et al., 2000; Yin et al., 1997). In GBM, the frequency of $CD133^+$ cells vary from 1 to 30% (Beier et al., 2007). Several studies suggested a correlation between CD133 expression, glioma grading and poor prognosis in GBM patients (Pallini et al., 2008; Rebetz et al., 2008; Zeppernick et al., 2008). Moreover, $CD133^+$ cells showed an increased resistance to chemotherapeutic agents and radiation, both *in vitro* and *in vivo* (Bao et al., 2006). However, subsequent studies revealed that also $CD133^-$ cells, isolated from brain tumors, were able to induce tumor growth, when transplanted in mice (Joo et al., 2008; Wang et al., 2008), suggesting that an univocal GSC marker is still not available. Whatever, some technical issues, such as cell suspension preparation, tumor subtype or culture condition should be considered (Sarkar et al., 2009). At present, CD133 still should not be neglected, until a specific marker for GSCs is found (Huang et al., 2008). Furthermore, some recent investigations suggest that $CD133^+$ enriched tumor stem cell lines more closely mirror the primary brain tumor, both phenotypically and genotypically, than serum-cultured cell lines do, justifying the use of GSC lines to understand GBM pathogenesis (Ernst et al., 2009; Lee et al., 2006a).

MULTI-LEVEL ANALYSIS OF GENOME IN CANCER RESEARCH

Cancer is a disease based on genome alterations that arise at several levels: DNA mutations, copy number variations, chromosomal aberrations and DNA methylation changes, together provide the driving force of tumor initiation and development (Network, 2008). In particular, GBM is a heterogeneous disease, both at cellular and molecular level (Bonavia et al., 2011; Shapiro et al., 1981); this broad biological heterogeneity is still not unravel and the

histopathologic analysis alone is not adequate to classify this tumor properly (Idbaih et al., 2010). A comprehensive genomic characterization of GBM may complement histology-based classification (Klink et al., 2011) and the identification of molecular subclasses of GBM will allow stratification of treatments (Huse et al., 2011; Mischel et al., 2003; Phillips et al., 2006). This approach might enable the detection of genetic markers useful for diagnostic classification, prognostic assessment and development of new targeted therapeutic drugs. Hence, a more comprehensive molecular knowledge regarding GBM is needed, but considering the complexity of genomic changes, a single-level investigation is inadequate. As multiple levels of genomic disruption are instrumental to cancer development, a multi-dimensional approach to study cancer genomics is mandatory, in order to understand cancer initiation, progression and metastasis. Various mechanisms of genome alterations might achieve the same effect and specific genes may be altered by several processes. Mutations, deletions, methylation are different levels of genomic regulation that influence gene expression and function (Chari et al., 2010; Heng et al., 2004; Idbaih et al., 2010; Network, 2008). Thus, the use of integrative platforms is necessary to relate these multiple DNA dimensions.

Numerous techniques are employed to identify genomic signature and key genes in GBM biology, including karyotype analysis, fluorescence *in situ* hybridization (FISH), array comparative genomic hybridization, microsatellite analysis and epigenomic analysis, through genome-wide methylation studies. Aneuploidy, chromosomal aberrations and rearrangements are detected by means of cytogenetic techniques, such as Q or G-banding. These methods posses the advantage of identifying the major chromosomal abnormalities and assessing intratumor genomic heterogeneity. Anyway, conventional cytogenetic does not provide for detection of genomic variations smaller than 3-5 Mb (Iourov et al., 2008). Molecular cytogenetic techniques, such as FISH or SKY (Spectral karyotyping), are used to refine variations detected by banding techniques or to identify subtle chromosomal rearrangements and marker chromosomes. Anyway, these techniques are based on chromosomal preparations, which can be considered a limiting-step in the analysis process. Recent innovation in genome-

wide analysis tools, such as array comparative genomic hybridization (aCGH), has lead to additional information on karyotypic rearrangements and the discover of extensive genomic structural variations called copy number variations (CNVs). CNVs are alterations of genomic DNA that result in variation in the number of copies of a genomic segment. CNVs arise from deletions, duplications, insertions and translocations and accounts for roughly 12% of human genomic DNA (Redon et al., 2006). CNV size varies from about 1 Kb to several megabases (McCarroll, 2010; Sebat et al., 2004; Stankiewicz and Lupski, 2010). CNVs might represent normal genomic variations, as well as pathological variations; however the phenotypic effects of CNVs are still unclear and depend mainly on whether sequences are affected by genomic rearrangements (Stankiewicz and Lupski, 2010). When pathologic, CNVs may be addressed as copy number alterations (CNAs). Even if the role of CNAs in cancer is still not well understood, these regions are more susceptible to genomic rearrangements and may become hotspots for amplifications and deletions (Hastings et al., 2009). aCGH is a microarray based technique and provides information on CNVs, comparing the fluorescence intensity ratio between two DNA, the target and the reference DNA, labeled with two different fluorescent dyes and hybridized onto a single microarray (Pinkel et al., 1998). aCGH avoids cell culture preparation and metaphase chromosomes, using genomic DNA as starting material and is useful to uncover subtle chromosomal variations, because of its increased resolution (less than 100 Kb). However, the resolution of aCGH depends on array platforms. aCGH limitations involve the inability to detect balanced translocations or inversions, as well as some polyploidies, or to identify imbalances present in small subclones in the cell population (Heng et al., 2004).

Besides, abnormal epigenomic regulation affects cancer cells, for example through aberrant DNA methylation profiles. The study of the methylome of cancer cells might give a further insight in tumor biology (Esteller, 2008) and epigenomic regulation is only an additional dimension to be considered in cancer.

In order to achieve a deeper comprehension in cancer genomic, many sources of biological material have been employed, i.e. surgical specimen, primary cultures or cell lines. Recently,

many works on the genomic profiling of GBM have pointed out that not all these models are representative of the original tumor: only spheroid cell cultures, enriched in GSCs and maintained in serum-free medium, more closely mirror the original features of primary tumors (De Witt Hamer et al., 2008; Ernst et al., 2009; Huang et al., 2008; Lee et al., 2006a; Li et al., 2008), than classical serum cultures do. These works highlight both the relevance to use the right sample and the importance and reliability of established cell-lines from GBM that retain cancer-initiating stem cell properties, as the proper model to investigate the genomic complexity of GBM (Pollard et al., 2009).

CYTOGENETIC AND GENOMIC ABERRATIONS IN GBM

Currently, several works highlight that almost all the chromosomes are involved in aberrations and that aneuploidy, resulting in chromosome instability, appears to be a typical feature of brain tumors (Bayani et al., 2005; Iourov et al., 2008; Kramar et al., 2007). Cytogenetic and genomic studies of GBM, performed during the last 20 years, identified several recurrent chromosomal abnormalities. GBM is characterized by various numerical and structural aberrations, deletions, amplifications and loss of heterozygosity, that lead to inappropriate activation of intracellular signaling pathways.

Receptor-driven pathways may be activated through different mechanisms, including overexpression of ligands and/or receptors, genomic amplifications and mutations, all processes that result in constitutive receptor activation and continuous mitogenic signaling (Furnari et al., 2007). The first genetic abnormality detected in GBM was the amplification of the epidermal growth-factor receptor (*EGFR*) gene, which maps in 7p11-12, in 40% of cases (Huse and Holland, 2010; Libermann et al., 1985; Liu et al., 2000; Schlegel et al., 1994). Gain of chromosome 7 is one of the most common chromosomal alterations in approximately 60% of GBMs, with or without *EGFR* amplification (Ichimura et al., 2004; Liu et al., 1998). Nevertheless, all GBMs with *EGFR* amplification show *EGFR* overexpression (Chaffanet et al., 1992). *EGFR* amplification is often associated with rearranged transcripts and *EGFR* variant III

(*EGFRvIII* or *delta EGFR*) is the most common rearrangement, found in 50-60% of GBMs with EGFR amplification (Schwechheimer et al., 1995). The rearrangement results in an in-frame deletion of 801 bp of exons 2-7 of *EGFR* gene, leading to the expression of an aberrant protein, which does not bind ligand and is constitutively activated (Frederick et al., 2000; Sugawa et al., 1990). *EGFR* overexpression, or its constitutive activation, enhances tumorigenic potential of GBM cells, by reducing apoptosis and increasing proliferation (Nagane et al., 1996). In addition, another receptor-mediated signaling, altered both in lower-grade glioma and GBM, is platelet-derived growth-factor receptor (*PDGFR*) signaling, through amplification of 4q12, involving *PDGFRA* gene (13% of GBMs) (Lo et al., 2007) and/or its mutation or ligand overexpression (Westermark et al., 1995). Co-expression of the receptor and its ligand suggests a possible autocrine-paracrine loop sustaining oncogenic signaling (Hermanson et al., 1992).

Functional loss of the tumor suppressor *phosphatase and tensin homolog* (*PTEN*) occurs in more than 80% of GBMs by deletions, mutation or epigenetic mechanisms (Network, 2008). Loss of the long arm of chromosome 10 was detected in 70-90% of GBMs (Ichimura et al., 2004). *PTEN* is an important negative regulator of the PI3K-AKT-mTOR signaling, which is a well established anti-apoptotic and pro-survival pathway. In addition, recent studies highlighted other possible roles of *PTEN* in suppressing tumor progression. *PTEN* is expressed at high levels in differentiated cells and is believed to possess a role in the maintenance of genomic integrity, promoting DNA repair (Shen et al., 2007). The presence of three commonly deleted regions at 10q suggested the existence of several tumor suppressor genes: *PTEN* in 10q23; *MTXI1* located at 10q25.2, a negative regulator of Myc oncoprotein (Wechsler et al., 1997); and *DMBT1*, *deleted in malignant brain tumor*, in 10q26.13 (Mollenhauer et al., 1997).

Rb pathway has a central role in regulating G1/S transition. Unphosphorylated Rb normally sequesters E2F, a transcription factor that controls the transcription of genes required for S phase initiation. Under proliferative signals, Rb is serially phosphorylated by cyclin dependent kinases CDK4/6 and CDK2: hyperphosphorylated Rb releases E2F, activating genes involved in G1/S transition. Cyclins, such as cyclin D or cyclin E, positively regulate CDK activity,

promoting cell cycle progression. Instead, cyclin dependent kinase inhibitors (CKIs) negatively regulate Rb pathway. The INK4 family, a member of CKIs, is composed by INK4A (p16), INK4B (p15), INK4C (p18) and INK4D (p19) and blocks the activation of cyclin D-CDK4/6 complex (Zhu and Parada, 2002). Rb signaling is disrupted through several genetic alterations. Loss of Rb in 13q14 was identified in 14-33% of GBMs (Ueki et al., 1996), whereas amplification of *CDK4* gene, in 12q13-15, accounts for 14% of GBM cases (Ichimura et al., 1996). Rb activity might be influenced by some negative regulators, such as $p16^{INK4A}$ and $p14^{ARF}$, which map at *CDKN2A* locus and result deleted in 40-57% of GBMs (Schmidt et al., 1994). In addition, *CDK6* and *cyclin D1* are amplified in a small number of GBMs (Büschges et al., 1999; Costello et al., 1997).

The p53 pathway prevents the uncontrolled growth of cells, blocking the cell cycle in G1 phase or inducing apoptosis, primarily regulating the transcription of several genes. Functional loss of p53 occurs in 30-40% of GBMs by mutations of *TP53* gene or loss of chromosome 17p (Frankel et al., 1992; Furnari et al., 2007; Ichimura et al., 2000). 10% of GBMs show amplification of 12q14-15 region, containing *MDM2* gene, a negative regulator of p53 (Reifenberger et al., 1994). *MDM4* gene (1q32), a homologue of *MDM2*, encodes for a protein that inhibits p53 transcription and is amplified in 4% of malignant gliomas (Gu et al., 2002). The second protein encoded by *CDKN2A*, $p14^{ARF}$, controls the activity of Mdm2 and is also involved in the inhibition of progenitor cell renewal in the subventricular zone of aging mice (Molofsky et al., 2006). 9p21 region includes *CDKN2A* and *CDKN2B* loci. The latter gene encodes for $p15^{INK4B}$, a CKI involved in Rb pathway. The chromosomal region 9p21 is homozygously deleted in at least 30-40% of GBMs. This deletion has a critical role in GBM pathogenesis as it guides the simultaneous disruption both of Rb and p53 pathways (Jen et al., 1994).

1p deletion is a common abnormality in oligodendroglial tumors, whereas the understanding about its involvement in GBM pathogenesis is still limited (Ichimura et al., 2004). Anyway, 1p deletion and LOH analysis revealed that this alteration is present in approximately 20% of

astrocytic tumors (Mueller et al., 2002; Schmidt et al., 2002). 1p partial loss, involving 1p36 region in particular, is associated with a poorer prognosis than total 1p loss (Idbaih et al., 2005). Co-deletion of chromosomes 1p and 19q in oligodendriomas has a prognostic value, with larger progression free-survival rate and increased response to chemotherapeutic treatment (Cairncross et al., 2006). Nevertheless, 1p36 and 19q13.3 LOH is believed to be critical for malignant glioma and 1p/19q co-deletion results in neuronal differentiation and favorable outcome (Ducray et al., 2008; Mizoguchi et al., 2011), but target genes have not yet been identified.

Additionally, various signaling pathways involved in the maintenance of stemness and self-renewal are associated to GBM tumorigenesis. Shh is a key protein involved in self-renewal of normal stem cells and an increased activation of hedgehog pathway is related to reduced survival in GBM patients (Xu et al., 2008). Notch signaling influences glioma pathogenesis in two main ways. First of all, Notch is considered the "gatekeeper against differentiation" (Artavanis-Tsakonas et al., 1999) as it is able to increase the expression of the stem cell marker Nestin (Shih and Holland, 2006) and enhances the ability of glioma cells to form neurosphere-like colonies in serum-free medium (Wang et al., 2010). Secondly, Notch stimulates the expression of ABC transporters, which are involved in drug efflux, contributing to chemoresistance (Bhattacharya et al., 2007). Wnt/β-catenin pathway, whose role is well known in hematopoietic malignancies, has a critical role in cancer stem cells, enhancing the tumorigenic potential, controlling proliferation and differentiation (Reguart et al., 2005).

All these findings hint both several putative targets for GBM therapy and the importance of genomic study, to give further insight in the puzzling landscape of glioma stem cell biology.

EPIGENETIC MECHANISMS IN NORMAL CELLS

Epigenetics is defined as the study of mitotically and/or meiotically heritable changes in gene expression that occur without changes in DNA sequence (Berger et al., 2009). Epigenetic regulation includes DNA methylation, covalent histone tail modification, non covalent mechanisms, such as incorporation of histone variants, nucleosome remodeling and non-coding

RNA (Sharma et al., 2010). These processes cooperate in order to regulate genome function by influencing chromatin dynamics. In the mammalian genome, methylation occurs only at the fifth carbon in cytosine bases that are located in CpG dinucleotides, within the genome. These dinucleotides are not evenly distributed across the human genome, but are instead concentrated in short CpG-rich DNA stretches, termed 'CpG islands' (CGIs), and in regions of large repetitive sequences, such as centromeres, retrotransposones and rDNA (Bird, 2002). CGIs are genomic DNA regions with lengths of 0.5 Kb to several Kbs that are marked by a content of CG greater than 50% and an expected/observed CG ratio over 60% (Gardiner-Garden and Frommer, 1987). 50-60% of these CGIs are associated with promoter regions of 50-60% of human genes (Wang and Leung, 2004): the majority of CGIs are located at promoter regions of house-keeping genes, but some of them are found also in tissue-specific genes. Normally, CGI are devoid of methylation and allow the expression of genes with an appropriate transcriptional-prone environment. However, a subset of CGIs might be methylated during development, suggesting a programmed mechanism of DNA methylation (Bird, 2002; Kim et al., 2009). DNA methylation may lead to gene silencing, by preventing or promoting the recruitment of distinct subset of regulatory proteins to DNA. One mechanism is the blocking of transcriptional activation, by limiting the accessibility of transcriptional factors to target binding sites, or gathering methyl-binding domain proteins which mediate gene repression, through interactions with histone deacetylases (Sharma et al., 2010). DNA methylation pattern in the human genome is catalyzed by *de novo* DNA methyltransferases - DNMT3A and DNMT3B - which show specificity for both unmethylated and hemimethylated DNA, and the maintenance DNA methyltransferase - DNMT1 - that has a preference for hemimethylated DNA and acts during cell replication (Kim et al., 2002).

Another level of epigenetic regulation is histone modification, by means of covalent post-translational modifications at N-terminal tails. Modifications include different chemical group, such as methyl, acetyl and phosphate and different degrees of methylation (mono-, di- and tri-methylation). Ubiquitination, sumoylation, ADP-ribosilation, biotinylation and proline

isomerization are additional modifications of histone (Vaquero et al., 2003). Modifications influence different histone proteins and different histone residues such as lysine, arginine and serine (Hatziapostolou and Iliopoulos, 2011). These modifications play a critical role in several key cellular processes, such as replication, transcription and DNA repair (Kouzarides, 2007). Histone modifications work either by changing the accessibility of chromatin or by recruiting and/or occluding non-histone effector proteins. Besides, histone modifications can lead to either activation or repression, depending upon which residues are modified and the type of modification, adding multiple layers of complexity to chromatin regulation (Sharma et al., 2010). Histone modifications are governed by several chromatin-associated enzymatic systems, including histone acetyltransferases (HATs), that add acetyl groups on lysine and histone deacetylases (HDACs), which remove them. The most studied modification of histone is acetylation of lysine that neutralizes the positive charge of histones, resulting in the loosening of their interaction with the negatively charged DNA and leading to a more open chromatin structure, that is more accessible for the transcriptional machinery (Gregory et al., 2001; Kristensen et al., 2009). Thus, lysine acetylation correlates with transcriptional activation (Bernstein et al., 2007). Otherwise, lysine methylation may occur in activation or repression. For example, trimethylation of lysine 4 on histone H3 (H3K4me3) is found associated with transcriptionally active gene promoters, whereas trimethylation of H3K9 or 27 is present at gene promoters that are transcriptionally repressed (Kouzarides, 2007).

A further level of complexity in the epigenetic control is established by the links between these various levels of regulation. A key link is the interaction between covalent histone modification and DNA methylation: cytosine methylation attracts methyl-CpG binding domain proteins (MBDs) to hypermethylated CGIs. Subsequently, MBDs recruit HDACs to methylated promoters, which catalyze histone deacetylation, leading to a chromatin-repressed state of gene transcription (Esteller, 2002; Jones and Baylin, 2007). Moreover, DNA methylation can also direct histone methylation (H3K9) through the recruitment of -CpG binding domain protein 2 (MeCP2), establishing a repressive chromatin state (Fuks et al., 2003). Thus, DNA methylation

and histone modifications are firmly associated and work together to establish the global and local chromatin states that eventually determine gene expression (Rodríguez-Paredes and Esteller, 2011). The continuous interplay of all these processes creates an epigenetic landscape which contributes to the cellular identity and developmental stages, evidencing that distortion of this equilibrium may result in many physiopathological conditions, including cancer.

EPIGENETICS IN CANCER

Tumorigenesis is a process whereby cells undergo several changes that lead to unlimited cell proliferation, loss of checkpoint control and misregulated differentiation. Epigenetic regulation is involved in several physiological mechanisms of cells, such as X chromosome inactivation, differentiation, aging, stem cell plasticity and genomic imprinting (Hatziapostolou and Iliopoulos, 2011). Thus, accumulation of epigenetic abnormalities (also termed epimutations) in DNA methylation and histone modification, contributes to oncogenesis, introducing a new level of neoplastic transformation.

The 'epigenome' is profoundly distorted in cancer. DNA methylation undergoes a global overall hypomethylation and acquires site-specific hypermethylation at promoters of tumor suppressor genes (Esteller, 2008; Hatziapostolou and Iliopoulos, 2011; Kristensen et al., 2009). Cancer cells have been found to have 20-60% less methylation than matching normal cells (Esteller, 2005). Hypomethylation is generally associated to repetitive DNA sequencing, retrotransposones, coding regions and introns and may contribute to tumorigenesis resulting in genomic instability, increased rate of chromosomal rearrangements, activation and translocation of retrotransposones to other genomic regions (Eden et al., 2003; Howard et al., 2008). Additionally, hypomethylation may lead to weakening of transcriptional repression in normally silent regions of the genome, activation of protoncogenes and loss of imprinting (i.e. *IGF2* gene in Wilm's tumor) (Ogawa et al., 1993; Wilson et al., 2007).

Site specific hypermethylation of CGIs contributes to tumorigenesis by inducing inappropriate silencing of genes that are involved in growth regulation, DNA repair, apoptosis, angiogenesis

and tumor cell invasion. These evidences suggest that methylation imbalance contributes to malignancy (Costello et al., 2000). The first evidence of a link between CGI hypermethylation and tumor suppressor genes was provided by the work of Dryja and Horsthemke on *RB* gene. They indicated that tumor suppressor silencing might occur by an epigenetic pathway (Greger et al., 1989; Sakai et al., 1991). Subsequently, several works confirmed the involvement of hypermethylation in silencing of other key genes involved in the major cellular pathways, such as cell cycle control (*INK4A*), p53 network (*ARF*) and DNA repair (*MGMT* and *BRCA1*) (Esteller, 2007b). Probably, hypermethylation is a progressive process which requires several 'waves' of disregulated methylation to achieve a hypermethylated CGI 'phenotype' and to produce transcriptional silencing (Esteller, 2002). *De novo* methylation may occur through the breakdown of the normal compartmentalization of the genome into euchromatin and heterochromatin. The weakening of 'boundary elements', a sort of protective barriers to CGI methylation, that maintain active and silenced domains and prevents from a spurious spreading of DNA methylation, is the first step. Afterwards, the 'seeding' of methylation, from heavily methylated DNA that flanks a CGI towards the center of the gene, attracts more methylation, generating a positive cooperative process until hypermethylation is achieved (Esteller, 2002; Jones and Baylin, 2002). In addition, DNMT and HDAC are overexpressed in many types of tumors (Yoo and Jones, 2006). Anyway, it is still unclear how genes are targeted for aberrant DNA methylation; probably the silencing of some genes may provide a growth advantage to cells, resulting in their clonal selection and proliferation, or by a DNMT driven mechanism, through its association with oncogenic transcription factors (Esteller, 2002; Sharma et al., 2010).

Changes in histone modifications are also involved in cancer. A global loss of acetylated H4-lysine 16 (H4K16ac) and H4-lysine 20 trimethylation (H4K20me) have been identified in several malignancies (Fraga et al., 2005). HDACs mediate histone deacetylation and these modifications results in gene repression. Moreover, HDACs are found overexpressed in cancers, whereas HAT enzymes may be influenced by inactivating mutations, working in concert with

HDACs to disrupt normal histone acetylation level (Mahlknecht and Hoelzer, 2000; Sharma et al., 2010). In addition to the interference with the normal covalent histone modifications, also the incorporation of some histone variants, such as H2A.Z, is implicated in tumorigenesis, destabilizing chromosome, promoting cell cycle progression and spreading of repressive chromatin-domains (Svotelis et al., 2009).

Given all these evidences, epigenetic alterations may be considered as alternatives for genetic changes, by mimicking the effect of classical genetic changes. In 2006, Feinberg and colleagues proposed an alternative model of cancer. In particular, this model integrated the CSC theory and the epigenetic changes that characterize cancer, providing an integrated view of the different mechanisms involved in tumorigenesis. This model was called 'The epigenetic progenitor model of cancer' (Feinberg et al., 2006). CSC theory and the presence of epigenetic changes, even in early tumorigenesis and in normal tissues, before tumors arise, indicate that the epigenetic modifications may occur as a first step alteration in stem/progenitor cells and may be considered the key determinant of tumor initiation and progression. Interestingly, this epigenetic model could also explain cancer heterogeneity, one of the key characteristic of tumors, considering cell-growth, invasion, metastasis and resistance to therapy. The first step is the epigenetic disruption of stem/progenitor cells, which leads to a polyclonal precursor population of cells prone to cancer initiation. Moreover, epigenetic aberrations might perturb the physiological subtle balance of stem cell self-renewal, by stimulating the numerical increase of undifferentiated population or by modifying the differentiation capabilities of stem cells. These epigenetic alterations should effect the so called 'tumor progenitor genes', that are involved in the regulation of stemness, increasing stem cell capability to self-renew and reducing differentiation. The second step is the mutation of tumor suppressor genes or oncogenes in the epigenetically-disrupted population of progenitor cells. Subsequently genetic and epigenetic instability contributes to increased tumor evolution and heterogeneity (Feinberg et al., 2006).

Another evidence that supports this 'epigenetic progenitor model of cancer' is the presence of 'bivalent domains' in embryonic stem (ES) cells. These domains are characterized by the co-

existence of active and repressive histone marks at promoters of genes involved in development, creating a sort of poised chromatin state, since these cells should be able to relieve the silent chromatin state upon differentiation, to allow lineage specific gene expression (Bernstein et al., 2006). Bivalent domains are controlled by two critical regulators: the Polycomb group proteins (PcG) and the trithorax group proteins (trxG). The PcG functions as repressor of target genes and the trxG antagonizes the PcG function through activation of target genes. In particular, PcG is essential for maintaining ES cell pluripotency by silencing of cell-fate specific genes whereas trxG maintains active chromatin state during development (Kim et al., 2009; Ringrose and Paro, 2007; Sharma et al., 2010). This bivalent mark is essential for phenotypic plasticity of ES cells, indeed differentiated cells do not posses this bivalency and acquire rigid chromatin structure, important for the maintenance of cell fate (Mikkelsen et al., 2007). In the context of cancer epigenomics, the chromatin bivalent domains in stem/progenitor cells predispose tumor suppressor genes to DNA hypermethylation and hereditable silencing and PcG targets are more likely to have an aberrant DNA hypermethylation than non-target ones, supporting a stem cell origin of cancer (Ohm et al., 2007; Schlesinger et al., 2007; Widschwendter et al., 2007).

THE EPIGENOME OF GBM

The epigenetic features of GBM still remain partially defined. Global hypomethylation occurs in approximately 80% of GBM, but is very variable among tumors, ranging from nearly normal to 50% of normal brain levels (Cadieux et al., 2006). This decrease in 5-methylcitosine comprises the demethylation of approximately 10 million CpG sites per tumor cell. Both repetitive elements and single copy loci can be hypomethylated. High levels of hypomethylation parallel an increased GBM proliferation. DNA hypomethylation of repetitive DNA sequences contributed to genomic instability. The tandem repeat satellite (Sat2), located at the juxtacentromeric regions of chromosome 1, 9 and 16, displays a dramatic hypomethylation in GBM (22-50% of normal brain), leading to copy number alterations of the adjacent euchromatic regions and predisposing to chromosomal breakage (Cadieux et al., 2006; Fanelli et al., 2008). Regional hypomethylation at single-copy loci is associated to the activation of cancer-associated

genes, such as the melanoma antigen gene *MAGEA1*. *MAGEA1* is a member of the MAGE gene family and is a germline-specific gene that becomes transcriptionally activated in multiple human cancers, resulting in increased cell proliferation and inhibition of p53 function and response to chemotherapy (De Smet et al., 1996; De Smet et al., 2004; Yu et al., 2004). Locus-specific hypermethylation mostly occurs at promoter CGI of genes with diverse functions related to tumorigenesis, such as regulation of cell cycle, DNA repair, apoptosis, invasion, angiogenesis and drug resistance. Aberrant promoter methylation was identified in genes that are well known in GBM pathogenesis, for example *RB*, *CDKN2*/p16, *PTEN*, *TP53* and $p14^{ARF}$ (Baeza et al., 2003; Costello et al., 1996; Nakamura et al., 2001). The screening for promoter hypermethylation in GBM samples enabled also the identification of new tumor suppressor candidates. One example is the hypermethylation at 19q13.2 region of the epithelial membrane protein 3, *EMP3*, a myelin-related gene involved in cell proliferation. The reintroduction of *EMP3* in neuroblastoma cell lines results in a decreased ability of colony formation *in vitro* and a reduction of xenograft growth in mice, suggesting a tumor suppressor function (Alaminos et al., 2005). *EMP3* gene promoter was found hypermethylated in 80% of secondary GBM, but only in 17% of primary GBM, so *EMP3* methylation status might be considered a marker to distinguish between primary and secondary GBM (Kunitz et al., 2007). Promoter hypermethylation can also affect genes involved in invasion and metastasis. 87% of GBMs exhibit promoter hypermethylation of the *protocadherin-gamma subfamily A11* (*PCDH-gamma-A11*) gene, which is involved in invasion of cancer cells into brain parenchyma (Waha et al., 2005). Hypermethylation in cancer cells can also modulate drug sensitivity and response to therapies. In GBM, the best known example is *MGMT* gene, which is involved in the response to DNA alkylating agents. Alkylating drugs, such as temozolomide, kill cells through the formation of lethal crosslinks between adjacent strands of DNA, inhibiting DNA replication. MGMT is involved in DNA repair by removing these alkyl adducts from the O6 position of guanine (Esteller et al., 1999). The effectiveness of temozolomide or other alkylating drugs is impaired by the activity of *MGMT*. DNA methylation of *MGMT* promoter may reduce MGMT level. *MGMT* promoter methylation is currently considered a predictive biomarker for the

responsiveness to chemotherapy with alkylating agents: *MGMT* promoter hypermethylation is associated with an increased survival of GBM patients treated with temozolomide (Brandes et al., 2008; Hegi et al., 2005).

Moreover, hypermethylation can alter the differentiation properties of GSCs, linking the CSC theory and epimutations in GBM. Bone morphogenetic proteins (BMP) mediate astroglial differentiation through Jak/STAT pathway. Epigenetic silencing of BMP receptor 1B (*BMPR1B*) gene, by means of promoter hypermethylation, blocks GSCs differentiation. Moreover, forced BMPR1B expression restores the differentiation potential of GSCs (Lee et al., 2008). *CD133* marker is also influenced by epigenetic mechanisms and it was found hypomethylated in GBMs specimen, resulting in an aberrant expression of this stemness marker (Tabu et al., 2008).

Histone modifications also occur in GBM, alone or in association with DNA methylation contributing to the silencing or activation of cancer-related genes. Silenced genes are characterized both by CGI hypermethylation and loss of H3K9 acetylation. The presence of bivalent domains in normal stem cells along with histone modification may predispose tumor suppressor genes to DNA hypermethylation (Ohm et al., 2007). Mutations in many genes involved in epigenetic regulation were uncovered by large scale sequencing studies, including *HDAC2*, *HDAC9* and *methyl-CpG binding domain protein 1 (MBD1*) (Parsons et al., 2008).

The early epigenetic studies on the methylation status of GBM were performed on candidate genes and this kind of approach may introduce a bias in the analysis process. Recently, microarray analysis technologies with newly high-throughput techniques allowed the simultaneous analysis of CGI spanning on the entire genome, providing a more comprehensive insight in the epigenomic landscape of cancers. The scanning of the entire genome provides a more unbiased approach and the new employed methods are various, such as bisulfite sequencing and methylated DNA immunoprecipitation combined with microarray platform, in order to comprehensively interrogate the epigenome and to better understand the epigenomic

disregulation in GBM or other types of cancers (Esteller, 2007a; Kim et al., 2006a; Laird, 2010; Nagarajan and Costello, 2009). This genome-wide approach has different goals, as it can represent a new parameter in the classification of tumors or a prognostic and/or diagnostic marker. In particular the epigenetic status of GBM may define different clinical phenotypes, giving information about prognostic and predictive factors. Prognostic factors unveil information about the 'virulence' of the tumor, by improving tumor classification and by helping in the stratification of the degree of malignancy. Various works in the latter 10 years provided an initial attempt to the epigenomic classification of GBM (Foltz et al., 2009; Kim et al., 2006b; Laffaire et al., 2011; Martinez and Esteller, 2010; Noushmehr et al., 2010; Uhlmann et al., 2003; Wu et al., 2010). In particular Noushmehr and co-workers characterized a distinct molecular subgroup in human gliomas, identifying a proportion of GBM with highly concordant DNA methylation, which was defined as CpG island methylator phenotype (G-CIMP). These GBMs are a subclass of the GBM pro-neural subtype, defined by Phillips et al. and Verhaak et al. (Phillips et al., 2006; Verhaak et al., 2010). G-CIMP positive tumors were associated with secondary or recurrent tumors and showed a favorable prognosis within GBMs (Noushmehr et al., 2010). In addition, Wu and colleagues identified an overrepresentation of methylation of homeobox genes and 31% of the most commonly methylated genes in their cohort represent targets of Polycomb complex. Functional annotations of methylated promoter genes revealed genes mainly involved in neuronal differentiation, supporting the disregulation of differentiation process in GBM cells (Wu et al., 2010). All these evidences sustain the development of a methylation fingerprinting for GBM, as the study of promoter methylation may contribute to understand the biology of GBM and represent a new biomarker for diagnosis, classification, prognosis and drug response.

GBM TREATMENT

Conventional therapies for GBM include maximal safe surgical resection, radiotherapy and chemotherapy, but these treatments provide only palliative effect on GBM. The current standard of treatment includes adjuvant chemotherapy with temozolomide (TMZ). TMZ is a small

lipophilic agent, which is able to cross the blood-brain barrier effectively and which can be orally administered. Addition of temozolomide to radiotherapy resulted in increased median survival of GBM patients from 12.1 to 14.6 months and improved 2-year median survival from 10.4 to 26.5% (Stupp et al., 2005). Although TMZ treatment may slow GBM tumor growth, tumor recurrence is typical, indicating the presence of a TMZ-resistant subpopulation of cells within GBM (Liu et al., 2006b). GSCs are resistant to standard therapies because they are mostly quiescent and current therapies target proliferating non-tumorigenic cells (Eyler and Rich, 2008). Several other potential mechanisms of GSC drug-resistance have been highlighted. Bao and co-workers demonstrated that GSCs promote chemoresistance through the activation of DNA damage response (Bao et al., 2006). GSCs also show an increased expression of ABC (ATP binding cassette) transporters, which are involved in the efflux of chemotherapeutic drugs (Hirschmann-Jax et al., 2004).

These peculiar features of GSCs provided the driven-force for the development of molecularly targeted agents that inhibit specific tumor associated pathways. Genomic profiles of GBM revealed several genes implicated in the pathogenesis of GBM, such as *EGFR* and *PDGFR*, whose abnormal function and/or overexpression are associated with increased proliferation of GBM cells. These pathways have been specifically targeted using small inhibitors of tyrosine kinase receptors. The monoclonal antibodies Gefitinib and Erlotinib are selective EGFR inhibitors and have been tested in several solid tumors, including GBM. Despite targeting a specific pathway which is altered in GBM, only 10-20% of patients respond to EGFR inhibitors (Mellinghoff et al., 2005). Imatinib mesylate is a PDGFR inhibitor (well known for chronic myeloid leukemia therapy), but as with EGFR inhibitors, phase II trials have largely been disappointing, showing only little benefits (Wen et al., 2006).

Angiogenesis may constitute another therapeutic target for malignant glioma. Vascular endothelial growth factor (*VEGF*) is the dominant pro-angiogenetic factor, which increases vascular permeability and stimulates endothelial proliferation and migration (Hicklin and Ellis, 2005). Bevacizumab is a monoclonal antibody that targets VEGF and a phase II trials showed

that the combination of Bevacizumab and Irinotecan provided an increase in the survival of patients with grade VI gliomas (Vredenburgh et al., 2007a; Vredenburgh et al., 2007b).

Taking together these observations, the complete eradication of GSCs is essential, in order to really improve GBM patient survival. The total eradication of the stem subpopulation may be achieved by blocking the signaling pathways involved in self-renewal, such as Wnt pathway, Notch pathway and Hedgehog signaling. Another alternative approach is the use pro-differentiation drugs, which are able to induce differentiation of GSCs, affecting self-renewal abilities (Cinatl et al., 1996), or modulating neural developmental signaling, such as BMP pathway (Piccirillo and Vescovi, 2006).

VALPROIC ACID

Valproic acid (VPA, 2-propylpentanoic acid) is an eight-carbon branched-chain fatty acid, derived from valeric acid and is widely used in the treatment of epilepsy and other seizure disorders (Pinder et al., 1977). In the human brain, VPA influences the activity of Gamma Amino Butyrate (GABA) neurotransmitter, through the increase of GABA inhibitory activity, by means of several mechanisms, such as inhibition of GABA degradation, increased GABA synthesis or decreased turnover (Mesdjian et al., 1982). Moreover, VPA directly interacts with the neural membrane blocking voltage-dependent sodium channels (Löscher, 1999). Recently, VPA was shown to have anti-tumoral properties, by inhibiting cell proliferation and inducing differentiation of neuroblastoma cells in vivo (Cinatl et al., 1997; Cinatl et al., 1996). Soon after these findings, the mechanism of action of VPA was investigated and VPA was shown to be an effective inhibitor of HDAC (HDACi) (Göttlicher et al., 2001; Phiel et al., 2001). VPA inhibits HDAC activity, by binding to the catalytic center and consequently, blocking substrate access (Phiel et al., 2001). VPA specifically targets class I HDACs and induces proteasomal degradation of HDAC2 (Yoo and Jones, 2006). Inhibition of HDAC increases histone acetylation, leading to chromatin relaxation, releasing the DNA and allowing transcription. Thus, VPA can induce de-repression of genes epigenetically silenced in cancer (Blaheta et al.,

2005; Van Lint et al., 1996) and involved in different cellular processes, including cell cycle control, differentiation, DNA repair and apoptosis (Chateauvieux et al., 2010). Moreover, HDAC inhibition is associated with DNA demethylation, probably because of the increase of acetylation that enables methylated DNA to be more accessible to DNA demethylase proteins, even if the exact mechanism is not yet known (Cervoni and Szyf, 2001). VPA administration is also associated to a down-regulation of expression of specific proteins involved in chromatin maintenance, such as DMT1 (DNA methyl transferase 1) and HP1 (heterochromatin protein 1) (Marchion et al., 2005). Many works highlighted the antineoplastic effect of VPA in several malignancies, including brain neoplasm, acute myeloid leukemia, ovarian, thyroid and prostate cancer (Camphausen et al., 2005; Catalano et al., 2005; Kuendgen et al., 2004; Takai et al., 2004; Thelen et al., 2004). Even if the mechanism of action of HDACi is cell-type-specific, anyway some general responses to HDACi administration are known, such as modulation of multiple pathways including cell cycle arrest, apoptosis, angiogenesis, metastasis, differentiation and senescence (Duenas-Gonzalez et al., 2008). VPA represents an attractive and valuable agent in the treatment of cancer because of its antineoplastic activity, minimal toxicity profile and long half-life (Shen et al., 2005). VPA has a serum-half life of 9-18 hours (Perucca, 2002), it can be administered orally and, at therapeutic concentration, produces mild adverse side effects, even when serum levels exceed the normal therapeutic range (Göttlicher et al., 2001). Adverse effects include mild transient gastrointestinal symptoms, sedation and ataxia (Löscher, 1999). VPA penetrates the blood brain barrier and can be chronically administered, due to its minimal toxicity (Camphausen et al., 2005). Epigenetic drugs seem to be the real promising agents for cancer treatment: they target aberrantly heterochromatic regions, reverting malignant epigenetic markers, leading to the re-expression of tumor suppressor genes or genes related to a normal functioning of cells. Moreover, epigenetic drugs are able to overcome chemotherapy resistance by chemosensitizing cells, which can be then targeted by other type of drugs (Yoo and Jones, 2006).

PACLITAXEL

Paclitaxel (PTX), a natural product isolated from Taxus brevifolia (Wani et al., 1971), is a member of taxane family and have been used to treat several solid malignancies, such as ovary, breast, non-small-cell lung and head and neck cancers (Crown and O'Leary, 2000). PTX strongly binds to the β-subunit of tubulin in microtubules, with the binding site located inside, in the lumen of the polymer surface (Nogales et al., 1995). The stoichiometric binding induces a conformational change in paclitaxel-bound tubulin, enhancing its affinity to the surrounding tubulin molecules and resulting in stabilization of microtubules (Nogales, 2000; Stanton et al., 2011). Thus, PTX affects microtubule dynamics, which is necessary for cell cycle progression, by preventing the dividing cancer cells from progressing from metaphase into anaphase (Jordan and Wilson, 1998). Indeed, mitosis requires highly dynamic microtubules, to ensure a timely and precise chromosome segregation, thus the spindle microtubule stabilization promotes mitotic arrest in G2-M phase of cell cycle (Schiff and Horwitz, 1980). Blocked cells eventually exit mitosis and undergo apoptosis (Jordan et al., 1996). However, PTX shows dose limiting toxicity, including febrile neutropenia, neuromuscular toxicity, peripheral neuropathy, anemia and thrombocytopenia (Markman, 2003).

Resistance to PTX involves the P-glycoprotein (P-gp) efflux pump, which is a product of the *multidrug resistance gene MDR1* (Gottesman, 2002). P-gp is a membrane associated ATP-binding cassette transporter (ABC-transporter) and it was found overexpressed in a number of tumors cell lines (Leonard et al., 2003): P-gp overexpression leads to an increased drug efflux, limiting the intracellular drug levels and consequently limiting drug cytotoxicity (Perez, 2009). In addition, alterations of tubulin-binding sites or microtubules dynamics are other important mechanisms of resistance to PTX treatment. Expression of some specific tubulin isotypes, such as βI isotype or βIII-tubulin isotype, is associated to increased resistance to taxanes (Giannakakou et al., 1997; Kamath et al., 2005).

In vitro, PTX was also shown to be active against glioma cell lines and brain metastases (Cahan et al., 1994; Tseng et al., 1999), but brain neoplasms represent a difficult problem and the therapeutic benefit of PTX in patients with recurrent primary brain tumors have been variable or low (Chamberlain and Kormanik, 1995). Probably, the low efficacy is attributable to its limited permeability into the CNS or to P-gp drug mediated efflux (Fellner et al., 2002; Heimans et al., 1994). Anyway, the blood brain barrier of patient with GBM is compromised, the blood capillaries are leaky and moreover, several strategies to improve PTX delivery in the brain are under investigations (Coomber et al., 1987). Drug delivery nanoparticles or PTX-conjugated peptides, as vectors to increase the permeabilization of the blood brain barrier, have been successfully employed in different models of brain tumors (Nikanjam et al., 2007; Régina et al., 2008). In addition, the co-administration of PTX with specific P-gp inhibitors seems to be an effective strategy (Fellner et al., 2002).

The dual-drug approach is a valuable tool in order to reduce drug toxicity and improve the efficacy of a single treatment. In particular, the co-administration of HDACi with standard chemotherapeutic agents is able increase the apoptosis of tumor cells, by erasing the epigenetic marks associated with the chemoresistance and therefore sensitize tumors to chemotherapy (Perez-Plasencia and Duenas-Gonzalez, 2006). Many models have been proposed to explain the efficacy of a dual approach. HDACi mediated hyperacetylation may contribute to chromatin exposure to drugs that specifically target DNA, enhancing their cytotoxic effect (Marks and Xu, 2009). Moreover, HDACi are able to induce DNA damage *per se* (Gaymes et al., 2006), enhancing the effect of other genotoxic agents and they are also able to abolish DNA repair and influence the apoptotic pathway, regulating the expression of apoptosis associated genes (Frew et al., 2009; Munshi et al., 2005). In particular, VPA was found to synergize with TMZ administration in U87 glioma cell line (Chen et al., 2011). The dual use of VPA and PTX has been shown to be effective on anaplastic thyroid cancer cell lines, as VPA is able to induce α-tubulin acetylation and therefore to increase the effectiveness of PTX, which acts on β-tubulin, by enhancing the microtubule stabilization (Catalano et al., 2007). The same effect was

observed by Yagi and colleagues on a scirrhous gastric cancer cell line (Yagi et al., 2010). The general reason why VPA synergizes PTX effect is due to the pro-differentiatiation ability of VPA: VPA is able to induce the differentiation of the stem cell subpopulation of the tumor, whereas PTX should be consequently able to eliminate cells further down the tumor hierarchy (Zhou et al., 2009).

AIM OF THE WORK

Glioma stem cells (GSCs) are the main actors in glioblastoma multiforme (GBM) pathogenesis and the full understanding of the key properties of this subpopulation is far from being achieved. Several levels of genetic and epigenetic disruption are instrumental to cancer development and the employment of a multi-level approach is mandatory to improve cancer-related knowledge. Thus, we decided to evaluate the cytogenetic, genomic and epigenomic features of GSCs in order to unravel their complexity and to deeply understand GBM heterogeneity. Drug-sensitivity is an additional level in the landscape of tumor biology. Pharmacological treatment with valproic acid (a histone deacetylase inhibitor) and Paclitaxel (a microtubule-stabilizing agent) was assessed on GSC lines, both to evaluate cell sensitivity to drug treatment and to characterize cytomorphological and epigenomic changes induced by drug administration. Moreover, the ability of VPA to induce differentiation of cancer stem-like cells was evaluated to unveil the potentiality of a differentiation therapy in GBM, which should be able to specifically target the stem cell subpopulation.

MATERIALS AND METHODS

CELL LINES

Glioma stem cell (GSC) lines have been isolated from patients affected by GBM. GBM2 and GBM7 cell lines were kindly provided by Dr. Antonio Daga from the Department of Translational Oncology, National Institute for Cancer Research, Genova, Italy. G144, G166, G179 and GliNS2 cell lines were kindly provided by Professor Austin Smith from Wellcome Trust Centre for Stem Cell Research and Department of Biochemistry, University of Cambridge, UK and stored by BioRep Srl. These GSC lines have been extensively characterized for their stem cell properties in Griffero et al., 2009 and Pollard et al., 2009, respectively (Griffero et al., 2009; Pollard et al., 2009). All the GSC lines were isolated from GBM specimen, whereas G179 cell line was derived from a particular subtype of GBM, termed giant cell GBM. Moreover, GBM2 and GBM7 were found insensitive to EGFR inhibitor treatment. All the GSC lines were isolated from male patients. CB660 and CB660SP are human foetal neural stem cell lines, derived from forebrain and spinal cord, respectively (Sun et al., 2008) and were stored by BioRep Srl. These two cell lines showed a normal female karyotype 46,XX.

CELL CULTURE CONDITIONS

Cell expansion was carried out in a proliferation permissive medium composed by DMEM F-12 and Neurobasal 1:1 (Invitrogen), B-27 supplement without vitamin A (Invitrogen), 2mM L-glutamine, 10ng/ml recombinant human bFGF and 20ng/ml recombinant human EGF (Miltenyi Biotec), 20UI/ml penicillin and 20µg/ml streptomycin (Euroclone). GSCs and human foetal NSCs were cultured in adherent culture condition in T-25 cm^3 flasks coated with 10µg/mL laminin (Invitrogen), in 5% CO_2/95% O_2 atmosphere. GSCs were routinely grown to confluence, dissociated using Trypsin 0.05% (Euroclone) and then splitted 1:2 or more, depending on cellular concentration. Medium was replaced every 3–5 days. For differentiation, cells were cultured in RPMI 1640 medium (Euroclone), supplemented with 10% Foetal Calf Serum (FCS, PBI International), 2mM L-Glutamine, 20UI/ml penicillin and 20µg/ml streptomycin (Euroclone) for 15 or 30 days.

CONVENTIONAL CYTOGENETICS

Metaphase chromosome spreads were obtained using standard procedures. Briefly, cell cultures were treated with 0.2μg/ml Colcemid (Roche) for a variable period of time, depending on the growth rate of each specific cell line (ranging from 3 to 16hs). Subsequently, cells were harvested and incubated with a hypotonic solution of pre-warmed 0.56% w/v KCl for 15 minutes at room temperature (RT). Then, cells were pre-fixed with 20% fixative solution composed of 3:1 methanol : acetic acid. The sample was collected by centrifugation and treated two times with fixative solution for 15 minutes at RT. Metaphase spreads were spotted onto glass slides and allowed to air-dry. The chromosomes were QFQ-banded using quinacrine mustard and slides were mounted in McIlvaine buffer. Slides were analyzed using Nikon Eclipse 80i fluorescence microscope (Nikon), equipped with a COHU High Performance CCD camera. The number of metaphases analyzed depends on the quality of chromosome preparations. The karyotype was defined following the guidelines of the International System for Chromosome Nomenclature 2009 (ISCN 2009).

FLUORESCENCE IN SITU HYBRIDIZATION (FISH)

Fluorescence in situ hybridization (FISH) was performed on metaphase chromosome spreads, using whole chromosome painting (wcp) probes. Specifically, Octochrome Chromoprobe Multiprobe System (Cytocell) was used and the procedures were assessed according to the manufacturer's protocol. This kit combines the utility of an 8 square slide and whole chromosome painting probes, which are labeled with 3 different fluorescent dyes in order to allow all 24 chromosomes to be identified on a single slide. A minimum of 10 metaphases were evaluated for each specific square.

ARRAY CGH

For array-CGH analysis, genomic DNA was extracted from cell cultures using the Wizard Genomic DNA Purification Kit (Promega). Sample preparation, slide hybridization, and

analysis were performed using Human Genome CGH Microarray, 4x44K (Agilent Technologies), according to the manufacturer's instructions. Sex-matched commercial DNA samples (Promega) were used as reference DNA during array-CGH. Data were analyzed as previously described (Panzeri et al., 2011). Briefly, the arrays were scanned at 2µm resolution using Agilent microarray scanner and analyzed using Feature Extraction v10.7 and Agilent Genomic Workbench v5.0 softwares. The Aberration Detection Method 2 (ADM2) algorithm was used to compute and assist the identification of aberrations for a given sample (threshold=5; log2 ratio=0.3). The estimated percentage of mosaicism was calculated using the formula determined by Cheung SW et al. (Cheung et al., 2007).

MICROSATELLITE ANALYSIS

Loss of heterozygosity (LOH) analysis of chromosome 1p35-36, chromosome 10 and chromosome 13 was assessed by means of PCR-based assays. Amplimers were selected on the basis of the heterozygosity rate in the population and they are listed in Table 1. Specific information about primer sequence, melting and annealing temperatures can be obtained referring to the UCSC Genome Browser (http://genome.ucsc.edu/). Amplification of each microsatellite was done in 20µl volume with 20ng/ml of genomic DNA, 1x PCR Buffer, 1µM primers, 200µM dNTPs, 1.5mM $MgCl_2$ and 1 unit of AmpliTaq Gold DNA Polymerase (Applied Biosystems). Amplification products were resolved on 6% polyacrylamide gels and electrophoresed for 5hs at 160V. Gels were stained with 0.1% ethidium bromide and LOH was determined by visual observation.

DRUGS AND TREATMENTS

Valproic acid (sodium salt, Sigma) was dissolved in sterile water to a stock concentration of 500mM and stored at -20°C. Paclitaxel (Lc laboratories) was dissolved in absolute ethanol to 10mM stock concentration and then diluted to the required concentrations, with complete cell

Table 1. List of STS markers.

STS marker	Position	Forward and reverse primers	PCR product size (bp)
D1S468	1p36.32	AATTAACCGTTTTGGTCCT GCGACACACACTTCCC	173-191
D1S214	1p36.31	CCGAATGACAAGGTGAGACT AATGTTGTTTCCAAAGTGGC	120-142
D1S508	1p36.23	AGCTGGGGAATATATGTNTCATAT TGTGGAAGGCCAACTC	73-85 bps
D1S228	1p36.21	AACTGCAACATTGAAATGGC GGGACCATAGTTCTTGGTGA	116-129 bps
D1S199	1p36.13	GGTGACAGAGTGAGACCCTG CAAAGACCATGTGCTCCGTA	94-116 bps
D1S2734	1p35.12	GGTTCAAGGGATTCTCCTG TGGCACTCAGACCTCAA	108-134 bps
D10S249	10p15.3	AACTGGTTTTGGTAGTGAGA GAGGTGCCCGCTAGTA	118-134 bps
D10S594	10p15.3	GGGCAGCGTGCTGAGA GCACCCAGATAGGCATAGAGA	100-108 bps
D10S558	10p15.3	ATGAACATCACCAAGGCATATAG ATAGTAGGCCGCCAGTCTC	192-212 bps
D10S552	10p15.1	GTCCTTTAATCTGGGCTTTC AATAGGTGGGGGCTTATG	84-103 bps
D10S1653	10p13	CCTTTGGATAAAGCCTCCT TATCATTGTCTCATCCGGG	201-213 bps
D10S197	10p12.1	ACCACTGCACTTCAGGTGAC GTGATACTGTCCTCAGGTCTCC	161-173 bps
D10S1686	10q23.1	CTCTTCAGTTCCAACCACAC ATAACACAGGGCCATTTAAG	172-208 bps
D10S185	10q23.33	TCCTATGCTTTCATTTGCCA CAAGACACACGATGTGCCAG	143-159 bps
D10S212	10q26.3	GAAGTAAAGCAAGTTCTATCCACG TCTGTGTACGTTGAAAATCCC	189-201 bps
D13S263	13q14.11	CCTGGCCTGTTAGTTTTTATTGTTA CCCAGTCTTGGGTATGTTTTTA	145-165 bps
D13S170	13q31.1	TTGCACTGTGGAGATAAACACATAG TCACATTGTCTTTTAAGGCAGGAG	113-137 bps
D13S159	13q32.2	AGGCTGTGACTTTTAGGCCA CCAGGCCACTTTTGATCTGT	168-203 bps
D13S285	13q34	ATATATGCACATCCATCCATG GGCCAAAGATAGATAGCAAGGTA	92-106 bps

culture medium. The final concentration of ethanol was no greater than 0.1%. This concentration of solvent had no effect on cell growth. Dose-response studies were carried out in order to determine the suitable doses for further experiments. Cell culture treatments were assessed following two different schemes of administration (Figure 1). Single drug treatment was performed using 0.5-1-3-6-10-20mM VPA or 0.01-0.1-1-10-20-50µM PTX for 24, 48 and 72hs (Figure 1a). Dual drug treatment was performed treating cells firstly with different concentration of VPA for 24hs, followed by treatment with PTX at different concentrations for 48hs, in combination (Figure 1b).

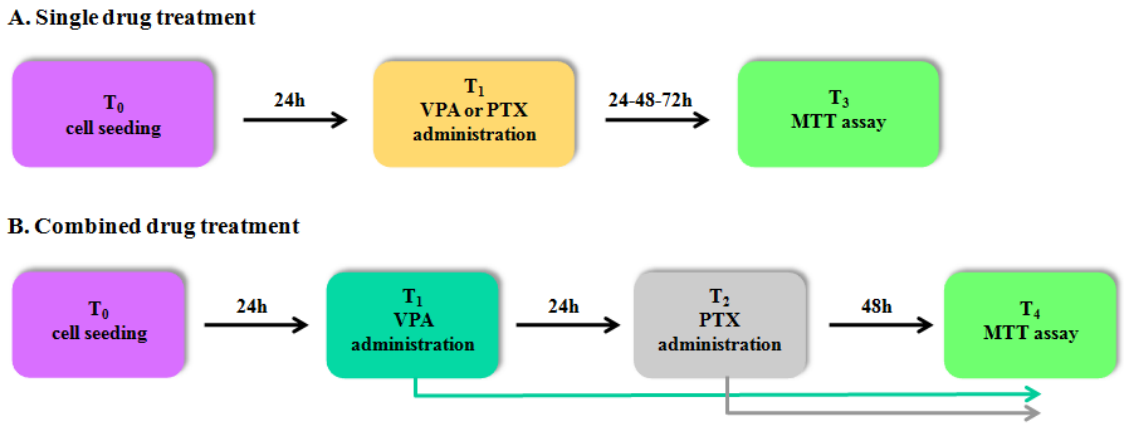

Figure 1. Drug administration plan: single drug treatment (A) and combined drug treatment (B).

CELL VIABILITY – MTT ASSAY

MTT assays was performed to evaluate the efficacy of antineoplastic drugs. MTT assay is a colorimetric test that measures cell metabolic activity and consequently, cell growth rate. MTT [3-(4,5-Dimethylthiazol-2-yl)-2,5-diphenyltetrazolium bromide] is reduced by the mitochondrial succinate-tetrazolium-reductase system to purple formazan that accumulates in cells as granules. The solubilized product is measured by a spectrophotometer. Formazan concentration is directly proportional to the number of viable and metabolically active cells. Cells were seeded at a density of 2-4x10^4 cells/well in a 96-well-plate in 100µL of culture medium and incubated at 37°C. After 24h, drugs were added to cell culture medium at various

concentrations. After the drug incubation time (24, 48, 72h), MTT solution (0.5mg/ml, Sigma) was added to each well and incubated for 3h at 37°C. Therefore, formazan was solubilized in absolute ethanol. The absorbance of the dye was measured spectrophotometrically at a 595nm wavelength using an automated microplate reader (Bio-Rad). The percentage of inhibition was determined by comparing the absorbance values of drug-treated cells with that of untreated controls: [(treated-cell absorbance/untreated cell absorbance)x100]. Thus, dose-effect curve can be drawn. The results are reported as the mean values of two different experiments performed at least in triplicate.

COOPERATIVE INDEX

In order to evaluate the effects of the combined treatment using VPA and PTX, the Cooperative Index (CI) was calculated, comparing the sum of cell death percentages obtained for each single agent to the percentage of cell death upon combined treatment (Aouali et al., 2009). CI values <1 indicate a synergistic effect, CI values = 1 an additive effect, while CI values > 1 indicate an antagonistic effect.

CYTOMORPHOLOGICAL ANALYSIS

In order to evaluate drug efficacy on some cytogenetic parameters, cells were seeded in T-25cm^3 at a concentration of 2x10^6 cell/5ml medium. Subsequently, cells in exponential growth phase were treated with 2mM VPA or with 10µM PTX for 24 and 48hs. After chromosomal preparation, cytomorphological parameters were analyzed. Mitotic index and polymorphic nuclei were evaluated counting the percentage of mitosis and aberrant nuclei, through the analysis of 1000 nuclei. Ploidy was investigated by evaluating the number of chromosomes/metaphase on 30-50 metaphases. Data were obtained as mean values, derived from two independent experiments.

To evaluate the cellular morphological changes after VPA treatment, cells were seeded in serum free medium at 3x10^3-10^4 cells/ml, depending on cell growth rate, specific for each GSC line. After 24hs, cells were treated with several VPA concentrations (2-3-6-10mM) for different

times of exposure (24-48 and 72hs). The morphological changes were evaluated through the observation at phase contrast microscopy, comparing VPA-treated and untreated cells. Representative images were taken for each cell line and for each treatment.

IMMUNOFLUORESCENCE

The immunofluorescence assays were performed on untreated and 2mM VPA-treated cultures for 72 h. The same parameters were evaluated on cultures maintained under differentiating conditions in RPMI-1640 (EuroClone), supplemented with 10% FCS (PBI International), after 14 and 30 days of cultures. The experiments were performed using Rabbit Anti-CD133 (Santa Cruz Biotechnology, 1:50), Mouse Anti-Nestin (Millipore, 1:50), Rabbit Anti-glial fibrillary acidic protein (GFAP, Dako, 1:200), Rabbit Anti-βIII tubulin (TuJ1, Covance, 1:100) and Goat-Anti-Myelin basic protein (MBP, Santa Cruz Biotechnology, 1:50) as primary antibodies. Cells were grown on coverslips or placed onto slides by means of Cytospin, washed with Dulbecco's modified phosphate-buffered saline (PBS), fixed with 4% paraformaldehyde for 15 minutes and treated for 10 minutes with 0.1 M glycine (in PBS). Slides were incubated 30 minutes at RT in blocking solution (5% Bovine serum albumine, BSA, 0.6% Triton X-100 in PBS) and treated for 30 minutes in RNAse 70 U/mg (1:30, Sigma) in blocking solutions. Cells were incubated with the primary antibodies at 4°C overnight. Then, slides were rinsed with washing buffer (0,3% Triton X-100 in PBS) and incubated with secondary fluorescent antibodies and 2.5 mg/ml propidium iodide (PI) for 1h at RT. Alexa Fluor 488-conjugated Goat Anti-mouse or Anti-rabbit and Donkey-Anti-goat (1:200, Molecular Probes) were used as secondary antibodies. Alexa Fluor 647-conjugated phalloidin (Molecular Probes, 1:200) was used to visualize the actin filaments. Then, cells were washed with PBS and coverslips were mounted using Polyvinyl alcohol mounting medium (Fulka Analytical). Fluorescent cell preparations were examined using a Radiance 2100 confocal microscope (Bio-Rad, Hercules, CA, USA), evaluating 100 cells for each sample. Noise reduction was achieved by Kalman filtering during acquisition.

MeDIP-Chip

MeDIP-Chip technology combines methylated DNA immunoprecipitation (MeDIP) with microarray technology, in order to give a detailed profile of genome-wide CGI methylation. Each experiment was carried out following the guidelines of Agilent Microarray Analysis of Methylated DNA Immunoprecipitation Protocol (Version 1.0), which is summarized in Figure 2.

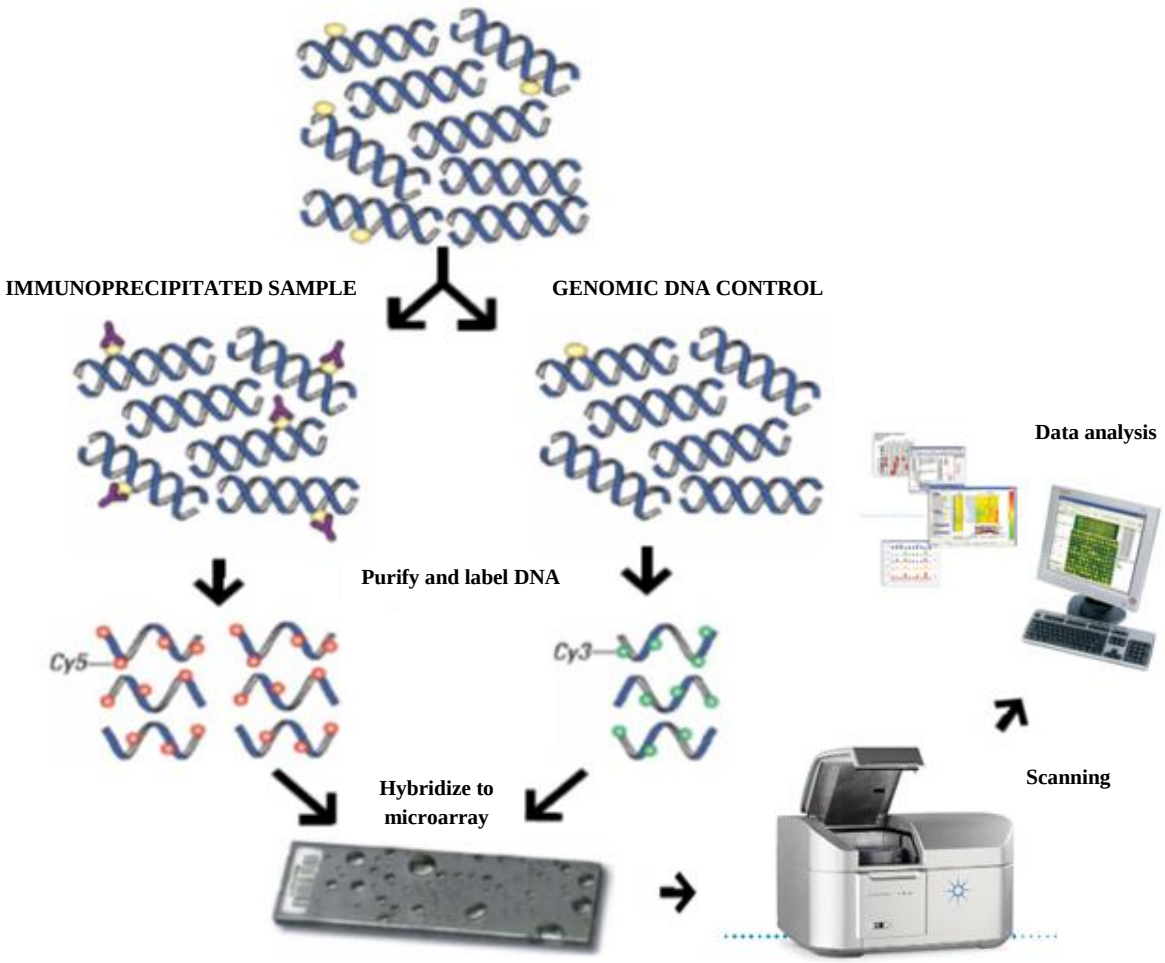

Figure 2. Agilent MeDIP-Chip protocol for DNA methylation analysis.

For beads preparation, 50µl of pan-mouse IgG Dynal magnetic beads (Invitrogen) were washed twice in PBS+0.5% BSA. Subsequently, beads were incubated with 5µg of 5-methylcytosine antibody (Eurogenetec) in PBS+0.05% BSA at 4°C on a rotator overnight. The next day, beads were washed three times with PBS+0.05% BSA and resuspended in 50µL of the same solution.

5µg of purified genomic DNA were resuspended in 250µL of PBS and then sonicated in order to achieve sheared DNA, with fragments ranging from 200 to 600 bp in size. 50µl of each sample were retained as the reference sample and stored for next steps in this protocol. The remaining 200µL of solution containing fragmented DNA were immunoprecipitated by incubation with the antibody/bead complex in PBS with 5µg/ml BSA and 25µg/ml yeast tRNA at 4°C, on a rotator overnight. Immunoprecipitated (ip) DNA was eluted from the beads by incubation at 65°C for 5 minutes in TE with 1% SDS. In order to achieve a complete elution of ipDNA from the beads each sample was incubated with 5µl 10mg/ml proteinase K (Roche) at 50°C for two hours. Then, ipDNA and reference DNA were purified through phenol-chloroform protocol. DNA from each sample was incubated with one volume of phenol:chloroform:isoamyl alcohol (25:24:1) and precipitated in two volumes of absolute ethanol containing 200mM NaCl and 1.5µL of 20µg/ml glycogen (Invitrogen). Precipitated DNA was washed in 70% ethanol, air dried and resuspended in 31µl of nuclease-free water. 5µl of each sample were stored for any additional analysis. Target (ipDNA) and reference samples were labeled with Cyanine 5- and Cyanine 3-dUTP nucleotides, respectively, using Agilent Genomic DNA labeling Kit Plus (Agilent Technologies). The clean-up of labeled genomic DNA was performed using Microcon^{TM} YM-30 columns (Millipore) and eluted in 42µl of Tris-EDTA (TE) buffer. The yield and specific activity of the labeling of each sample were evaluated using the NanoDrop ND-1000 UV-VIS Spectrophotometer (Thermo-Scientific). Then, cyanine 5- and cyanine 3-labeled samples were combined in a single mixture. Hybridization of labeled ip and reference DNA was performed essentially as described in the Agilent aCGH protocol using a 1x244K slide format, except hybridization, which was performed at 67°C for 40hs, in the presence of 15% formamide. Agilent Human CpG Island Microaray Kit 1x244K contains approximately 237˙000 oligonucleotide probes covering 21Mb of 27˙800 CpG islands, with average probe spacing of 100 bp and with ~8 probes per island. The full list of CpG islands can be downloaded from the UCSC genome browser (hg18, NCBI build 26.2, March 2006). Microarrays were scanned using a Agilent microarray scanner and images analyzed with Agilent Feature Extraction software v10.7, which is able to carry out linear normalization and calculation of the

log2 ratio value, obtained comparing the fluorescence intensity of Cy5 and Cy3 dye. Data were further analyzed by means of Agilent Genomic Workbench v5.0 software. A specific algorithm associates to each probe a combined Z-scores and p-values, which give the probabilities and confidence values for methylated and unmethylated probe populations. A methylation logOdds is then calculated which gives the relative probability that a probe is more likely methylated than unmethylated. The output file is an Excel spreadsheet that associates to each specific probe, the relative position on the genome and the associated values of log2 ratio, combined Z-score and logOdds.

Data were further analyzed according to the methodological approach conceived by Dr. Ravid Straussman and colleagues in 2009 (Straussman et al., 2009). First of all, the values of combined Z-scores for each specific CpG island were averaged to obtain the Island Methylation Score (IMS). Thus, each CpG island was associated to a specific IMS. Subsequently, data were plotted on a chart, comparing IMS versus the number of CpG islands associated to that specific IMS value. The resulting curve has a clear bi-modal distribution. Threshold values were calculated in order to determine the methylation status (methylation or un-methylation) of each CpG island. Firstly, the distance between the unmethylated (H1) and methylated IMS peaks was calculated (ΔH). Then, the lowest point (L) in the bimodal distribution was determined and the 10% of the ΔH was added to or subtracted from the L point, setting the upper or lowest limits (Figure 3). Values above the lower cut-off were associated to unmethylated CpG islands, whereas values over the upper cut-off were associated to methylated CpG islands. Values located between the two limits were considered undetermined, as it was not possible to clearly associate a methylation status. Consequently, data were converted in a binaric code: methylated CpG islands were referred as +1, while unmethylated islands were referred as -1. Undetermined islands were marked as 0. It is necessary to point out that this is a qualitative analysis, as this approach allows the identification of the methylation status of each CpG island, but does not provide any information about the amount of methylation at a specific CpG island sites.

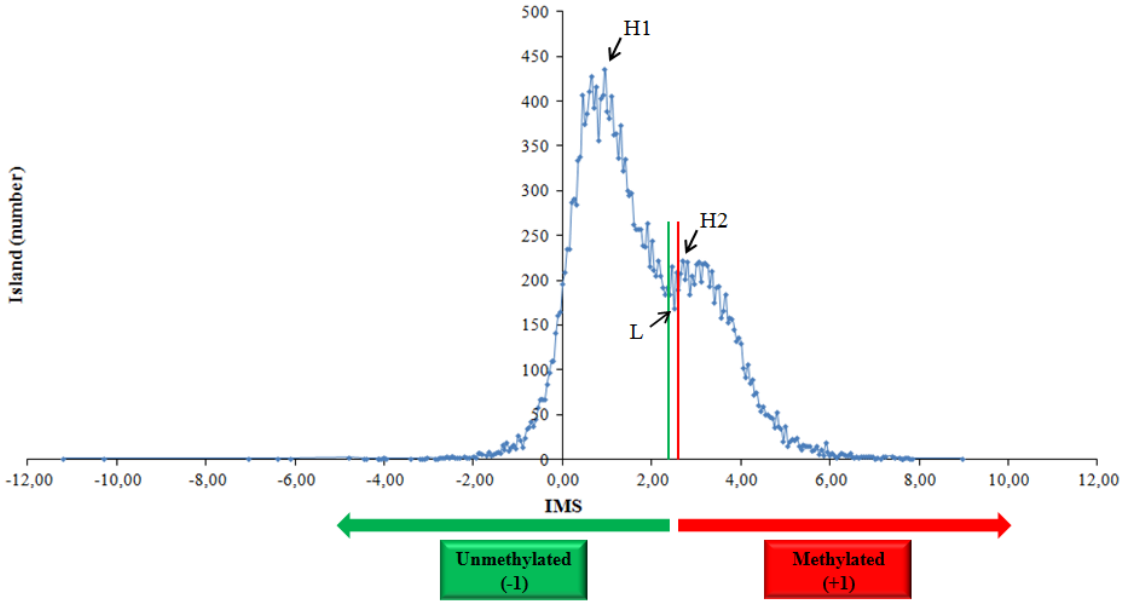

Figure 3. Determining the cut-off values for the methylation status of each MeDIP-Chip experiment. The chart shows an example of the analysis approach performed to determine the upper and lower limit for DNA methylation status. Specifically, this chart refers to CB660 cell line. H1: unmethylated IMS peak; H2: methylated IMS peak; L: lowest point.

BIOINFORMATIC ANALYSIS

The Gene Ontology (GO) analysis was performed using GOstat software (http://gostat.wehi.edu.au/) (Beissbarth and Speed, 2004) in order to identify possible enrichment of functional groups, related to 'biological process', in a specific input list of genes. GOstat software output file is a list of p-value for each GO term, estimating the probability that the observed counts could have occurred by chance. In order to limit the number of GO terms, a class should comprise more than five genes to be considered for further analysis (Aronica et al., 2008). GO terms were divided in cancer-relevant functional categories. Several functional categories were identified: 1. *cell cycle*; 2. *cell death and apoptosis*; 3. *response to external stimulus*; 4. *cytoskeleton organization*; 5. *cell signaling*; 6. *development & morphogenesis*; 6. *cell differentiation*; 8. *immune response*; 9. *cell motility*; 10. *metabolism;* 11. *transcription & gene expression*; 12. i*ntracellular transport*; 13. *DNA repair & chromatin remodeling*. Each category was associated to a frequency, which was calculated evaluating the ratio between the

number of genes associated to a specific category on the total number of genes associated to at least one GO term. The pathway analysis was generated through the use of Ingenuity Pathway Analysis software (IPA, Ingenuity System, Redwood City, CA, USA, www.ingenuity.com). IPA software examines functional relationships within an input list of genes. IPA analysis identified the pathways from the IPA library of canonical pathways that were most significantly associated to the data set. The significance of the association between the data set and the canonical pathway was measured in 2 ways: 1) a ratio of the number of molecules from the data set that map to the pathway divided by the total number of molecules that map to the canonical pathway is displayed; 2) Fisher's exact test was used to calculate a p-value determining the probability that the association between the genes in the dataset and the canonical pathway is explained by chance alone. Network analysis displays regulatory relationships existing between the genes in the input dataset and the involved networks are ranked by score. Networks are selected if their score is major than 3, which means that there's less than 1/1000 chance that the clustering would have occurred by chance.

STATISTICAL ANALYSIS

Statistical analysis was carried out performing chi-square, Fisher's exact test or t-test on raw data, by means of Excel spreadsheet (Microsoft Office 2007, Microsoft Corporation) or OpenEpi software v2.3.1, available on line at http://www.openepi.com/. The critical level of significance was set at $p<0.05$.

RESULTS

CYTOGENETIC AND MOLECULAR CYTOGENETIC ANALYSIS

Cytogenetic analysis is an essential tool to identify chromosomal abnormalities in tumors and to unmask specific genomic regions involved in tumorigenesis, as sequentially acquired chromosomal abnormalities are pathogenetically fundamental in the development of malignancy. Thus, a careful cytogenetic investigation of GSCs is needed. Specifically, the karyotype of each GSC line (GBM2, GBM7, G144, G166, G179 and GliNS2) was assessed, through QFQ-banding, in order to determine the major chromosomal abnormalities. GBM, as many other solid tumors, is characterized by great cytogenetic heterogeneity within the tumor. Thus, all the chromosomal aberrations are described in a composite karyotype (cp), which contains all clonally occurring abnormalities and gives the range of chromosome number in the analyzed metaphases. The clonal abnormalities are defined as two or more cells with the same additional chromosome or structural rearrangement, or three or more cells with the same chromosome missing, as stated in the International System for Human Cytogenetic Nomenclature 2009 (ISCN 2009). Subsequently, a molecular cytogenetic analysis by means of FISH was performed on GBM2, G166 and GliNS2 cell lines, using a panel of whole chromosome painting (wcp) probes, spanning on all the 24 chromosomes.

All the chromosomal abnormalities are summarized in Table 2 and result from the complementary analysis of QFQ-banding and FISH analysis. GBM2 cell line was characterized by the highest number of structural abnormalities, whereas G179 cell line showed two subpopulation of cell, defined as G179 and G179*, with a different modal number of chromosomes and so they have been analyzed separately. Firstly, a high heterogeneity was noticed both inter and intra-cell lines, showing numerical and structural aberrations. Ploidy was extremely variable, ranging from near-diploidy (G166 and GliNS2 cell lines) to near-pentaploidy (G179*). Moreover GBM2 and G179 cell lines were near-triploid and G144 and GBM7 are near-tetraploid. In order to identify the chromosomes mainly involved in numerical aberrations, the frequency of all gains and losses of whole chromosome

Table 2. Chromosomal aberrations identified in the 6 GSC lines through QFQ-banding and FISH analysis. The aberrations identified and/or supported by FISH analysis are marked in red. -: loss of whole chromosome; +: gain of whole chromosome; ++: more than two sovranumerary copies; /: lack of alterations.

	Cell line	GBM2	GBM7	G166	GliNS2	G179	G179*	G144
	<ploidy>	62~83<3n>,XXY	67~96<4n>,XXY	48~59<2n>,XXXXY	41~47<2n>,XY	64~79<3n>,X	101~117<5n>,XX	63~95<4n>,XXYY
Chromosome	X	-	-	/	+	- del(X)(p11.22)	- del(X)(p11.2)	-
	Y	-	+	-	-	- rea(Y)	+,- rea(Y)	-
	1	+ der(1)t(1;9)t(p36.3;q13) del(1)(p34)	+,- del(1)(p36.1),del(1)(p34) add(1)(p36.3)	+der(1)t(1;21)(q11;?) +rea(del(1)(p11))	inv(del(1)(p34.3))	del(1)(p33)	+ del(1)(p33)	- der(1)t(1;?)(p13;?) del(1)(q21)
	2	+,-	+ del(2)(q?)	+rea(del(2)(p11))	- der(2)t(2;20)	+	-	- del(2)(p11.2)
	3	-,del(3)(q13)	-	+ rea(3)(p?)	del(3)(p22?p25?)	+	+	+,-
	4	+,- der(4)t(3;4)(p21;p16)	+ del(4)(p12)	-	-	-	-	-
	5	+ del(5)(q12;q13)	+	+ der(5)t(5;11)(p11;?)	+der(5)t(2;5) (?;q35.3)	/	-	+,- rea(5)
	6	+,- del(6)(q14) der(6)t(6;7)(q27;?)	-	+ +del(6)(q16.1)	der(6)t(3;6)(?;q27) der(6)t(del(6)(q25.1); 21)(p21?;p13)	+	+	+,-
	7	++ del(7)(q31)	++	-	+	++	++ del(7)(q11.21)	++
	8	+,-	-	+	-	+	+	-
	9	+ del(9)(q11) dic(9;del(9)(p11)) (q34;q34)	-	+	/	/	-	+,- rea(9)(p?)
	10	+,-	-	-	- del(10)(q21.3)	-	-	+,-

	Cell line	GBM2	GBM7	G166	GliNS2	G179	G179*	G144
Chromosome	**11**	+,- add(del(11)(p11))(p11)	-	+rea(11)	rea(del(11)(q13))	/	-	- rea(11) del(11)(p15)
	12	+,- del(12)(p12)	+,- del(12)(p12)	-	+	+der(12)t(12;?)	+,- +der(12)t(12;?)	+,- del(12)(q?) der(12)t(12;?)(q11;?)
	13	-	+ der(13;14)(q10;q10)	+,-	-	/	-	+,-
	14	+,-	+,-	-	-	-	-	+,-
	15	+,-	-	+	+,-	-	+	+,-
	16	+,- rea(16)	+,-	+	+ rea(16)	+	+	+,-
	17	+ del(17)(p12) add(del(17)(p12))(q25)	-	- +i(17)(q10)	+	/	-	+,-
	18	+,- add(18)(q23)	+,-	der(18)t(7;18)(?;p11)	+ del(18)(p11.2)	/	/	-
	19	+,-	+	+,- der(19)t(19;22)(q13;?)	-	/	/	+
	20	+,-der(20)t(12;20) (q13;p11.2)	+	+	-	/	-	-
	21	+	+	-	- der(21)t(6;21)	-	-	+,-
	22	+	-	-	-	-	-	+,-
	mar	1~3	1~2	1~2	/	/	/	1

was calculated, by averaging each specific numerical abnormality on the total number of metaphases analyzed, for all the 6 GSC lines (Figure 4). Specifically, this analysis showed that numerical changes involved all the chromosomes. Anyway, gain of chromosome 7 was the most frequent numerical aberration, identified in 73% of metaphases analyzed and usually in more than two sovranumerary copies in 4/6 cell lines (GBM2, GBM7, G179 and G144). Moreover, a high percentage of metaphases were characterized by loss of chromosome 13 (43%) and loss of sexual chromosome (28% for X and 39% for Y chromosomes). Loss of chromosome 10 was identified in 32% of metaphases. Other high frequencies of chromosomal numerical aberrations concerned chromosomes 14, 16, 20, 21, 22.

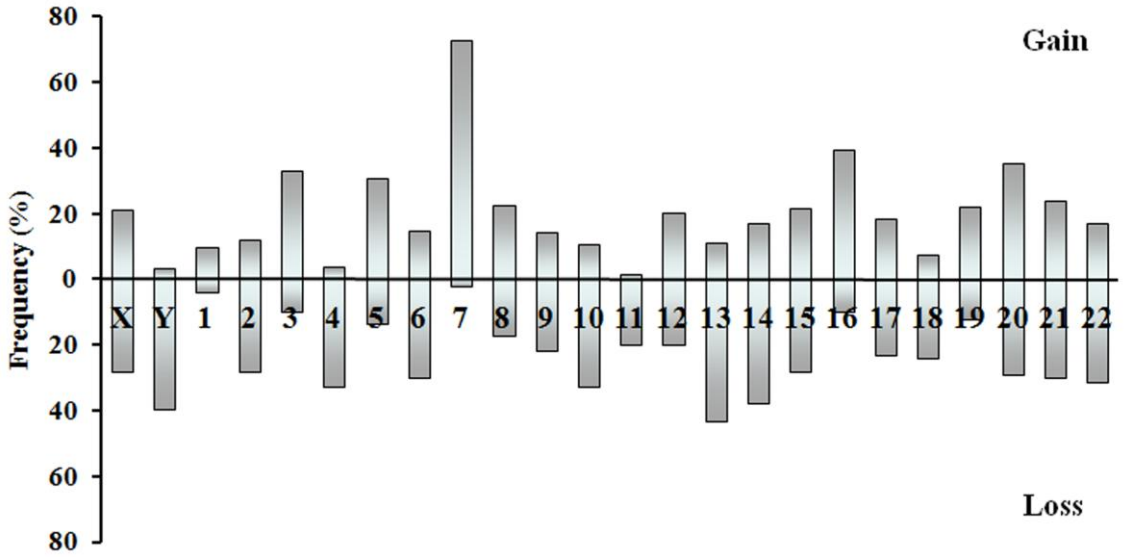

Figure 4. Frequency of gains and losses of whole chromosomes, in the 6 GSC lines analyzed by QFQ-banding. Data represent the average value of each numerical change identified in the karyotype of the 6 cell lines.

A total of 63 clonal chromosomal aberrations were found among the 6 cell lines. Generally, the aberrations involved mainly centromeric or telomeric breakpoint regions. The most frequently involved chromosome in structural rearrangements was chromosome 1, in 6/6 cell lines, showing both deletions, inversions and translocations. Translocations involving chromosome 1 were characterized by FISH analysis: der(1)t(1;9)t(p36.3;q13) in GBM2 (Figure 5A) and der(1)t(1;21)(q11;?) in G166 cell line (Figure 6A). GliNS2 cell line showed a deleted

chromosome 1, which was further involved in an inversion defined as inv(del(1)(p34.3)) (Figure 7A). All the cell lines showed deletions of the short arm of chromosome 1, with different breakpoint locations, ranging from the terminal deletion to the loss of the entire short arm. Deletions of the long arm of chromosome 6 were observed: del(6)(q14) in GBM2 and del(6)(16.1) in G166. An additional deletion of 6q was observed also in GliNS2 cell line, associated to a translocation with chromosome 21 (Figure 7G). Moreover, add(6)(q27) was found in GBM2 and GliNS2 cell lines. FISH analysis allowed the identification of the additional material added to the q arm telomere of chromosome 6 in both cases. Specifically, these abnormalities were defined as der(6)t(6;7)(q27;?) for GBM2 and der(6)t(3;6)(?;q27) for GliNS2 cell line (Figure 5D and 7F, respectively), showing a sort of telomeric breakpoint on chromosome 6q. Chromosome 12 was also seriously involved in structural aberrations (4/6 cell lines), showing deletions of both the short (GBM2 and GBM7) and the long arm (G144) and translocations (GBM2, G179 and G144). Deletion of chromosome 17p was identified in 2 cell lines through a proper deletion in GBM2 (del(17)(p12)) and the presence of an isochromosome of the entire long arm of chromosome 17 (iso(17)(q10)) in G166 cell line (Figure 6F). Moreover, FISH analysis allowed the identification of other complex rearrangements.

GliNS2 cell line was characterized by the presence of der(2)t(2;20) (Figure 7C) and der(5)t(2;5)(?;q35.3) (Figure 7D). A derivative chromosome 5 was identified also in G166 cell line (der(5)t(5;11)(p11;?)) (Figure 6D). Unfortunately, some chromosomal aberrations remained unidentifiable as both QFQ-banding and FISH analysis didn’t help in the unambiguous identification of such chromosomal materials. These structurally abnormal chromosomes are referred as marker chromosomes. The presence of double minutes (Figure 8) was noticed in all cell lines and their number was extremely variable between metaphases and cell lines. Furthermore, the cytobands involved in some translocations were not defined, due to the small dimension of the translocated region.

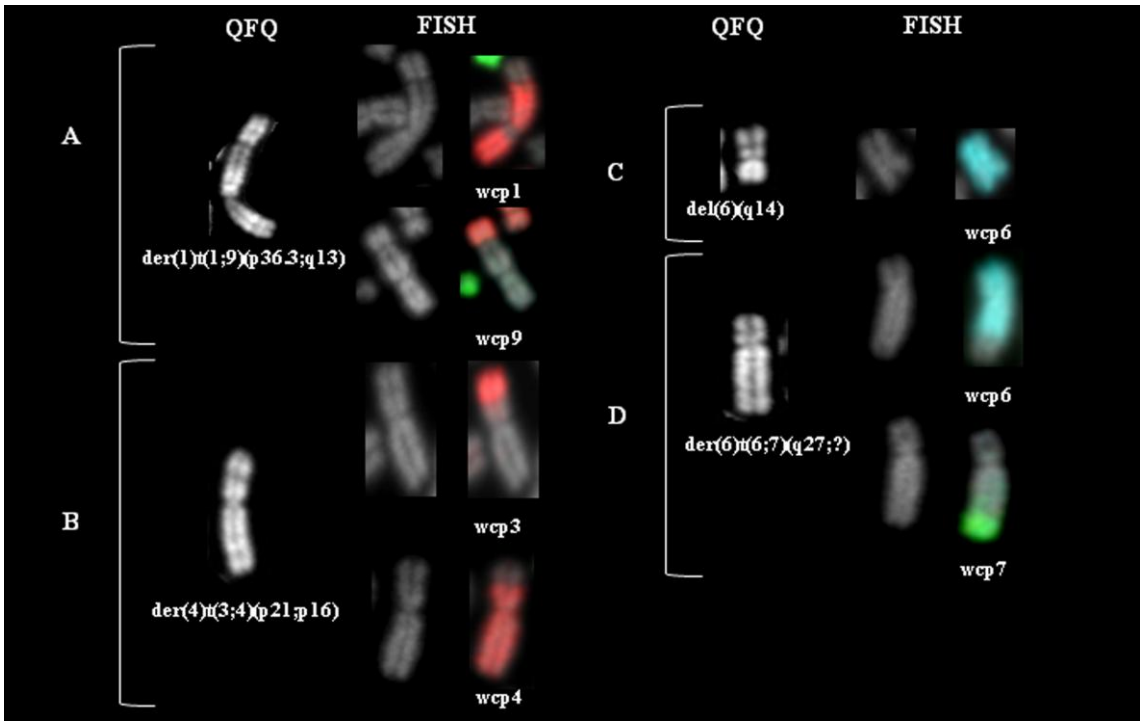

Figure 5. Panel of the chromosomal abnormalities of GBM2 cell line identified through FISH analysis. Each aberration is described by means of QFQ-banded chromosomes and the corresponding FISH results. A. der(1)t(1;9)(p36.3;q13), B. der(4)t(3;4)(p21;p16), C. del(6)(q14), D. der(6)t(6;7)(q27;?).

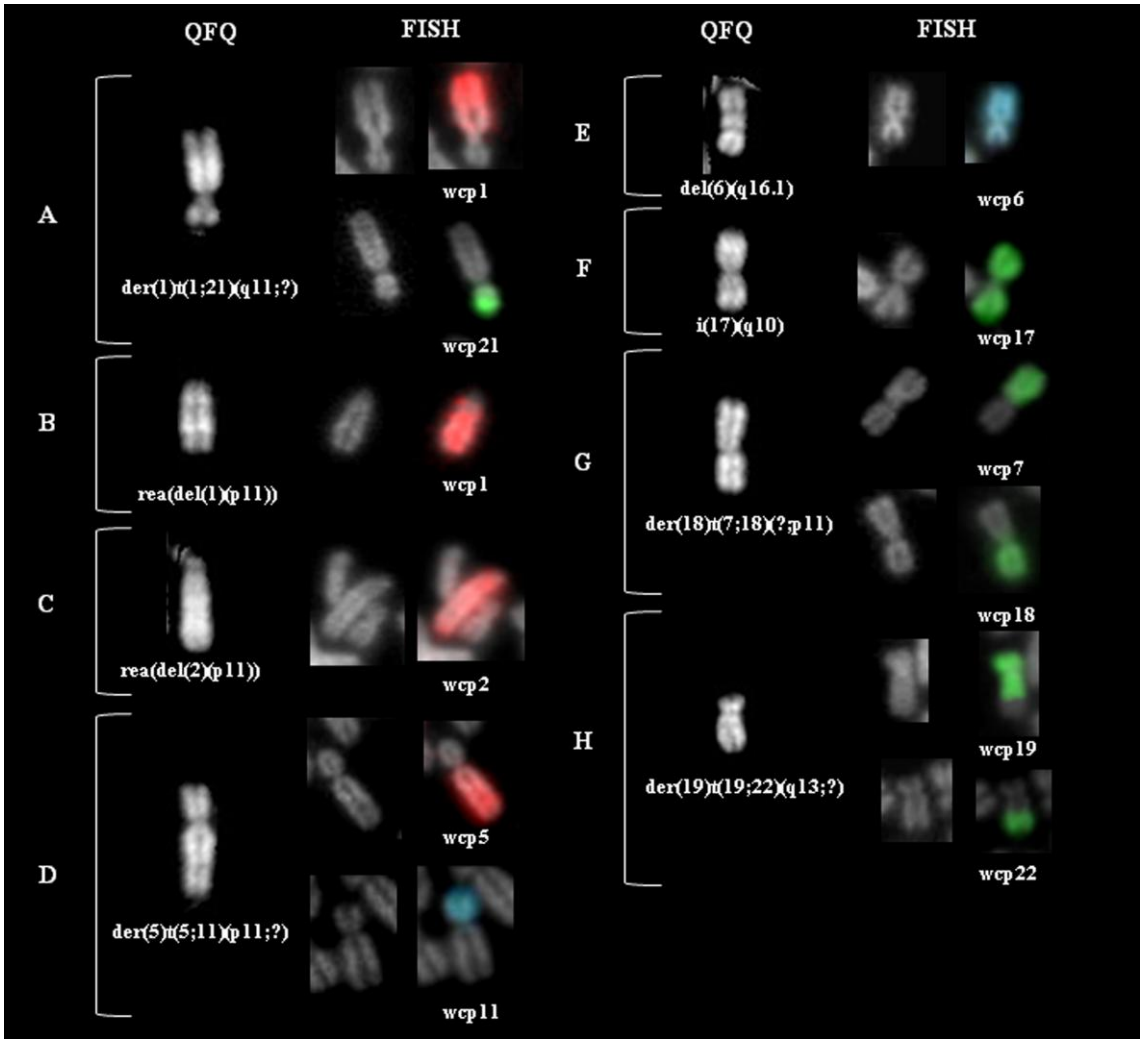

Figure 6. Panel of the chromosomal abnormalities of G166 cell line identified through FISH analysis. Each aberration is described by means of QFQ-banded chromosomes and the corresponding FISH results. A. der(1)t(1;21)(q11;?), B. rea(del(1)(p11)), C. rea(del(2)(p11)), D. der(5)t(5;11)(p11;?), E. del(6)(q16.1), F. i(17)(q10), G. der(18)t(7;18)(?;p11), H. der(19)t(19;22)(q13;?).

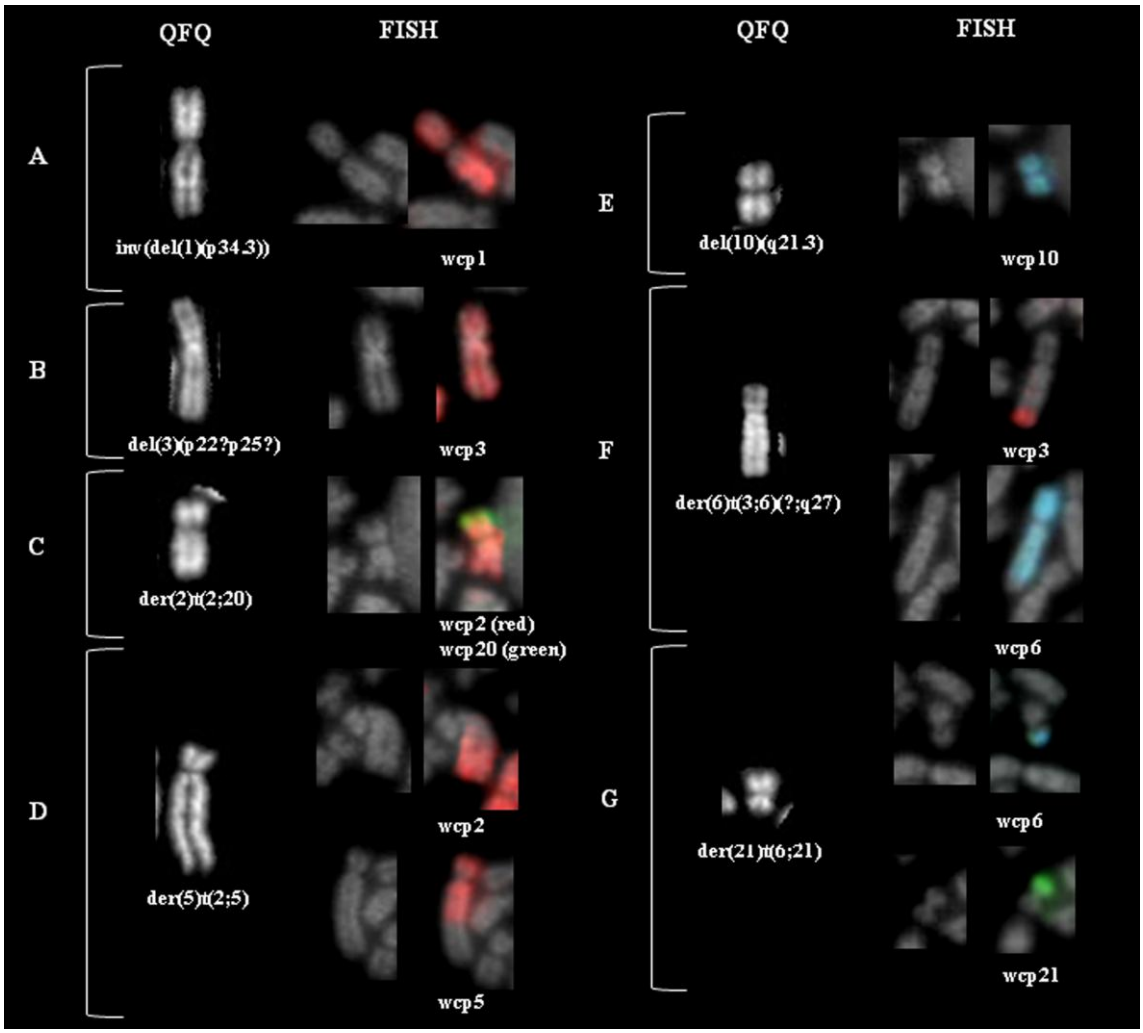

Figure 7. Panel of the chromosomal abnormalities of GliNS2 cell line identified through FISH analysis. Each aberration is described by means of QFQ-banded chromosomes and the corresponding FISH results. A. inv(del(1)(p34.3), B.del(3)(p22?;p25?), C.der(2)t(2;20), D. der(5)t(2;5), E. del(10)(q21.3), F. der(6)t(3;6)(?;q27), G. der(21)t(6;21).

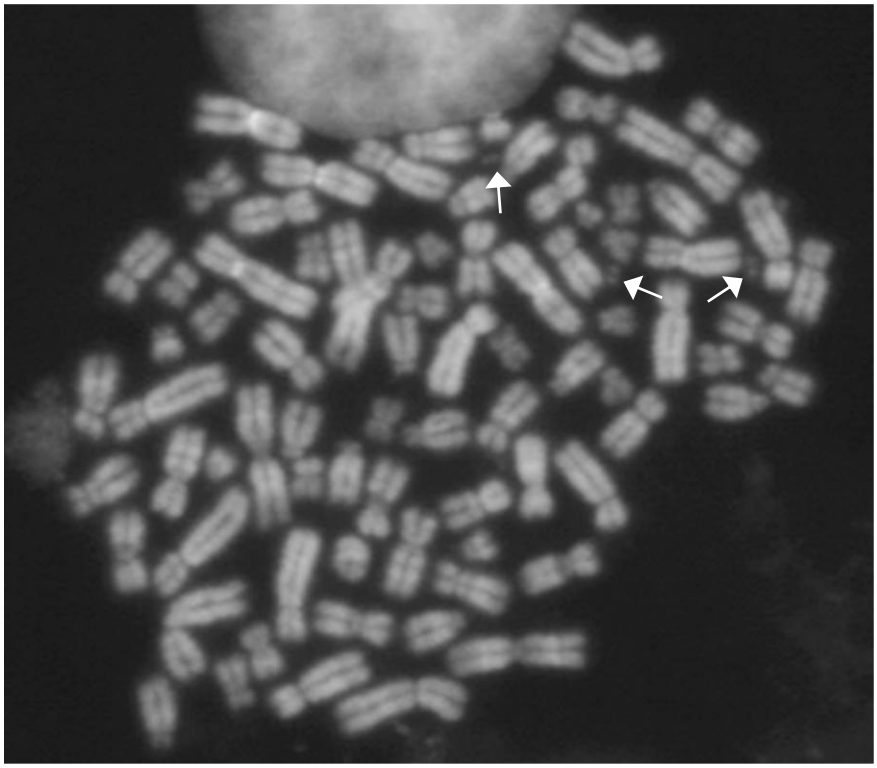

Figure 8. Metaphase chromosome spread (GBM2 cell line) showing an example of double minutes (dmin, arrows).

DETECTION OF COPY NUMBER ALTERATIONS (CNAS)

Array CGH on genomic DNA was assessed in order to screen for additional genomic alterations, which were not identified through QFQ-banding or FISH analysis, due to their lower resolution and the difficulty to obtain proper chromosomal preparations. CGH was performed to detect CNAs in GBM2, GBM7, G166, G179 and GliNS2 cell lines. aCGH of G144 was already carried out by Pollard and colleagues in 2009 (Pollard et al., 2009). A summary of the CNAs detected by aCGH in GSC lines is shown in Figure 9. Data comprise both homozygous and heterozygous deletions and both gains and amplifications. aCGH revealed complex genomic changes in these cell lines: no single chromosome was free from aberrations in the GSC lines analyzed. There was a variation regarding the frequency of each imbalance, but also which areas of the chromosome were implicated.

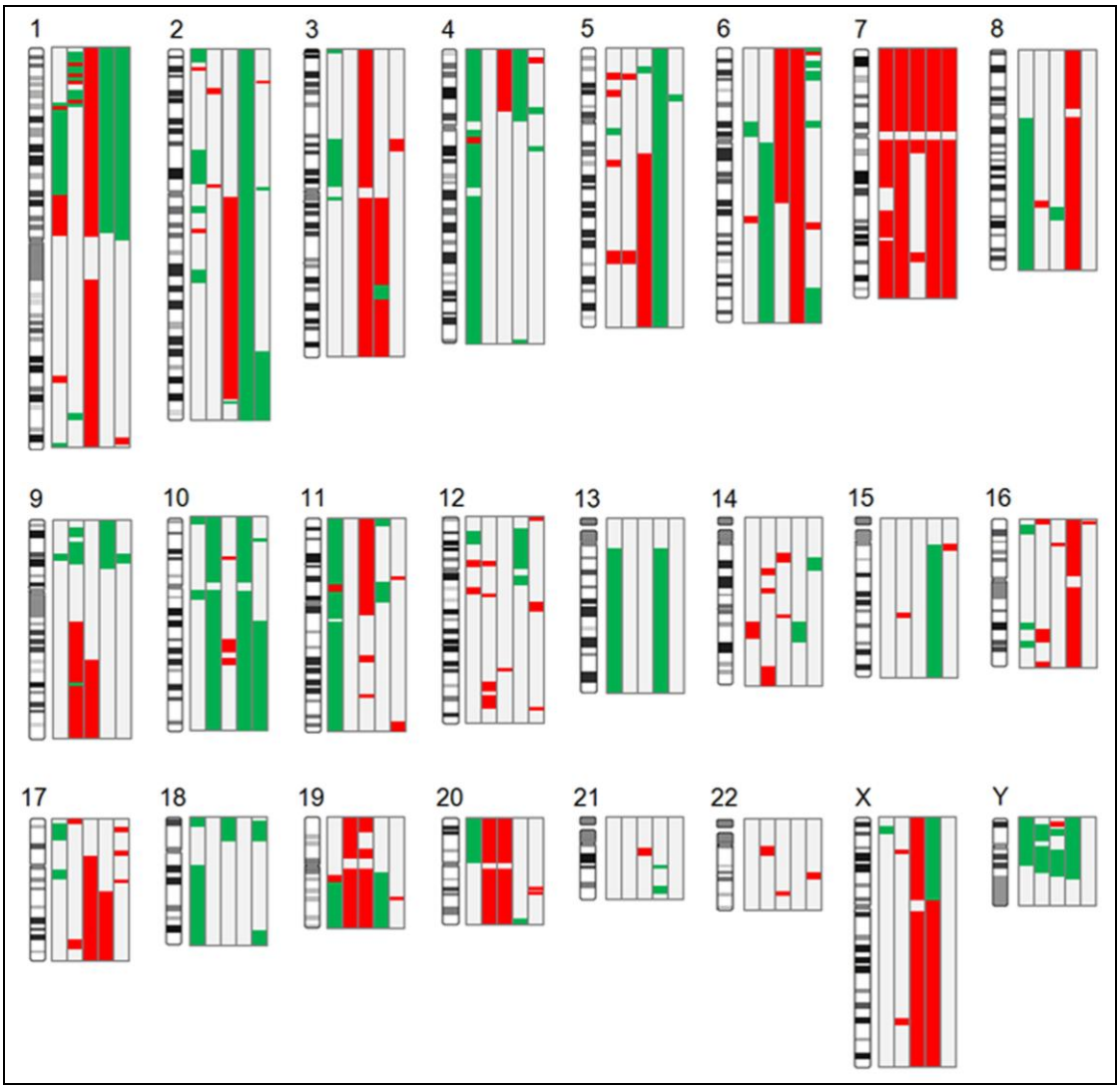

Figure 9. Composite array CGH profiles of GSC lines. Red bars indicate gains, whereas green bars indicate losses. Left to right: GBM2, GBM7, G166, G179 and GliNS2 cell lines, respectively.

The predominant imbalance in all the cell lines analyzed was gain of most (G166, 7p22.3-q11.1) or whole chromosome 7 (more than 4 copies in GBM2, GBM7, G179 and GliNS2 cell lines). *EGFR*, *CDK6* and *MET* genes map to this chromosome. Complete loss of chromosome 10 was noticed in 2 lines out of 5 (GBM2 and G179), whereas loss of 10q21.3-q26.3 was observed in GliNS2 cell line. These losses involve the deletion of *PTEN* and *DMBT1* genes. The long arm of chromosome 13 was lost in GBM2 and G179 cell lines and *RB* gene was at least one of the targets of this deletion. The entire or partial loss of 9p was observed in 4/5 GSC lines, encompassing the region containing known tumor suppressor genes CDKN2A and CDKN2B. Some of these deletions were homozygous deletions. Whole or partial loss of chromosome Y

was associated with 4/5 cell lines. Frequent alterations of chromosome 1 were identified, including gains and losses. Specifically, the 1p arm was characterized by loss of chromosomal material, spanning from the loss of the entire p arm in G179 and GliNS2 cell lines to a regional loss in GBM2 (1p34-p12) and GBM7 (1p34-36) cell lines. Moreover, loss of 1p and 19q, a common feature of oligodendriomas, were detected in GBM2 and G179 cell lines. Gain of 1q32.1 region, containing *MDM4* gene, was found in 2/5 cell lines (GBM2 and G166). Furthermore, the simultaneously gain of chromosome 19 and 20 appeared in GBM7 and G166 lines. Loss of 6q27-28 region, which includes PARK2, PACRG, QKI and PDE10A genes, was detected in GBM7 (6q11.1-27) and GliNS2 (6q25.1-27) cell lines. In addition to the common alterations, line-specific chromosomal alteration were identified, such as amplification of *PDGFRA* (4q14) and loss of *TP53* (17p13.2-13.1) genes in GBM2 cell line, or loss of whole chromosome 15 in G179 cell line.

Then, aCGH data from each cell line were examined in order to find functional annotations through a bioinformatic analysis. Genes in gain and loss regions were analyzed by means of GOstat software, to identify the biological functions of genes associated to these regions. Data were investigated separately and then results where compared in order to find common features between GSC lines. Cancer-related GO terms were analyzed further and were grouped in functional categories as described in 'Materials and methods' section. Categories were ranked in order of the percentage of genes found (Liu et al., 2010b) and are graphically represented in Figure 10. The most common biological functions identified through this analysis were *cell signaling* and *development and morphogenesis*. Thus, disregulation by amplification or deletions of genomic regions containing genes related to these two categories is functionally important in tumor biology. Moreover, *cell cycle* and *apoptosis* categories, which are important function in the regulation of cellular growth, were identified in CNA regions. Genes related to *cell differentiation* were also found affected by genomic copy number changes, with a

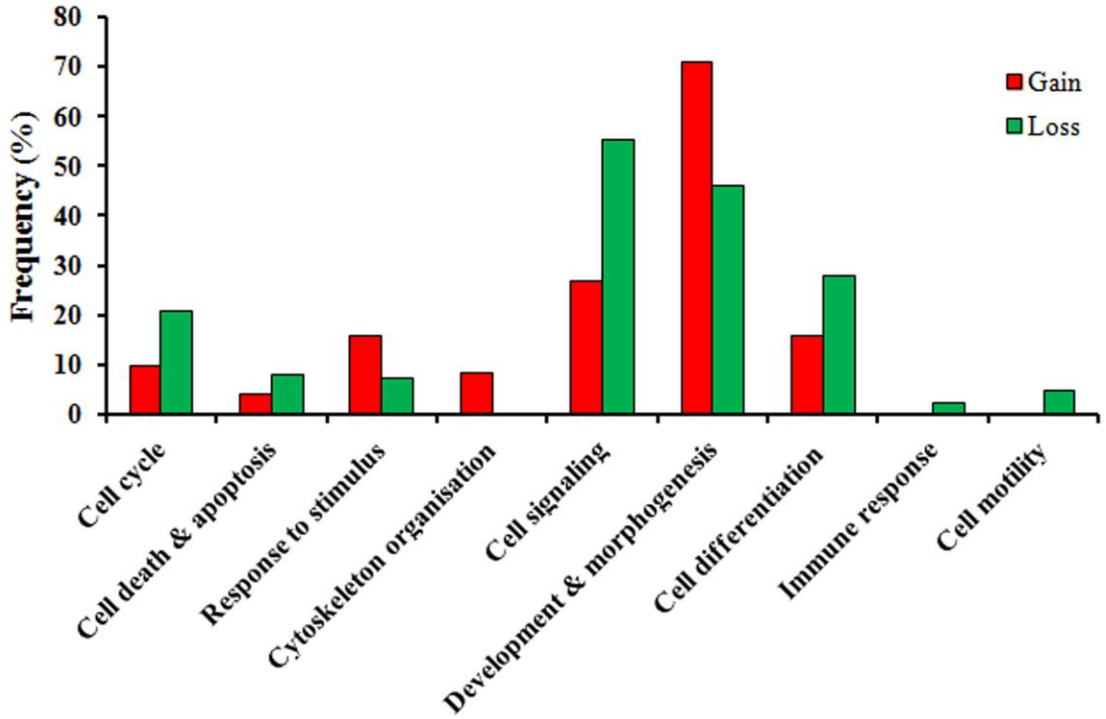

Figure 10. Categories of genes related to gain and loss regions and determined by GO analysis. Each category is associated to a percentage of frequency, which is calculated on the ratio between the number of genes associated to a specific category and the total number of genes associated to at least one GO term.

preponderance of loss of material, suggesting that cellular differentiation process might be impaired in this kind of cells. Other categories, such as *response to stimulus* and *cytoskeleton organization* were involved in these regions. Furthermore, even if at a lower frequency, cell motility and immune response categories were associated to deleted regions.

As we are investigating GSC lines, which are enriched in stem-like cancer cells, we decided to compare CNAs obtained by aCGH experiments on GSC lines to CNA data derived from 430 genomic profiles described in several literature studies (de Tayrac et al., 2009; Lo et al., 2007; Maher et al., 2006; Network, 2008; Nord et al., 2009), in order to find a specific 'stemness signature' associated to GSCs.

Figure 11. Tree topology of overlapping network established using IPA software. Genes in new 'exclusive' gain and loss regions identified in GSCs profiles of aCGH are assigned to gene networks, which are strictly interconnected one to each other and reveal cancer-relevant annotations. Different genes can be grouped in several networks, underlying the same mechanism (ie. cancer or cell cycle).

The reference profiles are derived from both surgical specimen and serum-cultured cell lines, so they can be considered as related to the bulk tumor. We identified several new 'exclusive' regions in our GSC lines (Table A1 of Appendix section), but unfortunately we didn't find any overlapping new CNAs among our stem-like cells. Anyway, genes mapping in these sites were analyzed through IPA software, in order to characterize these regions and to verify if these genes were involved in some shared network or pathway. Specifically, we found that these new 'exclusive' regions were associated to strictly interconnected networks, with several genes that represent the interface between different networks and are known to interact biologically (Figure 11). Different genes were grouped in several networks related to cancer, cell cycle and development, as these genes were differently interconnected forming diverse networks, underlying the same mechanism.

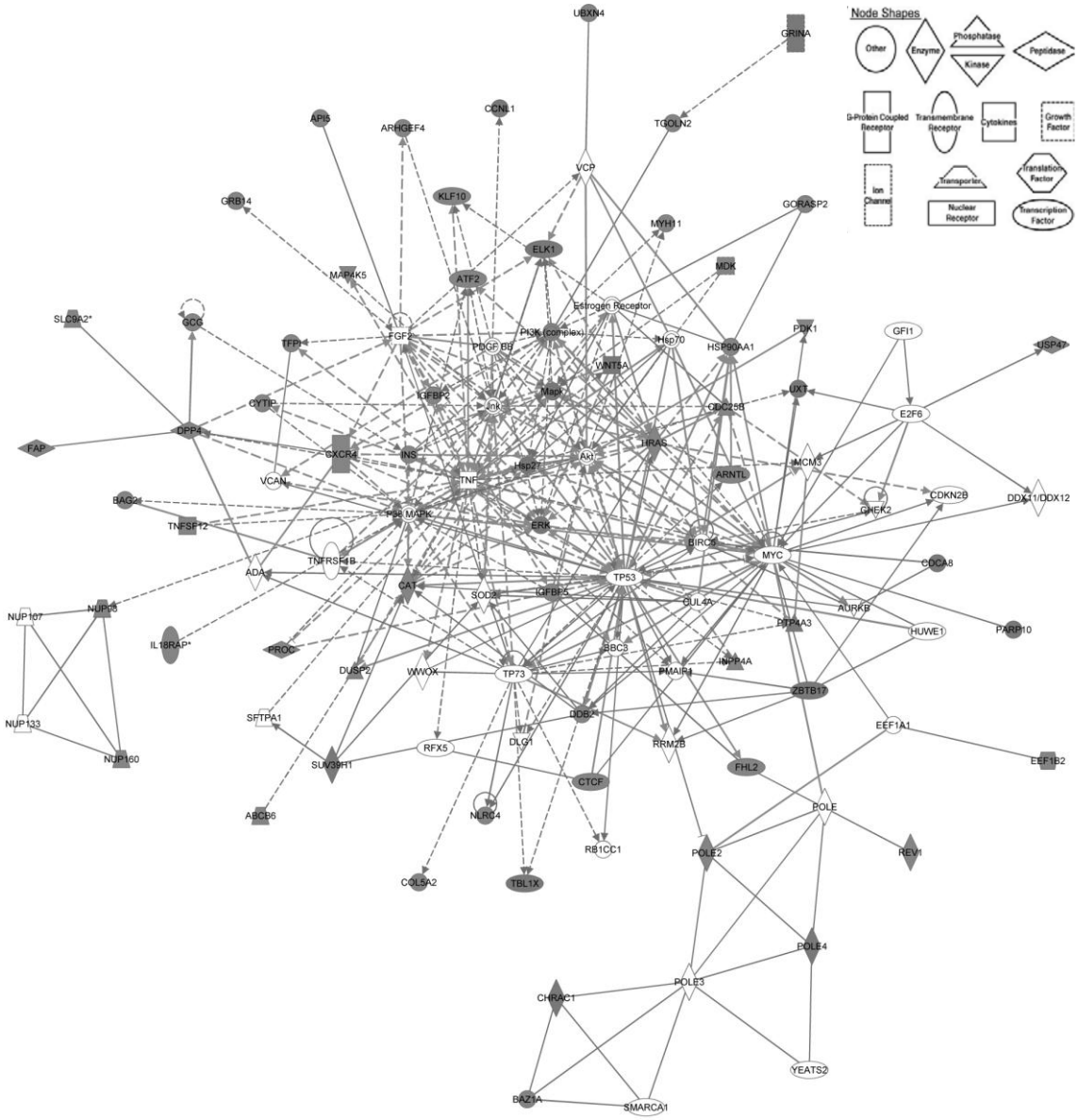

Figure 12. Connectivity of genes identified in the new 'exclusive' CNA regions of GSC lines. Figures in gray denote genes in gain or loss regions and others are those associated with the regulated genes based on pathway analysis. The network shows genes mainly involved in cell cycle. Solid interconnecting lines indicate genes that are directly connected and the dotted lines show indirect connection between genes and cellular functions.

These networks describe functional relationships between gene products based on known interactions in the literature. Thus, genes are not the same among the samples, but they share the same cellular functions and are able to interact, suggesting a sort of common regulatory feature among the GSC lines. Moreover, the specific functional annotations of these genes were cancer-relevant, such as *cellular growth and proliferation*, *cell cycle*, *cell death* and *development*.

Figure 12 shows an example of the strong interconnection between networks referring *to cell cycle process*. In addition, the pathways mainly involved new 'exclusive' CNA regions were *integrin* and *ephrin receptor signaling*, which are involved in motility and invasiveness of glioma cells; *PPAR signaling* which concerns cellular proliferation and differentiation; and *NF-kB signaling*, that is important for apoptosis, cell cycle and immune response. The immune response is additionally involved through *IL-6, IL-10* and *LXR/LXR signaling* pathways (the complete pathway list is available in Table A2).

LOSS OF HETEROZYGOSITY (LOH) ANALYSIS

LOH analysis on GSC lines was performed using a panel of microsatellite markers for chromosomes 1p, 10 and 13, as LOH of these regions is mainly involved in the pathogenesis of GBM. This approach allowed the distinction of the homologous chromosomes, as microsatellite markers with a high rate of heterozygosity were selected.

Microsatellite analysis of chromosomes 10 and 13 showed an overall heterozygosity of all tested markers (data not shown). Microsatellite analysis of chromosome 1p (Table 3) revealed discontinuous loss, defined as evidence of interstitial or small terminal deletions at one or more loci, with retention of heterozygosity at the proximal end of the evaluated region, with or without retention of heterozygosity at the distal end (Barbashina et al., 2005). In particular data displayed a discontinuous LOH at 1p36.31 and 1p36.21 in G144 and G166 cell lines; an interstitial LOH at 1p36.31 in G179 and GliNS2 cell lines; and a telomeric LOH in GBM2 and GBM7 cell lines at 1p36.32-p36.31 and 1p36.32-p36.23, respectively. Thus, 1p36.31 region (specifically D1S214 microsatellite) was identified as deleted in all the GSC lines (Figure 13).

Table 3. Loss of heterozygosity (LOH) study in 6 GSC lines. Abbreviations: homo, homozygote marker; hetero, heterozygote marker; ND, not determined.

	Markers and positions						
Cell line	**D1S468** 1p36.32	**D1S214** 1p36.31	**D1S508** 1p36.23	**D1S228** 1p36.21	**D1S199** 1p36.13	**D1S2734** 1p35.12	**Overall result**
GBM2	homo	homo	hetero	hetero	hetero	hetero	telomeric LOH
GBM7	homo	homo	homo	homo	hetero	hetero	telomeric LOH
G144	hetero	homo	hetero	homo	hetero	ND	segmental LOH
G166	hetero	homo	hetero	homo	hetero	ND	segmental LOH
G179	hetero	homo	hetero	hetero	hetero	hetero	interstitial LOH
GliNS2	hetero	homo	hetero	ND	hetero	hetero	interstitial LOH

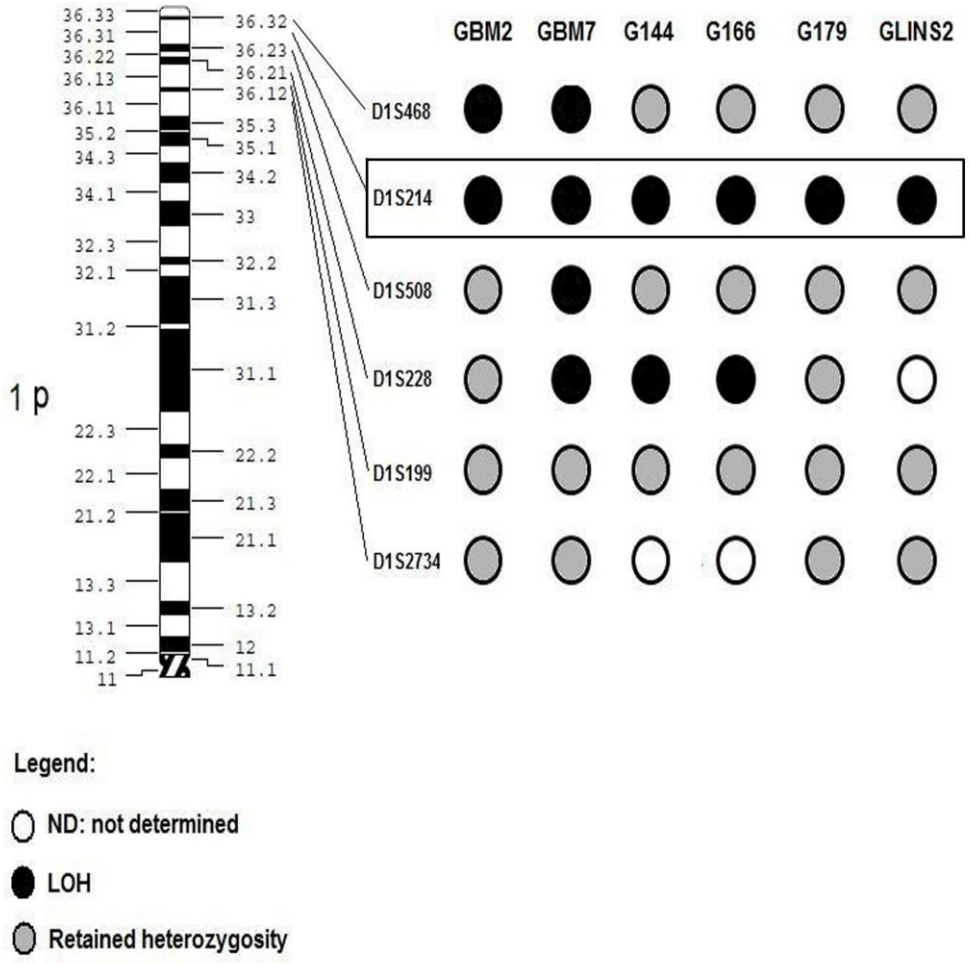

Figure 13. Detailed 1p LOH mapping of GSC lines. The square box highlights a common region of LOH in all the GSC lines, involving D1S214 microsatellite in 1p36.31.

CELL VIABILITY

The effect of VPA and PTX, either alone or in combination, on the cellular proliferation of GSC lines, was determined by means of MTT assays. Dose-response curves of each specific single treatment are shown in Figure 14 and individual p-value, obtained by t-test on raw data, are reported in Table A3. The proliferation rate of GSCs treated with the drugs at increasing concentration was compared to untreated cells at different time points (24, 48 and 72hs). The growth inhibitory effect of both drugs varied between cell lines. VPA treatment inhibited cell growth in a dose- and time-dependent manner in all the GSC lines. G179 and GBM2 were the most sensitive cell lines to treatment, showing a decrease in cell viability, at the highest dose of VPA and for 72h treatment, above 30% and 20% of control untreated cells, respectively. PTX treatment was less effective than VPA, anyway, a statistical significant decrease in cell viability was noticed at highest doses and for long incubation time (72hs) in all the cell lines. GBM7, G144, G166, G179 and GliNS2 cell lines were relatively resistant to PTX treatment and, even at the highest concentration (50μM) and for a long time of exposure (72hs), growth inhibition was observed in only 15%, 20%, 35%, 32% and 30% of the cells, respectively. GBM2 cell line again exhibited the largest growth inhibitory effect to drug treatment: PTX 50μM for 72hs induced a significant decrease in cell viability of approximately 70%. Next, the effect of the combined treatment of VPA plus PTX on the growth of GSC lines was examined. GSCs were treated with VPA 24hs before PTX administration; subsequently VPA and PTX in combination were incubated for further 48hs and then cell viability of GSCs was measured by MTT assay. The rationale for the time-scheduled administration of VPA prior to PTX was related to induction of cellular differentiation (using VPA) and then the inhibition of cell proliferation, through arrest of cell cycle and induction of apoptosis by PTX administration. The experiments were performed using a variety of doses of VPA and PTX in order to identify the best combinatorial treatment. Pretreatment of the cells with different concentrations of VPA significantly increased PTX effect. Anyway, all the GSC lines used in this study differed by their sensitivity to the combinatorial treatment. All the results are displayed in Figure 15.

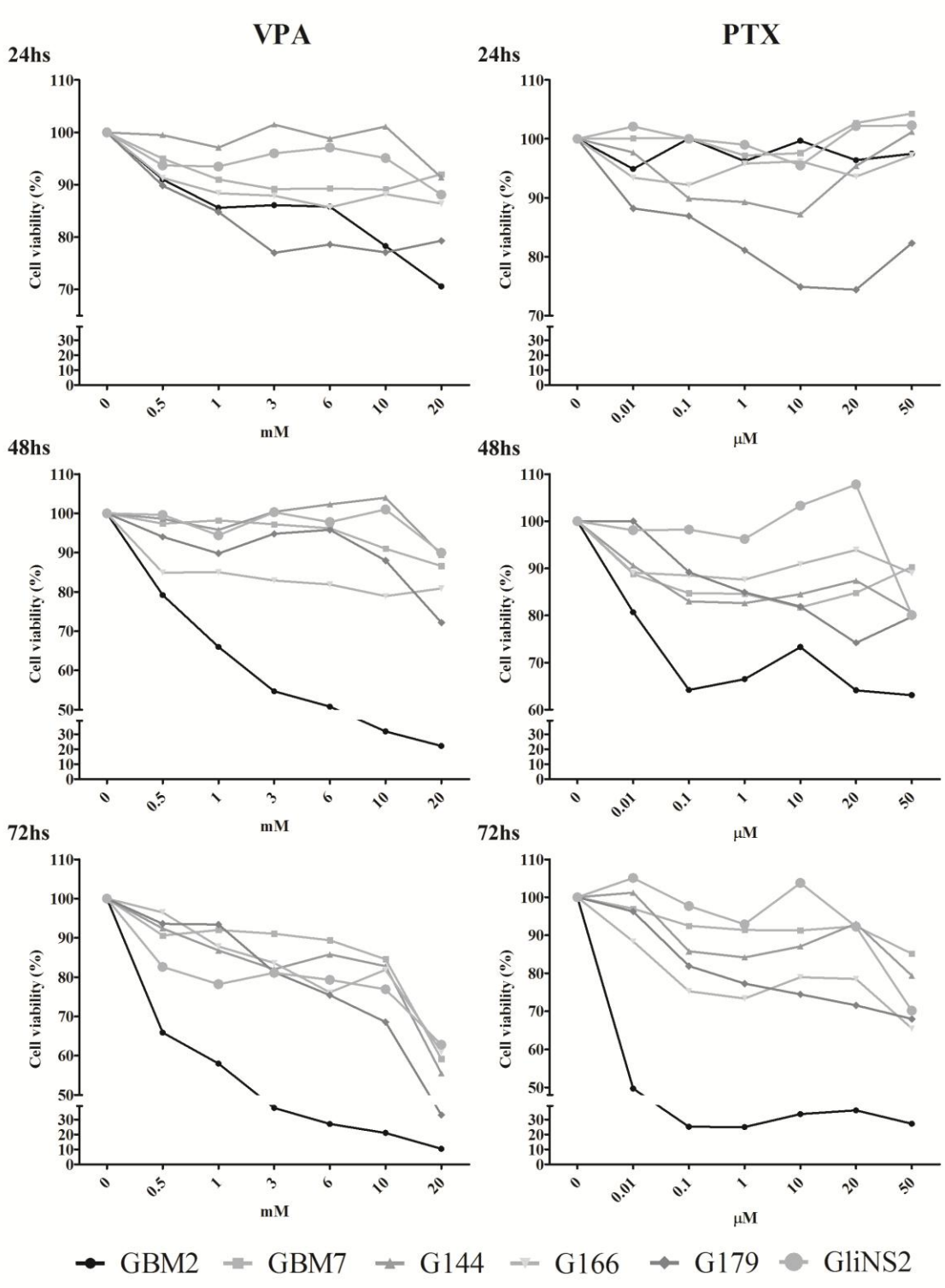

Figure 14. Cell viability assays on GSC lines using VPA and PTX. Cells were treated with different concentrations of the two drugs independently for 24, 48 and 72hs. Cell viability was measured as percentage of cell survival in drug-treated cells relative to untreated cells. Results are reported as means from two different experiments performed at least in triplicate. Standard error of the mean (SEM) was constantly lower than 5% of each mean value. Please note that the scale used in the charts may change.

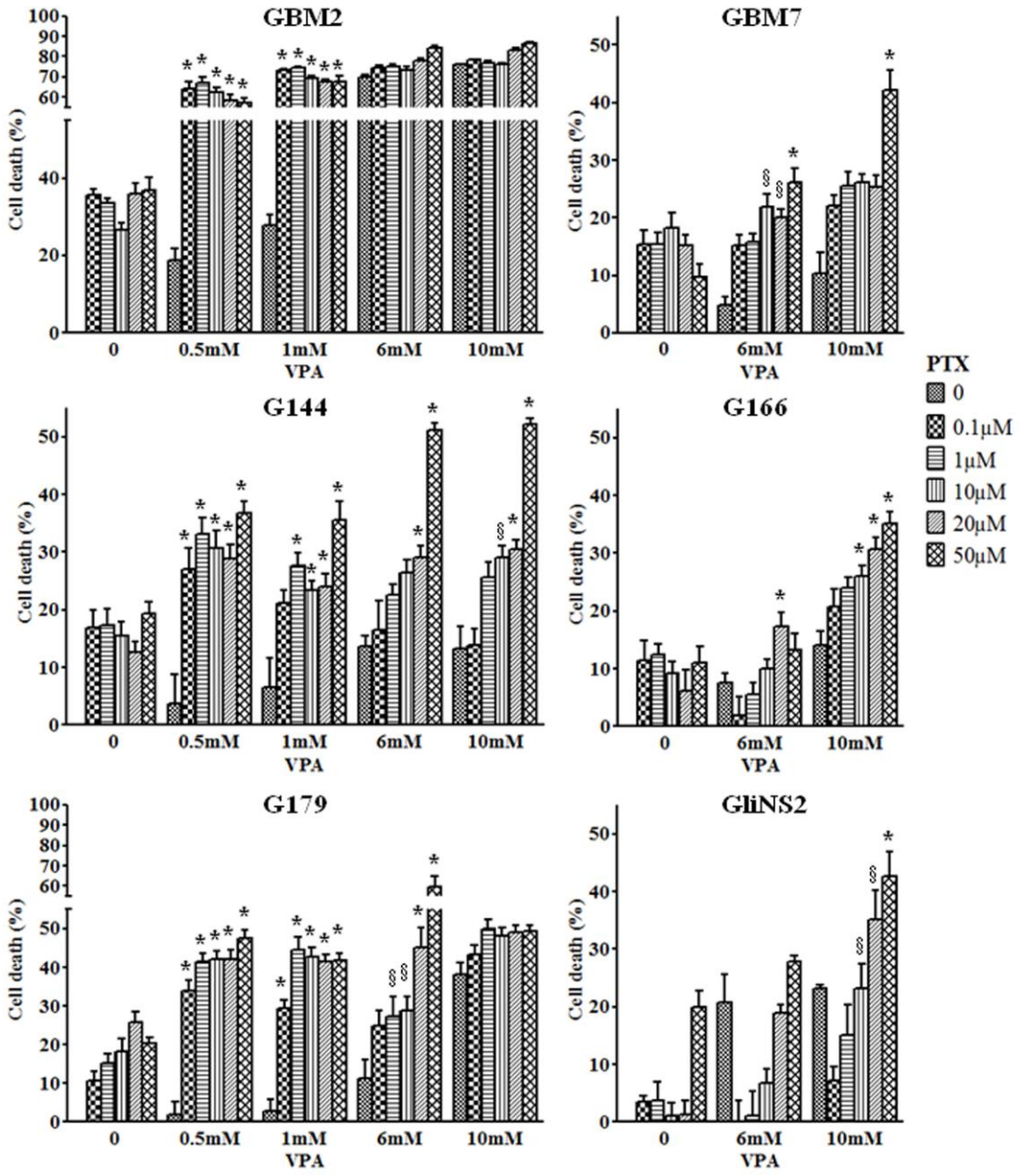

Figure 15. Combinatorial effect of VPA and PTX *in vitro*. The charts show the sensitizing effect of VPA to PTX in GSC lines. Cells were incubated for 24hs with VPA, before the addiction of PTX at different doses. After further 48hs, cell viability was determined by MTT assay. Cell viability was expressed as the ratio between treated cells and untreated controls. The results are reported as means ±SEM of two different experiments, performed at least in triplicate. *CI<1, synergistic effect; §CI=1, additive effect.

The effect of the combined treatment was evaluated through the cooperative index (CI) analysis (Aouali et al., 2009); CI values display the effectiveness of combined treatment, when CI<1 indicates synergistic effect and >1 indicates antagonistic effect. When CI is 1, the effect is

additive. CI values are reported in Table A4. Specifically, GBM7, G166 and GliNS2 cell lines were less sensitive to the combined treatment. Indeed, an additive, or slight synergistic effect was noticed only at the highest concentrations of both drugs (6-10mM VPA and 10-50µM PTX). On the contrary, GBM2, G144 and G179 cell lines showed a different pattern of growth inhibition after the coupled administration. Specifically, only G144 cell line displayed a significant increase in cell death at the highest doses of VPA and PTX. Moreover, the effect of the dual treatment was significant at 6mM VPA for G179 and 1mM VPA for GBM2 cell line. Generally, a marked synergistic effect of VPA and PTX was noticed at lower VPA concentrations (1 and 0.5mM), even ten times lower than the highest VPA dose used or less. For example, GBM2 cell line reached the 70% of reduction of cell viability, also at the lowest doses of VPA and PTX (0.5mM VPA and 0.1µM PTX). This effect was reached only by 6mM VPA alone, whereas PTX treatment, also at high doses, was unable to induce such an effect.

To determine the real effectiveness of the time-scheduled treatment (VPA administration 24h before PTX treatment), cell viability was evaluated also with the opposite treatment: PTX 1µM was administered to GBM2 and G144 cell lines 24hs before VPA treatment. The CI analysis revealed no additive or synergistic effect (data not shown, the CI values are reported in Table A4), suggesting that the efficacy of the dual treatment with VPA and PTX is time-dependent but also dependent on the specific biological effect of each drug.

CYTOMORPHOLOGICAL ANALYSIS

Cytomorphological analysis was performed to obtain some information about VPA and PTX effects on some cellular parameters, such as mitotic index, chromosome number or the percentage of polymorphic nuclei. In each experiment cell were treated with 2mM VPA or 10µM PTX for 24 and 48hs. These parameters were compared to those of untreated control cells. Unfortunately, after some treatment the metaphase chromosome spreads were absent or characterized by low quality, preventing the analysis (these results are marked as N.D., not determined). The results are displayed as means of two independent experiments.

MITOTIC INDEX

Mitotic index (MI) analysis was performed by counting the number of metaphases per 1000 nuclei. The MI was assessed on untreated and 2mM VPA or 10µM PTX treated cells for 24 and 48hs. Results were expressed as percentages and are displayed in Figure 16.

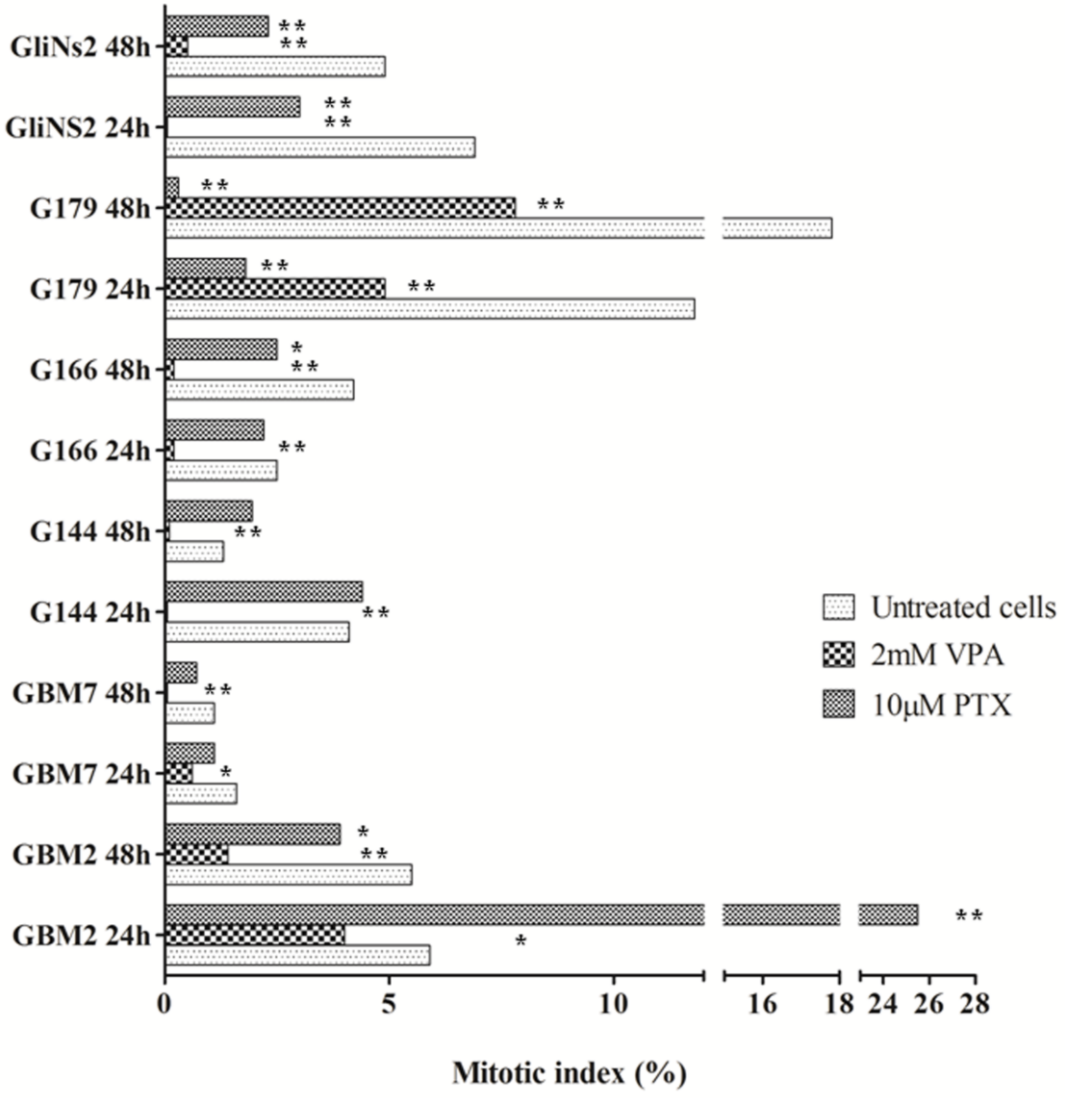

Figure 16. VPA and PTX effects on mitotic index of GSC lines. Cells were treated with 2mM VPA or 10µM PTX for 24 and 48hs. Results are reported as means of two independent experiments and are displayed as percentages. Chi-square test on raw data: *p<0.05; **p<0.0001.

Statistically significant differences were evaluated by chi-square test on raw data. VPA administration showed a decrease of MI in all the cell lines analyzed, both at 24 and 48hs of

treatment. PTX treatment showed differences in MI changes among the cell lines. GBM7 and G144 cell lines were insensitive to PTX treatment also at 48hs of exposure. PTX administration on G166, G179 and GliNS2 cell lines displayed a time-dependent decrease of MI compared to untreated control cells. GBM2 cell line showed a peculiar response of MI to PTX treatment. 24hs administration induced a considerable accumulation of metaphases in chromosome preparations. Moreover, this trend reversed after 48hs, indeed MI was statistically significant decreased, compared to untreated con cells.

PLOIDY

Ploidy was evaluated through the count of the number of chromosomes in at least 50 metaphases from each treatment. Several classes of ploidy were identified (listed in Table 4) and results were grouped according to this classification. Fisher's exact test was performed on raw data in order to identify any variation in ploidy after drug treatment. GBM2 was the most sensitive cell line to drug treatment, also referring to this parameter. Hyper- and hypo-triploid class had the highest frequency of metaphases, 71.9% and 18.6% respectively. The treatment with 2mM VPA for 24hs led to an increase of metaphases with a smaller number of chromosomes (near-haploid, hypo-diploid and hyper-diploid classes), with a concomitant reduction of hyper-triploid and hyper-tetraploid metaphases. 48hs administration resulted in a further increase of hyper-diploid metaphases and a sustained percentage decrease of hypo-tetraploid class. 48hs VPA treatment induced an overall decrease in chromosome number/metaphase and in the spreading of ploidy. In the same cell line, PTX administration for 24 and 48hs lead to a statistically significant reduction of hyper-triploid metaphases. Anyway, 48h PTX treatment, caused the appearance of a small number (1%) of hyper-tetraploid metaphases, but this result was not statistically significant. Also GBM7 cell line showed an

Table 4. Evaluation of ploidy after 2mM VPA or 10μM PTX treatment for 24 and 48hs.

		Class of ploidy (number of chromosomes/metaphase)										
Cell line	**Treatment**	**Near-haploid (≤34)**	**Hypo-diploid (35-46)**	**Hyper-diploid (47-57)**	**Hypo-triploid (58-69)**	**Hyper-triploid (70-80)**	**Hypo-tetraploid (81-92)**	**Hyper-tetraploid (93-103)**	**Near-pentaploid (104-126)**	**Near-hexaploid (127-149)**	**Near-eptaploid (≥150)**	**(overall) Fisher's exact test**
GBM2	**Untreated**	0.0	1.5	1.0	18.6	71.9	7.0	0.0	0.0	0.0	0.0	
	VPA 24hs	14.0***	8.0*	6.0*	13.0	58.0*	1.0*	0.0	0.0	0.0	0.0	***
	PTX 24hs	1.0	4.0	10.0**	23.0	61.0	1.0*	0.0	0.0	0.0	0.0	***
	VPA 48hs	2.1	5.2	4.2	22.9	57.3*	8.3	0.0	0.0	0.0	0.0	*
	PTX 48hs	3.4	2.2	5.6	24.7	57.3*	5.6	1.1	0.0	0.0	0.0	*
GBM7	**Untreated**	12.2	15.4	14.1	12.2	8.3	27.6	10.3	0.0	0.0	0.0	
	VPA 24hs	23.8*	22.5	12.5	10.0	8.8	17.5	5.0	0.0	0.0	0.0	
	PTX 24hs	N.D.	N.D.	N.D.	N.D.	N.D.	N.D.	N.D.	N.D.	N.D.	N.D.	
	VPA 48hs	16.0	9.9	12.3	12.3	3.7	32.1	13.6	0.0	0.0	0.0	
	PTX 48hs	N.D.	N.D.	N.D.	N.D.	N.D.	N.D.	N.D.	N.D.	N.D.	N.D.	
G144	**Untreated**	2.3	2.3	0.6	2.3	14.6	58.5	19.3	0.0	0.0	0.0	
	VPA 24hs	N.D.	N.D.	N.D.	N.D.	N.D.	N.D.	N.D.	N.D.	N.D.	N.D.	
	PTX 24hs	N.D.	N.D.	N.D.	N.D.	N.D.	N.D.	N.D.	N.D.	N.D.	N.D.	
	VPA 48hs	1.6	0.0	0.0	1.6	9.5	79.4*	7.9	0.0	0.0	0.0	
	PTX 48hs	3.1	1.0	1.0	1.0	5.2*	64.9	23.7	0.0	0.0	0.0	
G166	**Untreated**	1.1	1.7	1.1	2.2	3.4	11.8	60.1	16.3	1.1	1.1	
	VPA 24hs	6.0	9.0*	3.0	1.5	10.4	11.9	34.3**	7.5	3.0	13.4**	***
	PTX 24hs	N.D.	N.D.	N.D.	N.D.	N.D.	N.D.	N.D.	N.D.	N.D.	N.D.	
	VPA 48hs	1.0	0.0	1.0	0.0	2.0	16.0	52.0	23.0	1.0	4.0	
	PTX 48hs	0.0	0.0	4.7	1.2	3.5	8.2	58.8	23.5	0.0	0.0	
G179	**Untreated**	0.0	5.6	10.7	18.8	12.7	10.2	10.7	21.8	9.1	0.5	
	VPA 24hs	0.0	2.0	7.0	18.0	12.0	9.0	4.0	28.0	20.0*	0.0	
	PTX 24hs	1.0	12.0	17.0	12.0	15.0	8.0	5.0	24.0	6.0	0.0	
	VPA 48hs	N.D.	N.D.	N.D.	N.D.	N.D.	N.D.	N.D.	N.D.	N.D.	N.D.	
	PTX 48hs	N.D.	N.D.	N.D.	N.D.	N.D.	N.D.	N.D.	N.D.	N.D.	N.D.	
GliNS2	**Untreated**	1.2	73.5	22.9	0.0	0.6	0.6	1.2	0.0	0.0	0.0	
	VPA 24hs	2.3	88.6*	9.1*	0.0	0.0	0.0	0.0	0.0	0.0	0.0	**
	PTX 24hs	16.0**	56.0*	28.0	0.0	0.0	0.0	0.0	0.0	0.0	0.0	**
	VPA 48hs	8.3*	78.6	8.3*	0.0	0.0	4.8	0.0	0.0	0.0	0.0	**
	PTX 48hs	3.2	62.8	22.3	1.1	3.2	7.4*	0.0	0.0	0.0	0.0	*

Fisher's exact test (treated vs. untreated control cultures): *p<0.05; **p<0.001; ***p<0.0001. N.D., not determined

increased percentage of near-haploid metaphases after 24h VPA treatment, but this chance didn't affect the overall pattern. GliNS2 cell line was sensitive to both treatments. Specifically, this cell line was characterized by the prevalence of hypo-diploid and hyper-diploid metaphases (75.5% and 22.9%, respectively). VPA administration for 24 and 48hs led to a sequential decrease in chromosome number, through the increase of hypo-diploid metaphases after 24 hours and then, an increment of near-haploid metaphases, after 48h treatment. PTX administration induced a decrease of hyper-diploid metaphases and consequently an increase of metaphases with fewer chromosomes (near-haploid class). Anyway, there was also the onset of ploidy classes with a higher number of chromosomes, such as hypo-tetraploid class: the number of chromosomes was doubled compared to the modal number. G166 cell lines seemed to be affected by VPA treatment only after 24 hours. In particular, there was a decrease of the hyper-tetraploid class, with a consequent spreading of this difference in the other classes. G144 showed only some limited difference that didn't significantly affect the overall distribution of chromosome number among the ploidy classes.

POLYMORPHIC NUCLEI

The observation of chromosome preparations evidenced the presence of atypical nuclei, which are a hallmark of cancer and are peculiar features of malignant cells, in all the GSC lines analyzed. The nucleus shapes were irregular and various, donut-shaped, ring-shaped, polylobate nuclei and nuclei with multiple blebs are only some examples (Figure 17). A total of 1000 nuclei were counted in each sample, distinguishing between normally shaped nuclei and abnormal ones. The results are displayed in Table 5. Chi-square test was assessed to identify any statistically significant difference between untreated and drug treated cells. Two main groups were observed: the first group was composed by GBM7, G144, G166 and G179 cell lines. Indeed, these cell lines showed a high percentage of polymorphic nuclei in untreated cells (80-90%). In these cases a change in the percentage of aberrant nuclei after drug treatment might not be appreciated. GBM2 and GliNS2 cell lines had a low percentage of polymorphic nuclei in untreated cells, approximately 15% and 10%, respectively.

Table 5. Percentages of polymorphic nuclei in untreated, VPA and PTX treated cells

		Polymorphic nuclei (%)		
Cell line	**Time\Treatment**	**Untreated**	**2mM VPA**	**10μM PTX**
GBM2	24hs	19.3	23.4*	67.0***
	48hs	12.4	16.4**	83.8***
GBM7	24hs	81.2	85.8	86.4
	48hs	90.1	91.7	87.1
G144	24hs	96.3	97.7	95.5
	48hs	96.1	96.8	91.5
G166	24hs	97.0	93.0	96.0
	48hs	93.6	94.9	97.0
G179	24hs	91.6	91.9	90.4
	48hs	82.8	82.2	81.2
GliNS2	24hs	11.8	14.3	19.0***
	48hs	10.6	18.1***	31.3***

Chi-square test, treated vs. untreated cells: *p<0.05; **p<0.001; ***p<0.0001

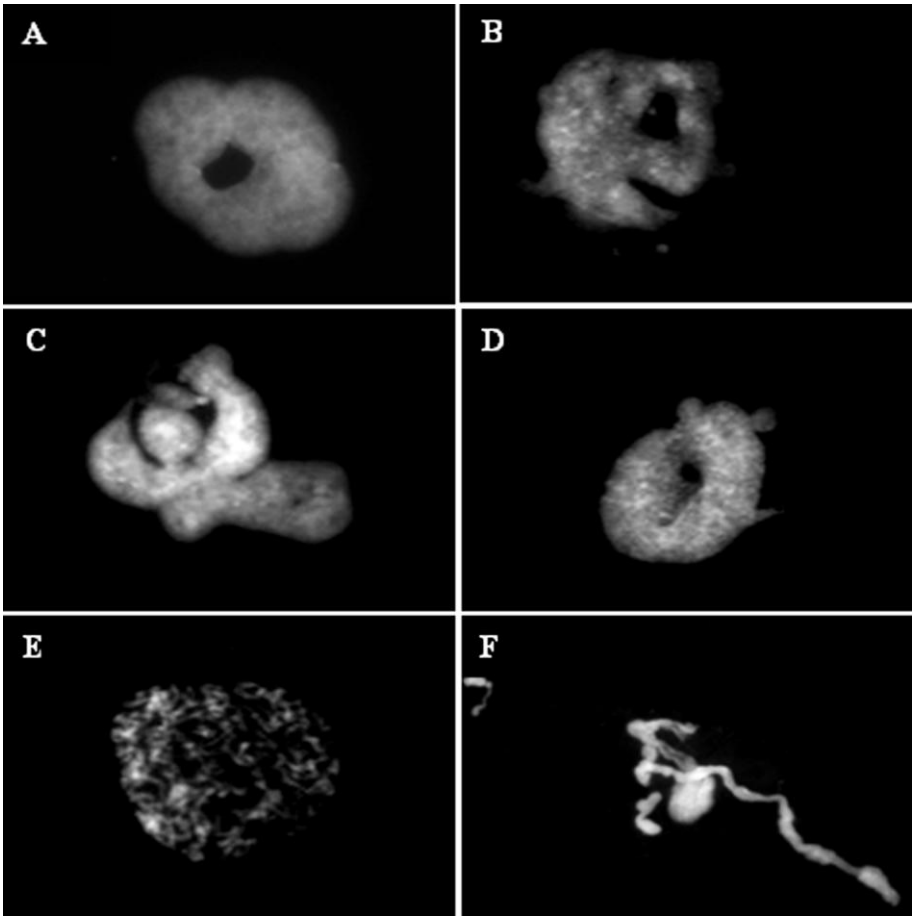

Figure 17. Examples of aberrant nuclei identified in chromosomes preparations, both in untreated and drug treated cells. The presence of donut-shaped, ring-shaped (A, D), polylobate nuclei (B, C) and nuclei with multiple blebs (D) was noticed. PTX treatment also induced the presence of de-condensed chromosomes, arranged in nuclei-like structures (E) and chromatin treads (F).

Both VPA and PTX induced an increase in polymorphic nuclei at 24 and 48 hours of treatment, compared to corresponding untreated control cells. The increment after PTX administration was higher than VPA administration and it was time-dependent. After PTX treatment, the presence of defective mitotic figures, such as uncondensed chromatin treads, chromosome fragmentation and de-condensed chromosomes, arranged in nuclei-like structures was noticed (Figure 17).

DIFFERENTIATION-INDUCING ABILITY OF VPA

The pro-differentiation effect of VPA was investigated through two main experiments. Firstly, the morphological changes were evaluated and subsequently the expression of stemness and differentiation markers was investigated by means of immunofluorescence analysis.

EFFECT OF VPA ON MORPHOLOGY

GSC lines were treated with 1-2-6 and 10mM VPA for 24, 48 and 72hs of exposure. Matching untreated control cultures were also assessed. Moreover, GSCs were cultured in a pro-differentiation medium, composed of RPMI+10% FCS, for 14 and 30 days, as a positive control of cellular differentiation. At each time point, cell morphology was evaluated through phase contrast microscopy and representative images were taken (Figure 18 and Figure A1). GSCs cultured under neural stem cell conditions, in serum-free medium, supplemented with EGF and bFGF, grew in non-adherent growth pattern as neurosphere, forming colonies varying in size. Medium implemented with FCS induced GSCs to grow as a monolayer and cells showed flat morphology, with elaborated processes and spindle-like structures. VPA treatment determined dramatic morphological changes in all the GSC lines, compared to untreated cells. Cells modified their morphology from rolling spheres to adherent cells. Most of the cells were star-shaped with cellular processes similar to neurite-like structures, indicating a sort of differentiation process. These changes were evident at lower concentration (2-3mM), whereas higher concentrations determined an inhibition of sphere growth and induction of cell death.

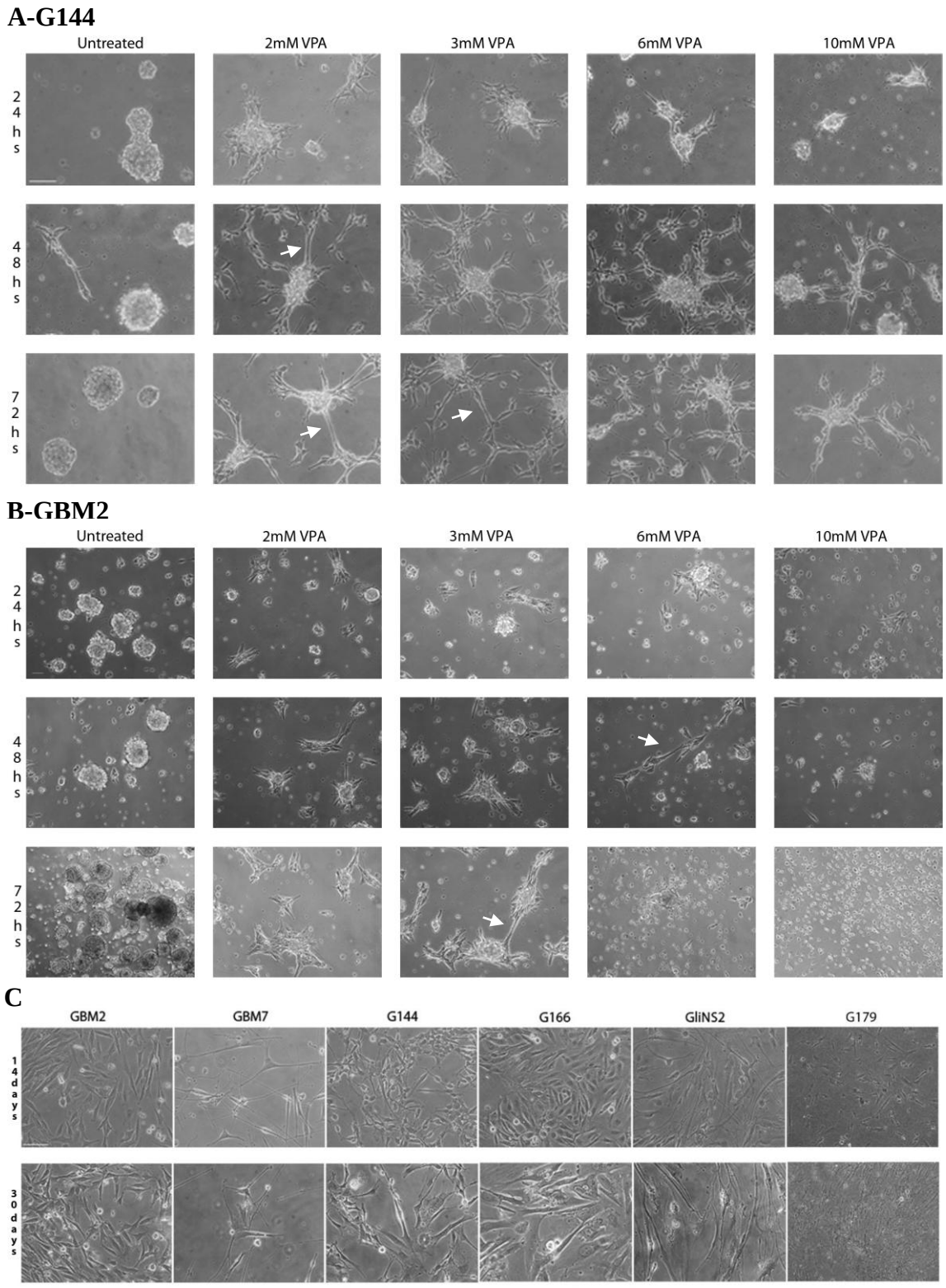

Figure 18. VPA induced differentiation in GSCs. Representative images taken by phase contrast microscopy of G144 (A) and GBM2 (B) cell lines treated with different doses of VPA for 24, 48 and 72hs. Drug treatment promoted growth of neurite-like projections (arrows) in GSCs. Higher doses of VPA for long time of exposure resulted in cell death and apoptosis (B). (C) Differentiation of GSCs in RPMI+10% FCS for 14 and 30 days. Scale bar = 100µM.

These analyses allowed the identification of 2mM VPA as the best dose, as it was able to induce morphological changes indicating differentiation ability and moreover, it is also a low dose, which would be better for a potential clinical use, due to good tolerability and poor side effects. Thus, 2mM VPA was the concentration used for further experiments.

IMMUNOFLUORESCENCE

The differentiation-inducing ability of VPA was evaluated through the expression analysis of stemness markers (CD133 and Nestin) and differentiation markers (GFAP, βIII tubulin and MBP) on untreated cells and 2mM VPA treated cells for 72hs. A positive control of differentiation was composed by cells cultured in RPMI+10% FCS for 14 and 30 days. In order to perform a semi-quantitative analysis for the expression of all markers, the number of immunoreactive cells was counted, evaluating at list 100 cells per sample and evaluating different areas of the slide. Staining intensity was scored in 5 categories: negative (-; 0-20% of immunoreactive cells); marginal (±; 21-40%); low (+; 41-60%); medium (++; 61-80%); and high (+++; 81-100%) (Li et al., 2005). Any statistical significant difference between treated and untreated cells was evaluated through Fisher's exact test on raw data. The summary of immunofluorescence experiments is reported in Table 6 and representative images are displayed in Figure 19. The overview of data showed that GSCs expressed both stemness and differentiation markers at variable proportions. Generally, Nestin was expressed at medium or high intensity in all untreated cell lines (range: 63.1-99.2%). CD133 immunoreactive cells were found as a high proportion of untreated GSCs in 5/6 cell lines (62.7-100%). Only G166 cell line showed almost a negative expression for this marker (7.3% of $CD133^+$ immunoreactive cells). Untreated cells were also positive for differentiation markers, although at very different levels among the various GSC lines. Thus, an aberrant co-expression of differentiation markers with stem/progenitor markers was not rare. This phenomenon is not surprising as tumor sphere populations are heterogeneous and committed progenitor cells can form neurospheres. GSC cultures recapitulate *in vitro* the hierarchical organization of tumor cells, being composed by promiscuously double-labeled cells, with both undifferentiated and differentiated markers

(Singh et al., 2004). VPA treatment caused a change in the percentage of cells positive for at least one stemness marker in 4/6 lines. GBM2 and G166 cell lines showed a decrease in Nestin immunoreactive cells from 75.4% to 53.8% and from 78.3% to 53.7%, respectively. Both cell lines displayed also a decrease in CD133 positive cells, but this variation was not statistically significant. VPA treatment on GliNS2 line induced a reduction of CD133 expression of approximately a half, form 100% to 55.5%. In G179 cell line, Nestin expression was relatively preserved after drug incubation, whereas a little decrease (but not statistically significant) in CD133 expression was observed. Surprisingly, GBM7 cell line showed an increased expression of Nestin after VPA treatment. The retained or increased expression of stemness markers might be interpreted as the ability of GSCs to resist differentiation (Günther et al., 2008). After VPA administration, 3 cell lines (GBM2, GBM7 and G166) exhibited a progressive enrichment of cells expressing βIII tubulin, indicating the capability of these cells to induce neuronal differentiation, upon VPA administration. In addition, GBM7 cell line showed an increased expression of GFAP positive cells. On the contrary, G144 cell line manifested a reduction of βIII tubulin-positive cells. The other cell lines didn't show any variation in differentiation marker expression, maybe due to the high expression rate, which was observed also in untreated cells. Induction of differentiation in RPMI+10% FCS showed a general retention of NSC markers and increased percentage of cells positive for both glial and neuronal markers. Unfortunately, MBP immunostaining was not informative in this type of analysis, as its expression remained at constant proportion between treatments. The presence of cells, co-stained for both glial and neuronal markers, suggests that differentiation pathways in GSCs are not entirely normal (Galli et al., 2004; Lee et al., 2006a). Moreover, aberrant type of cells may reflect the activation of an abnormal differentiation program in GSCs, as expected from developmentally de-regulated tumor cells (Galli et al., 2004). Thus, even if GSCs retain the ability to differentiate, efficiency and lineage choice differ impressively between cell lines. Another point to mention is marker localization, which may not mirror the normal pattern. CD133 is a surface marker, but it rarely shows a plasma membrane staining pattern, whereas

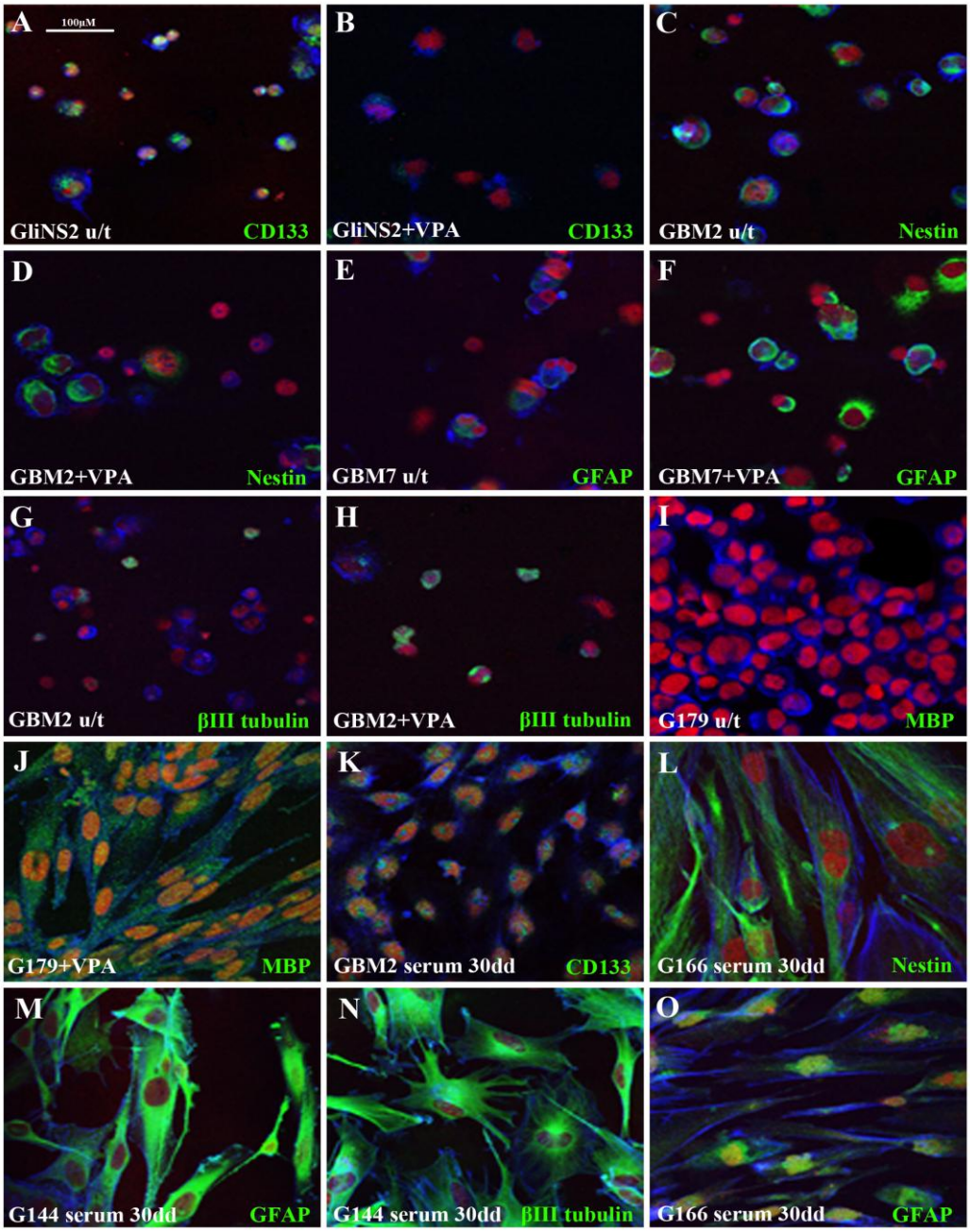

Figure 19. Selected representative images of immunofluorescence on untreated (u/t) GSCs, 2mM VPA treated GSCs (+VPA) for 72hs (spotted on glass slides using cytospin) and on GSCs induced to differentiate in RPMI+10% FCS (serum) for 14 and 30 days (directly grown on covers lips). Each specific maker is in green, phalloidin is in blue and propidium iodide in red. Undifferentiated cultures contained numerous immunoreactive cells for CD133 (A) and Nestin (C). Positive cells decreased after VPA treatment (B and D). Untreated cells may express differentiation markers at variable levels: GFAP (E), βIII tubulin (G) and MBP (I). VPA treatment was able to induce an increase of differentiation markers (F,H and J, respectively). After 30 days of differentiation GSCs may retain the expression of stemness markers CD133 (K) and Nestin (L). Differentiated GSCs contained clearly GFAP and βIII tubulin positive cells (M and N). Peculiar marker immunoreactivity was observed for CD133, which showed dense cytoplasmic staining with a fine granular pattern (i.e. K), and GFAP, which was mainly observed in nuclear/perinuclear pattern in G166 cell line after 30 days of differentiation. Scale bar=100µm.

Table 6. Summary of the analysis of stem and differentiation marker expression in GSC lines. Marker expression was evaluated in untreated and 2mM VPA treated cells for 72hs. Cells cultured in RPMI+10% FCS were considered a positive control of differentiation.

GSC line	Treatment	CD133		Nestin		βIII tubulin		GFAP		MBP	
		%	range	%	range	%	range	%	range	%	range
GBM2	Untreated	62.7	++	75.4	++	19.3	-	63.8	++	100.0	+++
	2mM VPA 72hs	56.5	+	53.8**	+	36.5*	±	64.8	++	95.0	+++
	RPMI+10% FCS 14 days	97.1**	+++	100.0**	+++	100.0**	+++	8.3**	-	100.0	+++
	RPMI+10% FCS 30 days	78.4*	++	68.9	++	100.0**	+++	5.9**	-	100.0	+++
GBM7	Untreated	94.4	+++	63.1	++	18.1	-	42.7	+	97.8	+++
	2mM VPA 72hs	100.0	+++	85.0**	+++	31.4*	±	71.8**	++	100.0	+++
	RPMI+10% FCS 14 days	100.0	+++	100**	+++	100.0**	+++	100.0**	+++	100.0	+++
	RPMI+10% FCS 30 days	98.0	+++	100**	+++	100.0**	+++	99.0**	+++	98.3	+++
G144	Untreated	78.4	++	91.4	+++	45.79	+	82.5	+++	100.0	+++
	2mM VPA 72h	67.9	++	87.9	+++	13.8**	-	80.9	+++	96.8	+++
	RPMI+10% FCS 14 days	100.0**	+++	100.0*	+++	0.0**	-	100.0**	+++	100.0	+++
	RPMI+10% FCS 30 days	100.0**	+++	100.0*	+++	100**	+++	100.0**	+++	100.0	+++
G166	Untreated	7.3	-	78.3	++	25.9	±	83.9	+++	100.0	+++
	2mM VPA 72hs	1.9	-	53.7**	+	43.5**	+	81.3	+++	100.0	+++
	RPMI+10% FCS 14 days	100.0**	+++	54.4**	+	100.0**	+++	100.0**	+++	100.0	+++
	RPMI+10% FCS 30 days	98.3**	+++	79.2	++	100.0**	+++	100.0**§	+++	100.0	+++
G179	Untreated	100.0	+++	99.2	+++	100.0	+++	98.2	+++	0.0	-
	2mM VPA 72hs	96.3	+++	100.0	+++	100.0	+++	100.0	+++	0.0	-
	RPMI+10% FCS 14 days	100.0	+++	96.5	+++	98.2	+++	100.0	+++	95.3*	+++
	RPMI+10% FCS 30 days	100.0	+++	94.1	+++	100.0	+++	100.0	+++	100.0*	+++
GliNS2	Untreated	100.0	+++	79.6	+++	71.4	++	93.6	+++	100.0	+++
	2mM VPA 72hs	55.5**	+	88.5	+++	63.0	++	89.3	+++	90.7*	+++
	RPMI+10% FCS 14 days	90.5*	+++	100.0**	+++	100.0**	+++	100.0	+++	100.0	+++
	RPMI+10% FCS 30 days	93.1	+++	97.2**	+++	100.0**	+++	100.0	+++	100.0	+++

*Fisher's exact test: treated vs. untreated cells, *p<0.05; **p<0.001. §Aberrant cellular location of marker.

most of the times CD133 displays a cytoplasmic staining with a fine granular pattern (Figure 19K) (Kim et al., 2011). In addition, after 30 days of culture in differentiation-inducing medium G166 cells showed re-distribution of GFAP staining to a nuclear/peri-nuclear pattern (Figure 19O) (Asklund et al., 2004; Benítez et al., 2008).

METHYLATION PROFILES

Epigenomics is another level of genome regulation and methylation is one key component of this process. To explore genome-wide DNA methylation, MeDIP-Chip (methylated DNA immunoprecipitation and array based hybridization, Chip) technology was employed. The enrichment of methylated DNA through immunoprecipitation is combined with genome-wide analysis using DNA microarray platform from Agilent Technologies (Agilent Human CpG Island Microaray Kit, 1x244K). In order to achieve further insight in the biology of GSCs, we analyzed the methylation profile of 3 GSC lines (GBM2, G144 and G166). As normal tissue controls, two foetal neural stem cell (NSC) lines were analyzed: CB660, derived from foetal human brain and CB660SP, derived from foetal human spinal cord (Sun et al., 2008). Moreover, the DNA from peripheral blood lymphocytes of 6 healthy male donors was pooled (PBL pool) and used as control for a differentiated tissue. In addition, the methylation status was investigated after 2mM VPA administration for 96hs on GBM2 and G144 cell lines, in order to evaluate the DNA methylation changes after the treatment with an epigenetic drug such as VPA, which is an HDACi. These two cell lines were chosen as examples of drug treatment-sensitive cell line (GBM2) and barely sensitive/insensitive cell line (G144) (see cell viability section). GBM2 and G144 cell lines were also treated with 10μM PTX for 96hs, in order to verify the specificity of the changes in the methylation status induced by VPA administration.

DNA METHYLATION PROFILES OF GSCS, FOETAL NSCS AND PBL POOL IN STANDARD CONDITIONS

Firstly, the methylation profiles of 3 GSC lines (GBM2, G144 and G166), two foetal NSC lines (CB660 and CB660SP) and one PBL pool were analyzed. This analysis was performed to

achieve some global information on the methylation status of these cell lines in standard conditions, to obtain a sort of basal-profile. The raw DNA methylation data, derived from each experiment, are summarized in Figure 20, which shows the mean average of Z-score values along chromosomes.

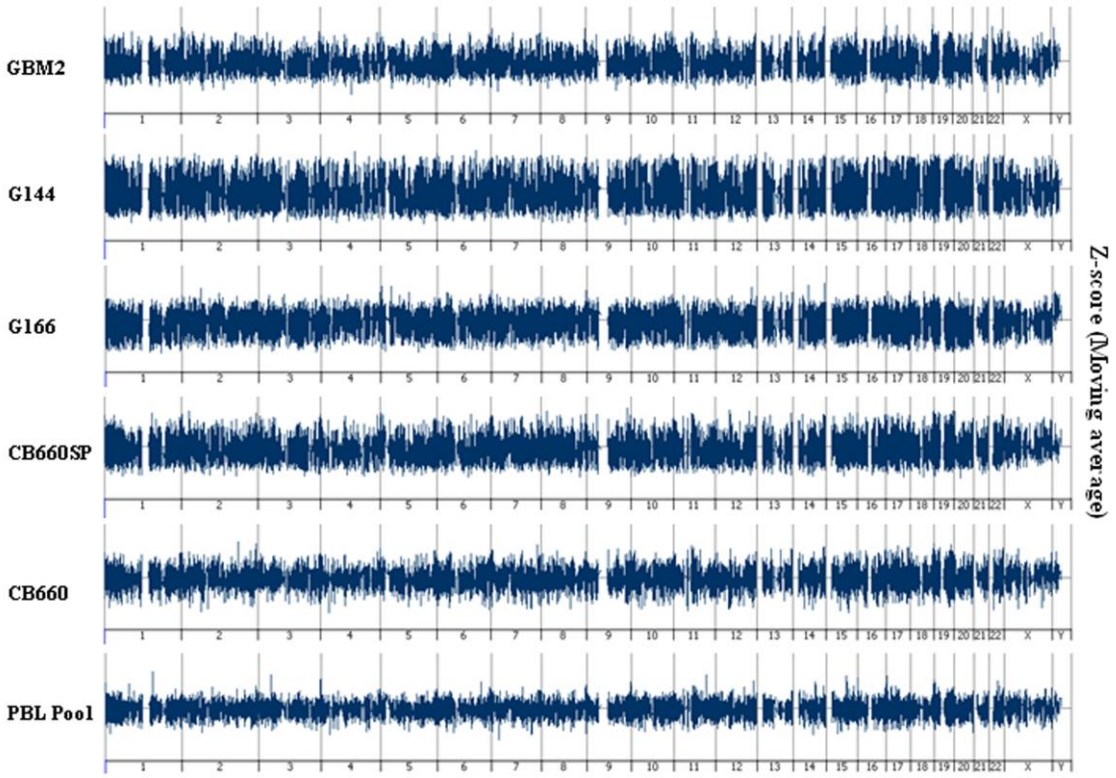

Figure 20. Global DNA methylation profiles along chromosomes, expressed through the mean average of combined Z-score values. The profile of methylated DNA sequences is displayed as the ratio of MeDIP-enriched DNA versus input (total) DNA signal. GBM2, G144 and G166 are GSC lines, CB660SP and CB660 are foetal NSC lines, isolated from human foetal spinal cord and forebrain, respectively; PBL pool is derived from DNA isolated from 6 healthy male donors. Chromosomes are displayed head-to tail, with p-arm at left, q-arm at right. Breaks in combined Z-score profile correspond to heterochromatin specific for secondary constriction regions (qh), which are not covered by probes.

Raw data have been processed as described in the 'Materials and Methods' section. Each CGI (CpG island) was associated to a specific methylation status and undetermined CGIs were excluded from the following analysis. To achieve some global information from each sample, the percentages of methylation and unmethylation for each chromosome were calculated and mean genomic values were determined (Figure 21). The detailed list of percentages is reported

in Table A5.

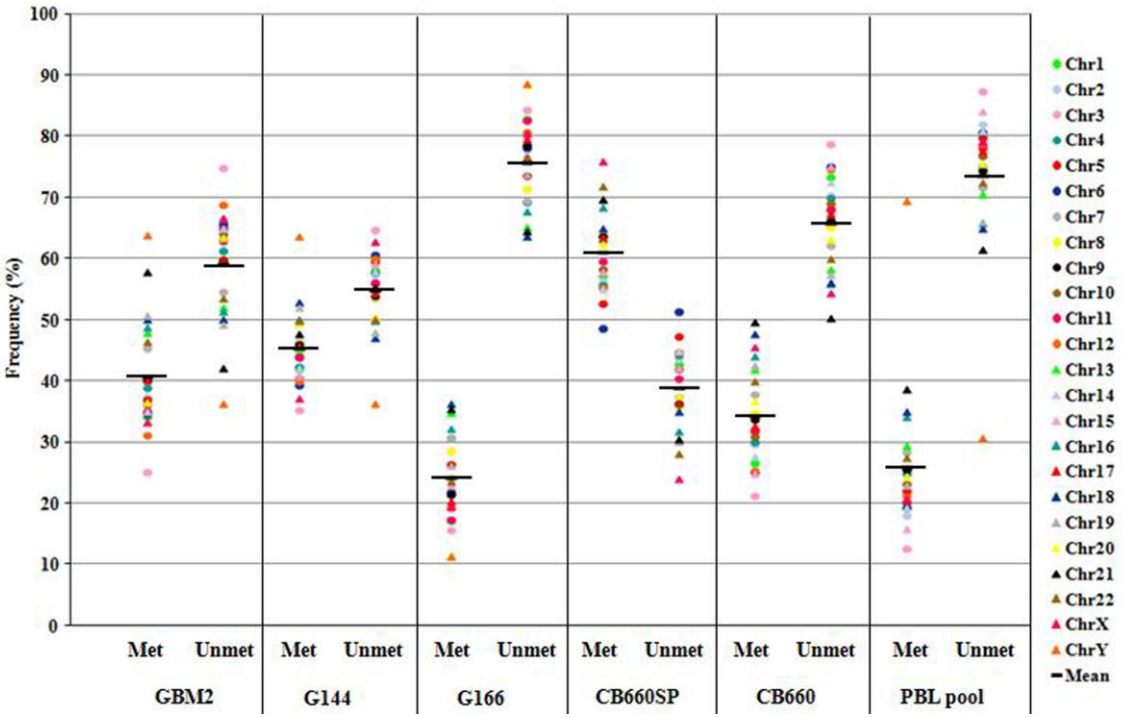

Figure 21. Frequency of methylation and unmethylation of CGIs for each sample. Chromosome-specific methylation status is reported and global genomic methylation scores are displayed as the mean values of all chromosome-specific values. Abbreviation: Met, methylation; Unmet, unmethylation of CGIs.

Firstly, a heterogeneous methylation pattern was observed in GSC lines. Generally tumors are characterized by a global hypomethylation and hypermethylation of specific gene promoters. Hypomethylation was variable, with unmethylation levels ranging from approximately 55% of G144 line to 76% of G166 cell line. Anyway, genome wide hypomethylation was observed in all GSC lines, as the 5-methylcytosine levels were always lower than 50%. Foetal NSCs differed in their methylation pattern. Specifically, CB660 cells were characterized by a global hypomethylation (66% of unmethylated CGIs), whereas CB660SP cells showed a hypermethylation, as 61% of CGI were found methylated. PBL pool displayed 74% of unmethylated and 26% of methylated CGIs. The more elevated 5-methylcytosine level in NSCs versus PBL has already been reported in literature (Cadieux et al., 2006). The comparison of global DNA methylation between GSC and foetal NSC lines showed that all the GSCs are more

similar to CB660 than to CB660SP. Thus, the methylation profile of GSCs resembles to NSCs derived from the forebrain.

In order to deeply investigate the similarities and differences between GSCs and NSCs, the genome-wide approach enabled the identification of specific methylation patterns shared between, or specific for these two groups. Firstly, gene promoters with the same methylation pattern, between all the 3 GSC lines were identified. Specifically, 378 promoters were methylated and 3514 unmethylated. The functional annotation analysis of these genes showed the involvement of genes among several biological processes (Figure 22). *Metabolism* was the most involved category, with a prevalence of unmethylated gene promoters. Cancer cells are characterized by a dramatically altered metabolic patterns and may also exhibit high energetic demand (Hsu and Sabatini, 2008). To this end, the presence of terms associated to biosynthesis of nucleotides, fatty acids and proteins may serve to support the synthesis of macromolecules in cancer cells. Increased level of unmethylation was found also in *transcription & gene expression* category, which could lead to activation of cancer-related genes. *Cell cycle*-related GO terms were enriched in unmethylated gene promoters in GSC lines, showing that cell proliferation is de-regulated in this type of cells, leading to possible increase of cell growth. A prevalence of methylated terms associated to *development & morphogenesis* and *nervous system development & differentiation* was found in GSCs, showing an inhibition of the developmental and differentiation processes, which characterize cancer stem-like cells. Cell death and apoptosis were two categories that showed a balance between methylated and unmethylated gene promoters, thus in these cases, epigenetic changes might act in order to maintain the malignant 'homeostasis' of tumor cells. Four categories were involved only in unmethylated gene promoters: *intracellular transport, DNA repair and chromatin remodeling, immune response* and *response to stress*. These functional annotations may increase the potential malignant phenotype of these cells.

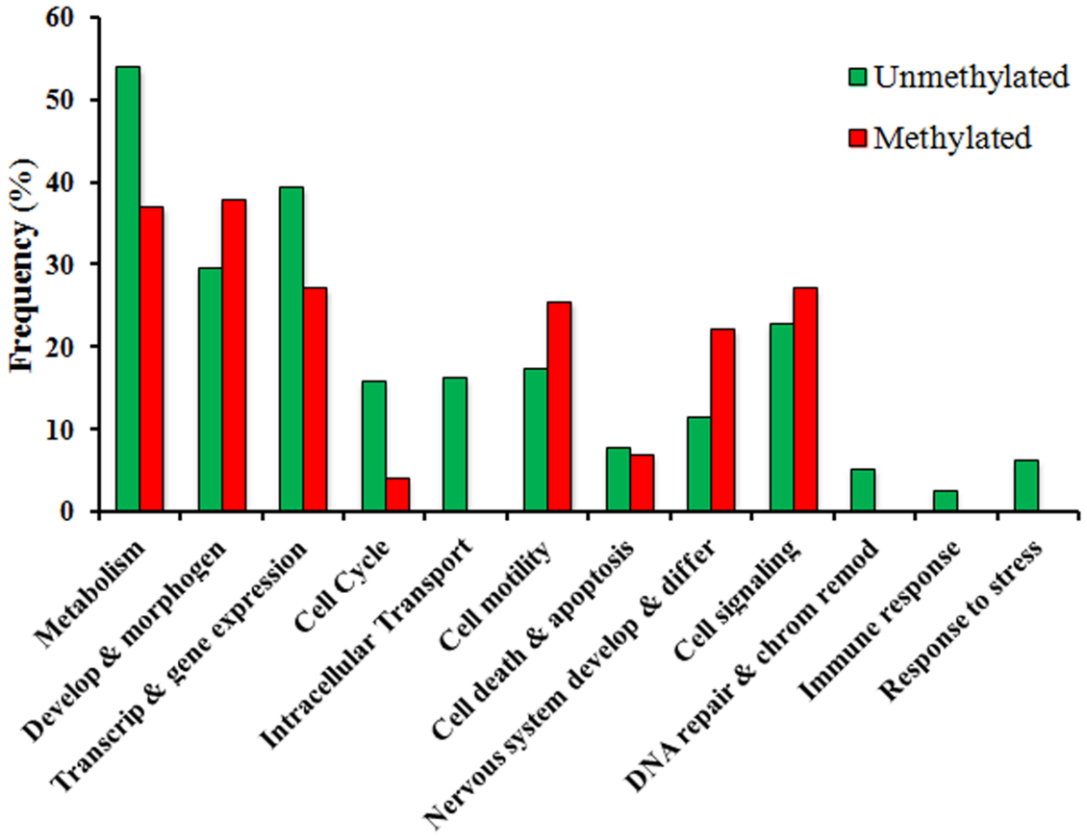

Figure 22. Functional annotation analysis of commonly methylated or unmethylated gene promoters in all the three GSC lines (GBM2, G144 and G166), performed using GOstat software. The y-axis shows the frequency (as a percentage) of each category compared to totally annotated genes.

Moreover, pathway analysis of genes that shared the same methylation profile at promoter regions, in all the GSC lines analyzed revealed the involvement of several cancer-related pathways (Figure 23 and Table A6). Two pathways were found in common with signaling specific for new 'exclusive' CNA regions of GSCs (see Table A2): *regulation of eIF4 and p70S6K signaling* and *ephrin receptor signaling*, indicating that genomic and epigenomic alterations act independently. Other specific pathway affected by methylation in GSCs are involved in *cyclins and cell cycle regulation*, *G1/S checkpoint regulation*, *PI3K/AKT signaling* and other mechanisms associated to several type of cancers.

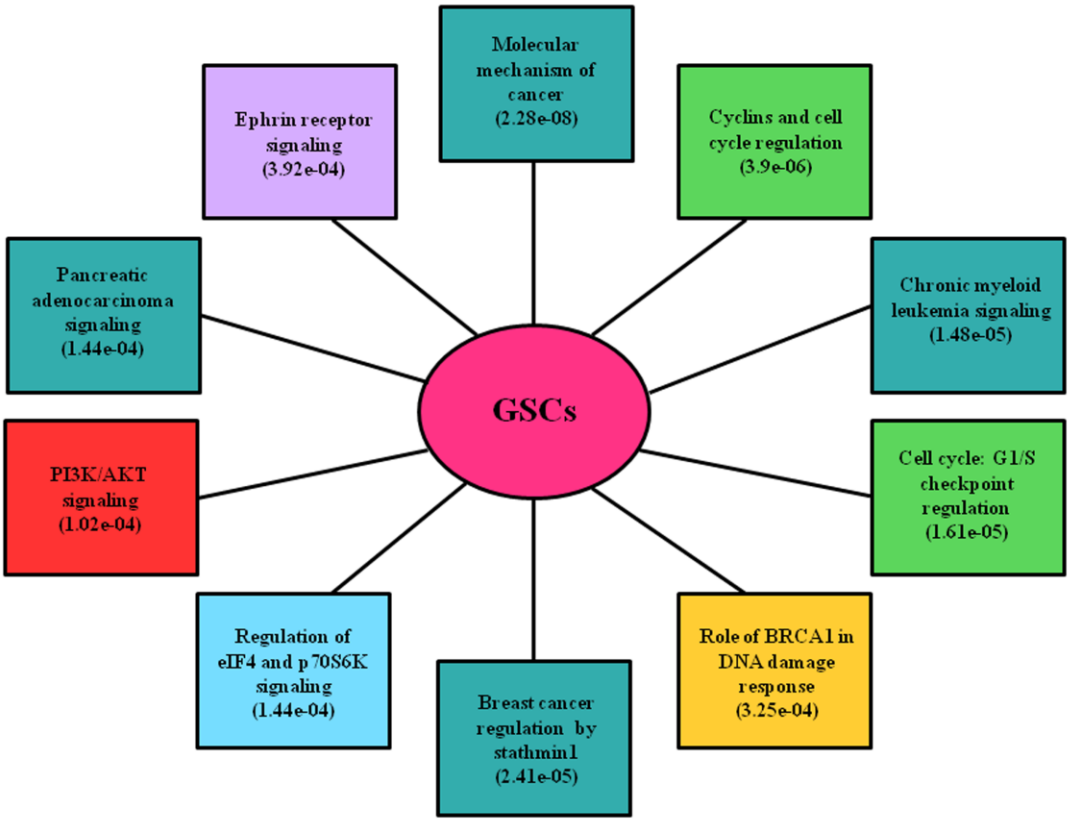

Figure 23. Top 10 pathways influenced by DNA methylation pattern in GSCs. Each pathway is associated with a p-value (calculated by the Ingenuity Pathway Analysis, IPA, software), which indicates the probability that such association could have occurred by chance.

To obtain further insight into the observed methylation pattern of GSCs and NSCs, we performed a comparison between the methylation profiles of these two groups and we classified the methylation of gene promoter regions into two categories: (i) promoters methylated in all the 3 GSC lines and unmethylated in both NSC lines; (ii) genes unmethylated in GSCs and methylated in NSCs. This latter group didn't show any significant functional annotation related to biological processes. 37 gene promoters were identified as specifically methylated in GSCs and unmethylated in NSCs and were referred as 'GSC-specifically methylated genes'. Thus, GSCs displayed aberrant methylation compared to normal foetal NSCs. The list of GSC-specifically methylated genes is reported in Table 7.

Table 7. List of GSC-specifically methylated genes. The significant GO annotations related to the nervous system, development and differentiation are listed.

Gene	Chromosomal location	Name	Significant GO terms related to the nervous system, development and differentiation
*BARHL2**	1p22.2	BarH-like homeobox 2	cell fate determination; nervous system development; neuron differentiation; neuron migration
CACNA1E	1q25-q31	calcium channel, voltage-dependent, R type, alpha 1E subunit	synaptic transmission
*SIX2**	2p21	SIX homeobox 2	anatomical structure morphogenesis, multicellular organism development
TBR1	2q24	T-box, brain, 1	axon guidance; brain development; hindbrain development
ECEL1	2q37.1	endothelin converting enzyme-like 1	neuropeptide signaling pathway
GHSR	3q26.31	growth hormone secretagogue receptor	none
NKX3-2	4p16.3	NK3 homeobox 2	none
*PHOX2B**	4p12	paired-like homeobox 2b	cell development; cell differentiation in hindbrain; glial cell differentiation; multicellular organism development; nervous system development; neuron migration; positive regulation of neuron differentiation
TEC	4p12	tec protein tyrosine kinase	none
*PITX2**	4q25	paired-like homeodomain 2	multicellular organism development
MAB21L2	4q31	mab-21-like 2 (C. elegans)	multicellular organism development nervous system development
*NEUROG1**	5q23-q31	neurogenin 1	cell fate commitment; multicellular organism development; nervous system development; neurogenesis; positive regulation of neuron differentiation
RPL26L1	5q35.1	ribosomal protein L26-like 1	none
*ETV7**	6p21	ets variant 7	none
PTPRK	6q22.2-q22.3	protein tyrosine phosphatase, receptor type, K	none
*TBX18**	6q14-q15	T-box 18	multicellular organism development
*TWIST1**	7p21.2	twist homolog 1 (Drosophila)	anatomical structural development; cell differentiation; multicellular organism development
*HOXA9**	7p15.2	homeobox A9	none
*TBX20**	7p14.3	T-box 20	none
MOGAT3	7q22.1	monoacylglycerol O-acyltransferase 3	none
MIR183	7q32.2	microRNA 183	None
NEFL	8p21	neurofilament, light polypeptide	anterograde axon cargo transport; axon transport of mitochondrion; intermediate filament organization neurofilament bundle assembly; neurofilament bundle assembly; retrograde axon cargo transport; synaptic transmission

Table 7. (Cont'd)

Gene	Chromosomal location	Name	Significant GO terms related to the nervous system, development and differentiation
PRDM14	8q13.3	PR domain containing 14	cell fate specification; cell morphogenesis
*DMRT2**	9p24.3	doublesex and mab-3 related transcription factor 2	none
*DMRT3**	9p24.3	doublesex and mab-3 related transcription factor 3	cell differentiation; multicellular organism development
*FOXE1**	9q22	forkhead box E1 (thyroid transcription factor 2)	none
*HMX2**	10q26.13	H6 family homeobox 2	none
SYT10	12p11.1	synaptotagmin X	none
*GSC**	14q32.1	goosecoid homeobox	multicellular organism development
ALDH1A2	15q21.3	aldehyde dehydrogenase 1 family, member A2	none
*ISL2**	15q23	ISL LIM homeobox 2	multicellular organism development
STAC2	17q12	SH3 and cysteine rich domain 2	none
DSC3	18q12.1	desmocollin 3	none
SALL3	18q23	sal-like 3 (Drosophila)	none
NKPD1	19q13.32	NTPase, KAP family P-loop domain containing 1	none
*SIM2**	21q22.13	single-minded homolog 2 (Drosophila)	cell differentiation; embryonic pattern specification; multicellular organism development
ESX1	Xq22.1	ESX homeobox 1	none

*genes targeted by Suz12 in ES cells (Lee et al., 2006b).

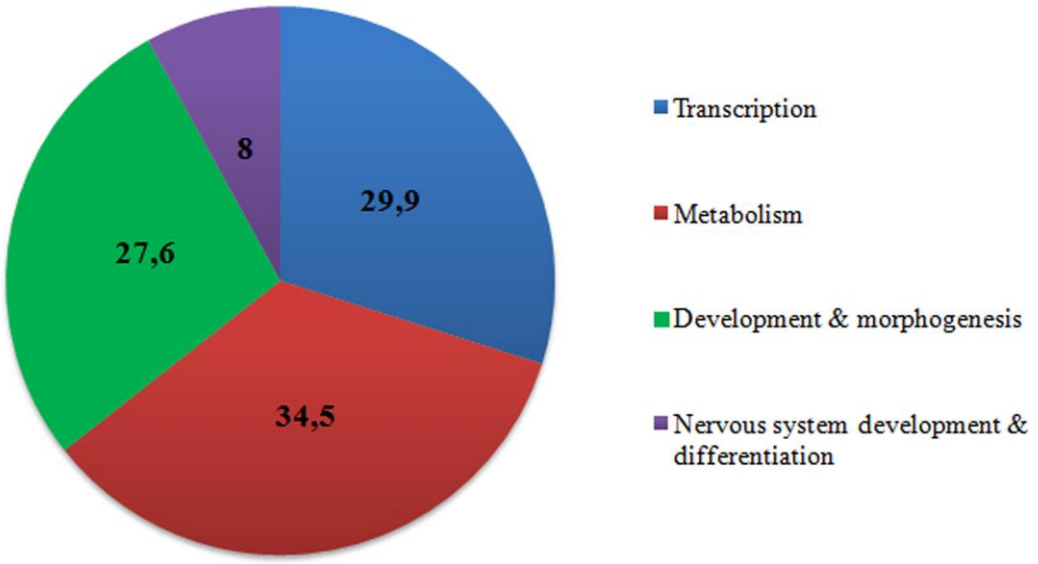

Figure 24. GO annotation analysis of GSC-specifically methylated genes. The chart shows the percentages of genes found in each functional category, compared to the total annotated genes.

GO analysis was performed to identify the biological functions associated to these genes and four main functional categories were identified (Figure 24). Besides, *metabolism* and *transcription*, GSC-specifically methylated genes showed an enrichment of terms related to *development & morphogenesis* (27.6%) and *nervous system development & differentiation* (8%), indicating that the methylation of these gene categories may be the real key components that distinguish GBM cancer stem-like cells from the normal counterpart. Moreover, to achieve a deeper insight into the mechanisms underlying DNA methylation in GBM, we evaluated if these 37 GSC-specifically methylated genes were targeted by Polycomb repressive complex 2 (PRC2) in embryonic stem (ES) cells (Lee et al., 2006b). 46% GSC-specifically methylated genes were found to be the target of Suz12 protein, a subunit of PRC2 and such enrichment was statistically significant (10% of genes are marked by PRC2 complex in ES cells, Fisher's exact test, $p<0.001$) (Lee et al., 2006b).

EFFECT OF DRUG TREATMENT ON METHYLATION PROFILES

VPA is an HDACi and it can be considered an epigenetic drug (Mai and Altucci, 2009). Acetylation and methylation are two epigenetic mechanisms, which are strictly interconnected and one process may influence the other one, in order to regulate gene expression. GBM2 and G144 cell lines were selected as examples of drug-sensitive and barely sensitive/insensitive cells, respectively. Cells were treated with 2mM VPA for 96hs, to identify DNA methylation changes due to the administration of an epigenetic drug. Cells were also treated with 10μM PTX for 96hs separately, to verify the specificity of VPA effect on DNA methylation profile of GSCs. Results on the genome-wide methylation status of treated cells were compared to the matching control untreated cells (Figure 25A). Raw data already showed the differences induced by drug administration on the methylation profile. The percentages of methylated and unmethylated CGIs in GBM2 and G144 were almost similar (40.8% methylated and 59.2% unmethylated CGIs for GBM2 and 45.3% and 54.7% for G144 cell line) (Figure 25B).

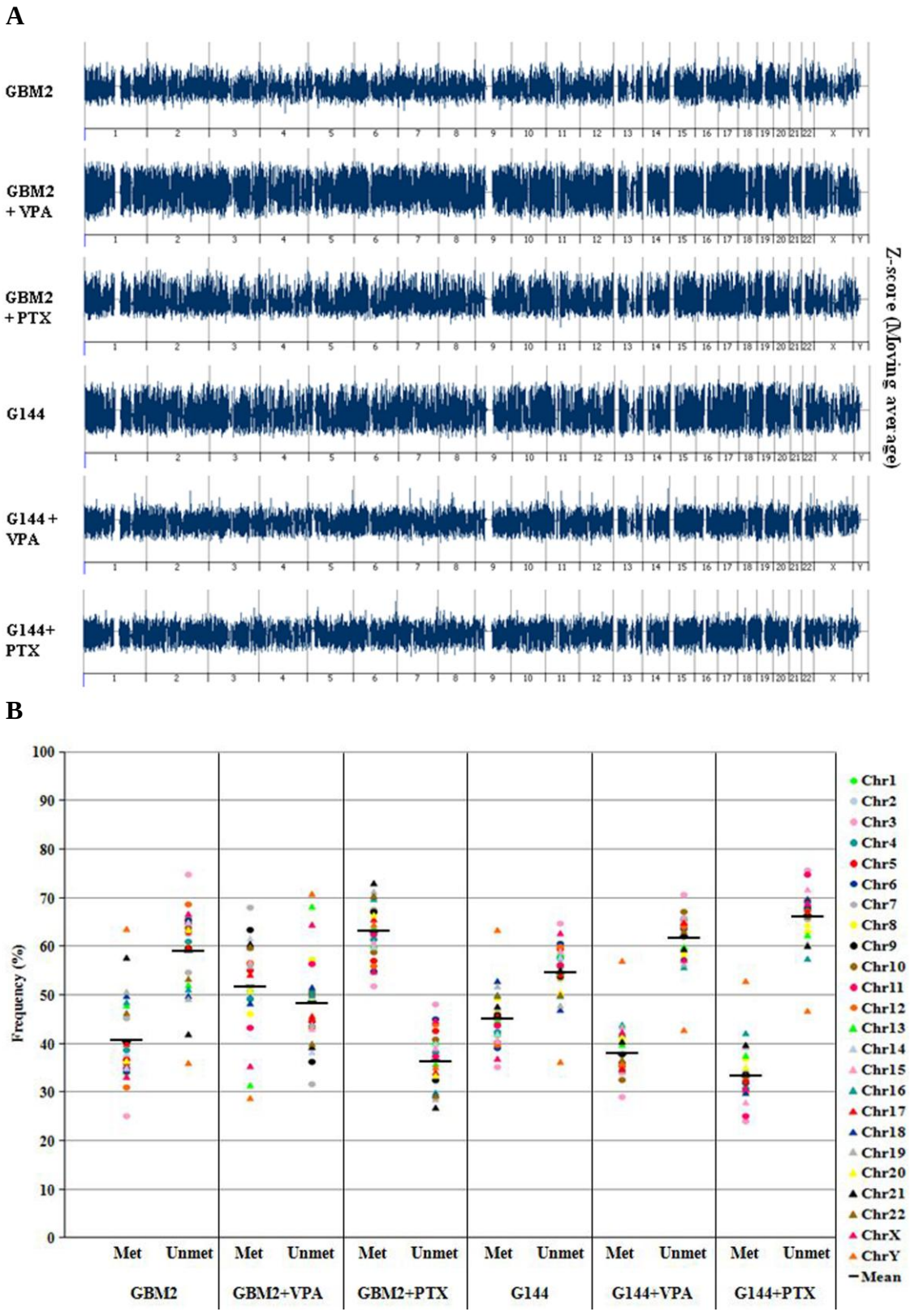

Figure 25. Methylation profiles of GSC lines after drug treatment. GBM2 and G144 cell lines were treated with 2mM VPA or 10μM PTX for 96hs. A. Global DNA methylation profiles along chromosomes, through the mean average of combined Z-score values. The profile of methylated DNA sequences is displayed as the ratio of MeDIP-enriched DNA versus input (total) DNA signal.

Chromosomes are displayed head-to tail, with p-arm at left, q-arm at right. Breaks in combined Z-score profile correspond to heterochromatin specific for secondary constriction regions (qh), which are not covered by probes. B. Frequency of methylation and unmethylation of CGIs for each sample. Chromosome-specific methylation status is reported and global genomic methylation scores are displayed as the mean values of all chromosome-specific values. Abbreviation: Met, methylation; Unmet, unmethylation of CGIs.

Anyway, drug treatment showed an opposite effect on cell lines. VPA induced an increase of methylated CGIs in GBM2, whereas a reduction of 5-methylcytosine in G144 cell lines. PTX induced the same modification pattern of VPA in each cell line, but with a stronger effect (the percentages of changes were higher). Nevertheless, these changes were merely global and it is important to understand if these alterations were due to a specific drug effect or to a general cytotoxic one. CGIs are located in several functional genomic regions, such as promoters and divergent promoters, inside or downstream the gene body and unknown regions. The changes in the methylation status of these regions were evaluated after drug administration (Figure 26 and Table A8). Specifically, GBM2 cell line showed major changes in the promoter and divergent promoter regions, compared to the expected variation calculated on the global genomic trend. These variations were more evident after VPA than PTX treatment. Instead, G144 cell line displayed a global spreading of changes among the different genomic functional regions. Maybe, this distinct mechanism of action is linked to the sensitivity of the cell line to the drug treatment.

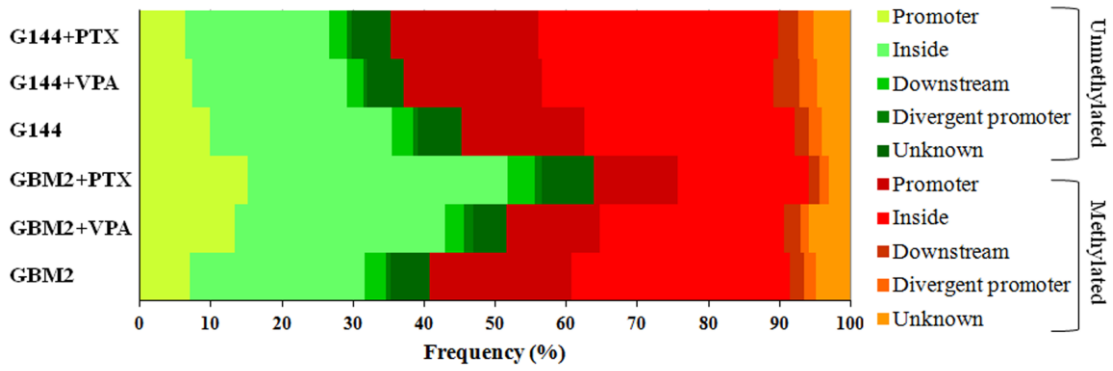

Figure 26. Changes in the distribution of methylated and unmethylated CGIs among functional genomic regions after VPA or PTX treatment of GBM2 and G144 cell lines.

In order to further investigate the features of methylation changes induced by drug treatment, we compared the methylation profile of drug treated cells to the matching untreated cells, focusing on promoter regions. After VPA treatment, 1797 and 379 genes changed the methylation status of their promoter regions in GBM2 and G144 cell lines respectively. Especially, 24.5% of genes were demethylated and 75.5% were methylated in GBM2 cell line, whereas 45.4% and 54.6% in G144 cell line. PTX treatment revealed a change in the methylation profile of promoter regions of 997 genes for GBM2 (2.7% demethylated and 97.3% methylated) and 272 for G144 cell line (89.3% demethylated and 10.7% methylated). Subsequently, genes that changed the methylation status at promoter regions, both after VPA and PTX treatment, were excluded from further analysis. Indeed, the methylation status of these genes might be influenced by the general drug cytotoxicity and not by a drug specific effect. To explore the function of these genes, GO analysis was performed to identify ontology categories that were significantly over-represented after drug treatment (Figure 27).

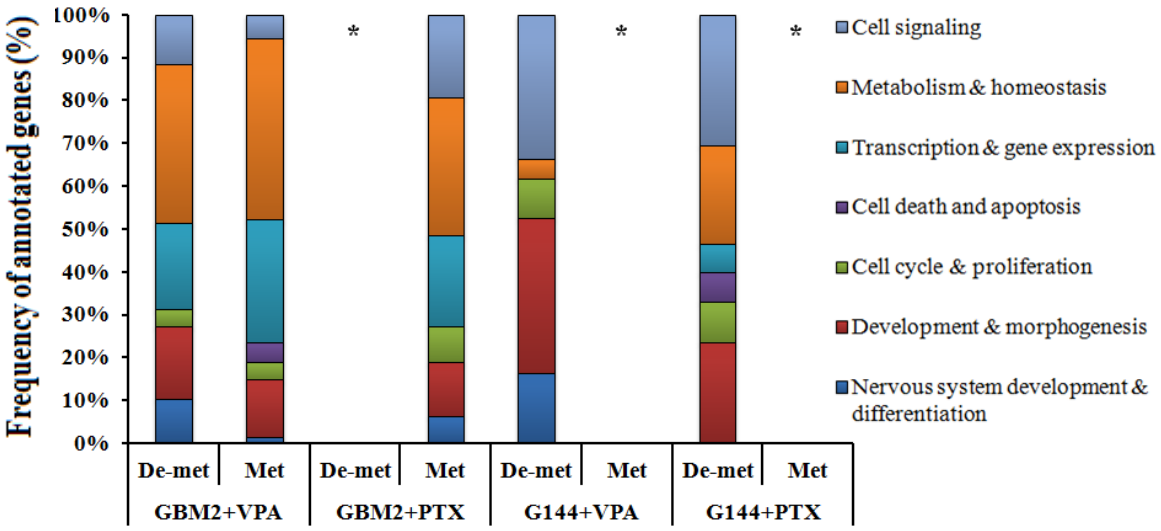

Figure 27. GO analysis of GBM2 and G144 cell lines after drug treatments. Each ontology category is represented by the frequency of annotated genes. *input list of genes didn't reveal any statistically significant annotations.

Some input gene list didn't reveal any statistically significant GO term (demet GBM2+PTX; met G144+VPA and met G144+PTX). This analysis evidenced that VPA induced a prevalent

demethylation of genes involved in *development & morphogenesis* and *nervous system development & differentiation* (27.5% for GBM2 and 52.7% for G144 cell line), in accordance to the pro-differentiatiation effect of VPA. This specific modification pattern of GO annotations wasn't induced by PTX treatment. GBM2 and G144 showed some differences related to the effect of drug treatment. Indeed, GBM2 cell line displayed an enrichment of terms related to *metabolism* and *transcription* (methylated and demethylated) after drug treatment, whereas in G144 cell line this category was less represented.

Probably, these differences are linked to the lower sensitivity of G144 to the drug administration. Moreover, G144 showed over-representation of terms related to cell cycle, whereas GBM2 didn't.

Drug treatment sensitive genes were further investigated to identify the molecular pathways influenced by drug treatment (complete list of pathway is available at Table A9-12). VPA administration on GBM2 cell lines showed a global methylation of genes (and so a possible down-regulation of expression) involved in cell proliferation pathways, such as *cyclins and cell cycle*, *G1/S checkpoint regulation* and *control of chromosomal replication* (Figure 28). Signaling pathways related to cancer mechanism were also potentially down-regulated (*small cell lung cancer signaling*; *molecular mechanism of cancer*; *pancreatic adenocarcinoma signaling*). In addition, 6 pathways (*cyclins and cell cycle regulation*; *cell cycle: G1/S checkpoint regulation*; *molecular mechanism of cancer*; *breast cancer regulation by stathmin1*; *regulation of eIF4 and p70S6K signaling*; *pancreatic adenocarcinoma signaling*) were associated to the genes that shared a common methylation status between the three GCSs analyzed. Importantly, Wnt/β-catenin signaling, a key pathway involved in stemness maintenance, showed a prominent methylation of its genes (Figure 29), indicating the effectiveness of VPA in blocking self-renewal and inducing differentiation. Also *TGFβ* and *SHH*, two important genes for stem proliferation and maintenance, were methylated after VPA treatment. G144 cell line showed few pathways that were influenced by VPA treatment, anyway

some critical genes in cancer, GBM pathogenesis and stem cell maintenance were modulated, such as *ROCK1*, *SLC1A2*, *GNG7* and *BAI1*.

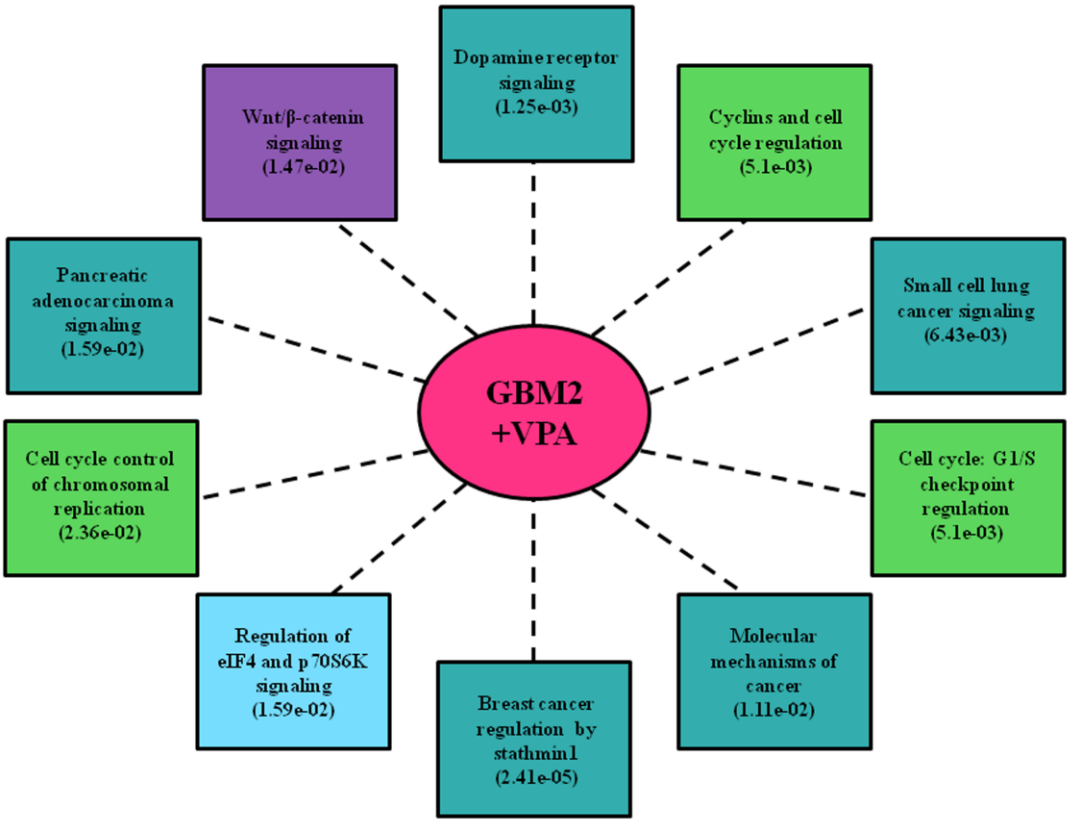

Figure 28. Top 10 pathways influenced by changes in the DNA methylation status after VPA treatment in GBM2 cell line. Each pathway is associated with a p-value (calculated by the Ingenuity Pathway Analysis, IPA, software), which indicates the probability that such association could have occurred by chance. Dotted lines indicate a global potential down-regulation, due to methylation in promoter regions of genes involved in these pathways.

PTX treatment didn't affect the methylation status of genes involved in self-renewal, but was generally associated to the epigenetic modulation of genes involved in several mechanisms of cancer, indicating a more general antitumor activity.

VPA administration allowed the demethylation of genes 20 and 11 genes that were specifically methylated in the untreated GBM2 and G144 cell lines, respectively. More than 65% of these genes were targeted by PRC2 complex. Finally, the methylation of 98 gene promoter regions was influence by VPA treatment both in GBM2 and G144 cell lines (Table A13). Moreover, 68 genes showed concordant changes after VPA administration in both cell lines.

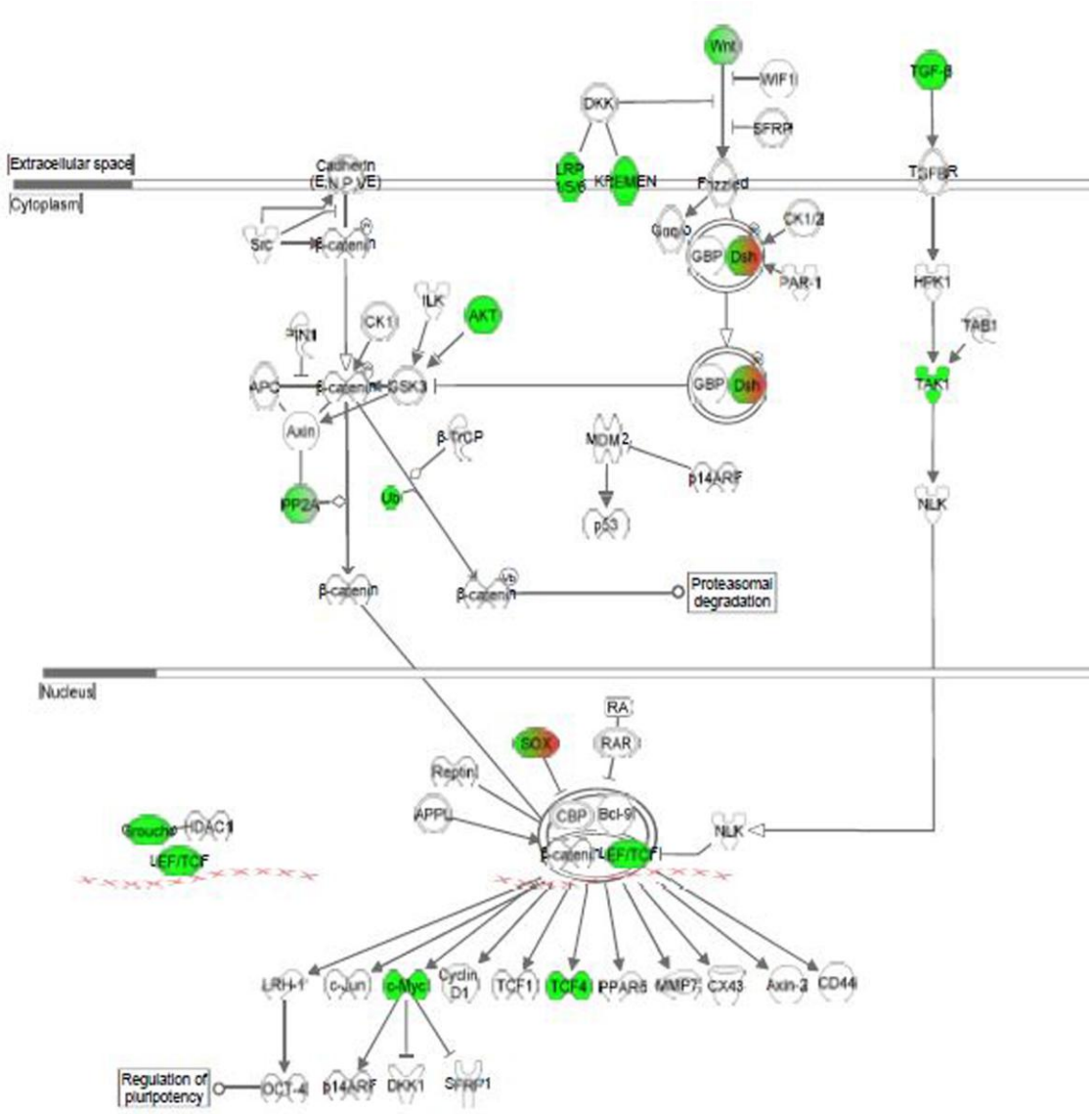

Figure 29. Wnt/β-catenin pathway is globally methylated after VPA treatment in GBM2 cell line. Green shapes indicate methylated gene promoters, whereas red shapes demethylated ones; genes/proteins with different isoforms may be both methylated or unmethylated (green and red), depending on the methylation status of each specific isoforms.

Thus, genome-wide methylation studies after drug treatment may help in the identification of aberrant methylation status in cancer cells. *MX1*, *POLG*, *STAT2*, *MIR542* genes were specifically involved in GBM, whereas other genes, such as *PIGU*, *PIM2*, *RPL30* and *SCTR* were linked to multiple malignancies. Importantly, VPA induced demethylation of 4 genes associated to aberrant methylation and targeted by PRC2 complex in ES cells: *HES3*, *OSR2*, *OTP* and *ETV7*.

DISCUSSION

Cultured glioma stem cell lines are a suitable model to study GBM onset, its genomic heterogeneity and to assess drug-sensitivity testing. In this work, GSCs have been investigated through a multi-level approach, in order to unravel GBM complexity. The cytogenomic and epigenomic profiles allowed the identification of key genes and molecular pathways specific for the stem-like counterpart. Drug testing enabled the evaluation of drug-sensitivity in GSCs specifically, trying to identify a suitable treatment for the eradication of the stem cell subpopulation, which is mandatory to achieve a real treatment for this type of tumor. Specifically, differentiation-inducing therapies are the most promising treatments, in order to affect self-renewal ability of cancer stem cell subpopulation. Furthermore, epigenomic analysis and drug administration were combined, in order to deeply decipher the effect of an epigenetic drug, such as VPA.

CYTOGENOMIC ANALYSIS IDENTIFIED GENETIC ALTERATIONS SPECIFIC FOR GBM

Solid tumors show an overall genomic complexity compared to hematological malignancies. GBM is the most common and malignant type of glioma (Central Brain Tumor Registry of the United States, CBTRUS, www.cbtrus.org) and is characterized by genomic heterogeneity (Bonavia et al., 2011), including structural and numerical aberrations, but also copy number alterations (CNAs). Thus, a comprehensive insight into the genomic landscape of GBM can be acquired only by an integrated analysis, comprising karyotyping in conjunction with molecular cytogenetic methods, such as FISH and aCGH, in order to bypass the limitations related to a single technique. Genomic analysis may result in the identification of prognostic and/or diagnostic markers and in pathogenetic subclassification. Genetic alterations induce the disease, promoting cell growth and survival, by altering oncogene and tumor suppressor gene dosage (Kubota et al., 2001; Lengauer et al., 1998). Firstly, all GSC lines showed complex karyotypes. Cytogenetic, aCGH and FISH results were consistent with each others, and some discrepancies are due to the inherent differences between these methods (Dahlback et al., 2009). Several shared cytogenetic alterations were identified by banding techniques and FISH analysis. aCGH enabled the fine determinations of these aberrations. Partial or whole gain of chromosome 7,

which leads to gain of *EGFR* gene (7p11.2), was identified in all the GSC lines and this alteration is associated to approximately 40% of GBMs (Network, 2008). Moreover, other oncogenes, such as *MET* (7q13) and *CDK6* (7q21-22) map on this chromosome and might be involved in the malignant transformation (Costello et al., 1997; Wullich et al., 1994). Loss of chromosome 10 was identified in 5/6 cell lines, which encompass *PTEN* gene (10q23). A second tumor suppressor gene locus on chromosome 10 at 10q25-26 has been identified, where the *DMBT1* gene maps (Rasheed et al., 1995). Loss of chromosome 13, the other classical alteration of GBM, was identified in 3/6 cell line and this alteration is associated to *RB1* gene loss, a tumor suppressor gene localized at 13q14 and deleted in 30% of GBM cases (Ichimura et al., 1996). Microsatellite analysis of chromosome 10 and 13 revealed retention of heterozygosity, so there wasn't prevalence in the loss of one homologue compared to the other. *CDKN2A* and *CDKN2B locus* at 9p21 was found deleted in 4/6 lines; the homozygous loss of these negative regulators of cell cycle was identified in 33-55% of GBMs (Izumoto et al., 1995) and it is associated with poor prognosis (Wiltshire et al., 2004). Cytogenetic analysis revealed 1p deletion in 5/6 lines, which is a common feature in GBM samples (Ichimura et al., 2008). The region deleted is usually quite large (1p32–1pter) and the breakpoints are variable, but the high incidence of deletions (30% of astrocytomas) indicates the presence of tumor suppressor genes (Smith et al., 1999). By means of microsatellite analysis, we identified a minimal deleted region at 1p36.31 in all the 6 GSC lines tested, including Calmodulin binding transcription activator 1 (*CAMTA1*) gene. This gene was found down-regulated in cancer stem cells compared with neural stem cells (Lottaz et al., 2010) and low *CAMTA1* gene expression was detected in $CD133^+$ cells compared to $CD133^-$ cells. Moreover, up-regulation of *CAMTA1* expression in glioblastoma cells reduced colony formation both *in vitro* and *in vivo* (Schraivogel et al., 2011). 1p/19q co-deletion was found in 2/6 cell lines and usually, it is associated to an increase of progression-free survival in oligodendroglial tumors (Giannini et al., 2008), but this combined alteration has no clear implication in astrocytomas (Smith et al., 2000). Deletions of the long arm of chromosome 6 were a common aberration between our GSC lines and in addition, 6q27 region was involved in a translocation event in two cell lines. Deletions at 6q25-

26 have been identified in 30% of GBMs, including *PARK2*, *PACRG*, *QKI* and *PDE10A* genes (Mulholland et al., 2006; Yin et al., 2009). Gain of 12q13 (*MDM2* and *CDK4*) and 1q32.1 (*MDM4*) regions and loss of chromosome 17 were identified and these imbalances are frequently found in GBM (Ohgaki et al., 2004).

Finally, GSC cultures may be considered a valuable model to investigate genomic alterations in GBM, as they retain genetic hallmark of human GBM and more closely mirror the genotype of primary tumors, than serum-culture do (De Witt Hamer et al., 2008; Ernst et al., 2009; Lee et al., 2006a). Therefore, the genomic profiling of GSC lines needs to be best investigated, in order to identify genomic alterations specifically associated to the stem-like subpopulation of tumor.

CYTOGENOMIC PATHWAYS SPECIFIC FOR THE GSC SUBPOPULATION

Functional annotation analysis of genes included in CNAs regions of GSC lines identified the enrichment of terms related to *development*, *differentiation* and *cell signaling*, rather than *cell cycle* or *cell death*, showing that GBM is characterized by development and differentiation impairment. Indeed, developmental regulators may support the malignant phenotype and the stem-like cell properties, including robust self-renewal potential, shifting the balance towards the maintenance of an undifferentiated phenotype (Ben-Porath et al., 2008; Jeon et al., 2008). The identification of core genes and pathways, sustaining the stem cell subpopulation within a tumor, is essential to unravel the specific features of this tumor component. We identified CNAs 'exclusive' for GSCs, compared to literature data (de Tayrac et al., 2009; Lo et al., 2007; Maher et al., 2006; Network, 2008; Nord et al., 2009), in order to highlight a 'genomic signature' specific for the stem cell properties of GBM cells. Network analysis revealed extensive interconnection between different pathways, pointing out cancer-relevant annotations and developmental pathways. Moreover, among the highly ranked pathways *NF-κB signaling* was identified. *NF-κB signaling* is involved in regulation of stem cell proliferation, migration and differentiation, its blockage induces a decrease in the proliferative capacity of NSCs (Widera et al., 2006) and constitutively activation of NF-κB signaling in NSCs drives their transformation

in tumorigenic cells (Kaus et al., 2010). I*nflammatory cytokines signaling pathways* (Il-10 and IL-6) were also involved in GSC specific CNAs. IL-6 activate NF-κB pathway, stimulating further cytokine production and inducing a positive feedback loop, that sustains CSC self-renewal (Korkaya et al., 2011). *Integrin and ephrin receptor signaling* pathways induce invasion and migration, promoting a more aggressive and metastatic phenotype, which is a key note of GBM (Campbell and Robbins, 2008; Liu et al., 2006a; Tabatabai et al., 2011). Thus, genomic analysis may help in the identification of specific signaling pathways, which play essential functional roles in cancer stem-like cells (Regenbrecht et al., 2008).

ABERRANT METHYLATION IN GSC LINES

Most studies on DNA methylation in cancer cells have focused on selected genes, usually involved in cell cycle regulation and cellular growth. Immuocapturing of methylated DNA with antibody against 5-methylcytosine results in a specific isolation of methylated DNA (MeDIP) (Weber, 2005). MeDIP in combination with array (Chip) technology, in the last years, enabled the identification of genome-wide methylation profiles specific for cancer cells, in a completely unbiased manner, allowing the investigation of *de novo* methylation (Keshet et al., 2006). CGI (CpG island) methylation plays a significant role in chromatin structure and gene expression, influencing the tumorigenic potential. Thus, epigenomic modifications, such as DNA methylation, are an integral part of the molecular pathways contributing to malignancy (Esteller, 2005). A general hypomethylation was found in the three GSC lines analyzed, as the percentage of unmethylated CGIs was higher than 50%. Genomic hypomethylation is a hallmark of many cancers, including GBM (Cadieux et al., 2006) and this event contributes to tumorigenesis, independently of CGI hypermethylation, by increasing genomic instability and allowing oncogene expression (Ehrlich, 2002). However, differences in the methylation percentages among cell lines were identified, because methylation profiles may vary and can be considered a peculiar background, such as genomic profile (Costello, 2000). These differences may be considered an epigenetic fingerprinting for gliomas (Uhlmann et al., 2003). Moreover, the array may not cover some regions affected by DNA unmethylation, which can contribute to genomic

instability (Cadieux et al., 2006). The identification of a shared pattern of promoter methylation among the three GSC lines allowed the discovery of specific biological functions endowed with the methylation profiles. *Metabolism* was the most enriched function. This is not surprising, as cancer cells may require high cellular turnover, according to their high replicative phenotype (Li et al., 2008). The others top ranked categories were *transcription*, *gene expression* and *development* and *nervous system differentiation*. The significant involvement of these categories in the methylation profile of GSCs indicates that the regulation of neurodevelopmental genes may be crucial for the full stem-like phenotype of glioma cells (Günther et al., 2008). The investigation of canonical molecular signaling, affected by DNA methylation patterns in GSCs, showed that only two pathways were shared with genomic alterations. Genetic and epigenetic changes are generally mutually exclusive in a given tumor (Chan et al., 2008) and these two mechanisms act synergistically on several signaling pathways, resulting in tumorigenesis (Sadikovic et al., 2008). The 37 genes showing aberrant de novo methylation in GSCs compared to normal NSCs, displayed a great involvement in *transcription*, *development* and *nervous system differentiation*. 47% of these genes were identified as Polycomb group targeted (PCGT) genes in ES cells and this enrichment was statistically significant compared to whole-genome frequency (Lee et al., 2006b). The overlap between Polycomb occupancy of genes in many non-cancerous cells and aberrant *de novo* methylation of gene promoters in malignant cells is impressive and strong supports the Polycomb connection. In ES cells, PcG (Polycomb group) proteins reversibly repress genes encoding transcription factors, which are involved in development and differentiation, forming the so called ‘bivalent domains’ (Bernstein et al., 2006; Ringrose and Paro, 2004). *De novo* methylation at promoter regions of these genes may lock cells in a stem cell phenotype and promote aberrant clonal expansion (Martinez and Esteller, 2010; Schuebel et al., 2006). These evidences indicate that PCGT genes are prone to gaining *de novo* DNA methylation in GBM development (Martinez and Esteller, 2010). Moreover, aberrant methylated genes in GSCs were found highly enriched in terms related to *nervous system development* and *neurogenesis*, increasing the evidence of a fundamental role in glioma stem cell biology. The aberrant methylation of genes involved in neural differentiation

in association with other genomic alterations may modify the balance of regulated differentiation towards aberrant proliferation of stem-like cells. Thus, an accumulation of a population of cells unable to differentiate can occur and novel transforming aberrations (both genetic and epigenetic) can be further acquired (Wu et al., 2010). The involvement of PCGT genes in many type of cancers points out the importance of this developmental gene class in tumorigenesis, highlighting a sort of conserved aberrant methylation pattern in cancer cells across various types of malignancy and it might be considered a sort of epigenetic hallmark (Ehrich et al., 2008; Martín-Subero et al., 2009). These data suggest that this kind of aberrations may preferentially originate in precursor cells with stem-like features, rather than in differentiating cells (Martín-Subero et al., 2009; Wu et al., 2010).

CELL VIABILITY AND CYTOMORPHOLOGICAL ANALYSIS ALLOWED THE EVALUATION OF GSC SENSITIVITY TO DRUG TREATMENT

Treatment of GBM should be focused on glioma stem cell subpopulation and GSCs lines provide a valuable model for *in vitro* drug-testing. Differentiation therapy could be a promising treatment approach, as it can resume cell maturation in aberrant undifferentiated cancer cells and weaken their proliferative capacity (Botrugno et al., 2009). Valproic acid (VPA) induces differentiation of several types of cancer cells, both *in vitro* and *in vivo* (Cinatl et al., 1997; Cinatl et al., 1996) and it is able to permeate blood brain barrier (BBB), with minimal toxicity profile, even after chronic treatment, thus representing an attractive agent for cancer treatment (Perucca, 2002; Shen et al., 2005). VPA administration inhibited cell growth, in a dose- and time-dependent manner, in all the GSC lines. VPA is able to modify the expression of genes involved in cell cycle, differentiation, DNA repair and apoptosis (Rosato et al., 2003; Savickiene et al., 2006). Specifically, it stimulates p21 expression, inducing G1/S block of cell cycle (Cheng et al., 2007), whereas it activates apoptotic program, through down-regulation of anti-apoptotic proteins, such as Bcl-2/Bcl-XL (Lagneaux et al., 2007; Ziauddin et al., 2006). A decrease of mitotic index was observed after drug treatment, indicating a G1 block performed by VPA (Martin et al., 1988; Regan, 1985). Moreover, VPA was able to reduce the spreading of

chromosome number and inducing a decrease in ploidy, indicating a sort of selective process: only cells with a smaller number of chromosomes were able to continue cell cycle, whereas other cells were negatively selected and showed a change in nuclear morphology compared to untreated cells (Kortenhorst et al., 2009). Probably, VPA induced a decrease in cell viability by inhibition of cell proliferation and induction of differentiation, rather than by apoptosis (Hrzenjak et al., 2006). Generally, cells arrested in G1 phase evolve towards differentiation and this process is mutually exclusive with apoptosis (Catalano et al., 2005), anyway, the factors determining cell fate (cycle arrest, differentiation or apoptosis) are still unknown. Probably, drug concentration is a key factor, but also the cell type may induce a substantial variability of VPA effects (Shen et al., 2005)

Paclitaxel (PTX) is a mitotic inhibitor, which binds to β-subunit of tubulin in microtubules, stabilizing their dynamics, leading to mitotic arrest and apoptosis (Jordan et al., 1996). PTX has a weak effect on GSC lines and only GBM2 cell line showed a considerable decrease in cell viability after 72hs incubation. Paclitaxel treatment is able to induce G2/M block, which leads to the accumulation of mitotic figures and increasing of mitotic index, as expected consequence (Scolnick and Halazonetis, 2000). The induction of mitotic arrest is the primary mechanism of action of drug affecting microtubule dynamics (Horwitz, 1992). Cells remained in mitosis for up to 24hs and then attempted to complete mitosis, however cytokynesis remained inhibited and cells became multinucleated or polyploid (Liebmann et al., 1994). Escaping from mitosis and entering in interphase are termed mitotic slippage (Elhajouji et al., 1998) and induce a multinucleated grape-like nuclear morphology of slipped cells (Riffell et al., 2009), identified as increased percentages of polymorphic nuclei. After 48hs treatment, the percentage of mitotic cells decreased, showing that the initially blocked cells attempt to complete mitosis. Cells escaping mitotic block bypass cellular division and this process results in endoreduplication and consequently, polyploidization (Lanzi et al., 2001). Subsequently, these cells undergo a non-apoptotic form of cell death, known as mitotic catastrophe (Erenpreisa et al., 2000). The cytotoxic effect of PTX is directly related to its ability to inhibit mitotic progression (Rakovitch

et al., 1999). Cells insensitive to PTX treatment may have mutations in genes involved in the mitotic checkpoint, which accelerate mitotic satisfaction and reduce the duration of mitosis. Indeed, these cells didn't show accumulation of mitotic figures after PTX treatment for 24h (Yang et al., 2009). The decrease of mitotic index in barely sensitive cells may be linked to a general induction of apoptosis by PTX, that may occur via signaling pathways independent from mitotic arrest (Chen and Horwitz, 2002). The variability in response to mitotic stress in GSC lines reflects their differential sensitivity to drug treatment and the measurement of cytomorphological parameters may serve as an important indicator of pathologic response to drug administration (Chakravarthy et al., 2006). PTX is extensively used in several types of solid cancer (Rowinsky et al., 1993) and recently it has been also shown to have a therapeutic effect both *in vitro* on glioma cells (Tseng et al., 1999; Zhang et al., 2008) and *in vivo* on GBM xenografts in mice (Karmakar et al., 2007; Karmakar et al., 2008). The weak permeability of PTX to the BBB may be a limiting aspect in the use of this drug, anyway, BBB is often compromised in GBM patient, the blood capillaries are leaky (Coomber et al., 1987) and moreover, several strategies to improve PTX delivery in the brain are under investigations (Yang et al., 2011).

DUAL THERAPY WITH VPA AND PTX SIGNIFICANTLY EFFECTS GSC SURVIVAL

In order to overcome the limitations linked to a single agent therapy, a dual approach was developed. The ability of VPA to induce differentiation is the rationale for its use in a combined treatment: the reduction of cell proliferation, with induction of differentiation of glioma stem cells can be coupled with a drug able to promote cell death, such as PTX (Roy Choudhury et al., 2011). After VPA induced-differentiation, PTX might be able to influence cell viability of downstream cells in the hierarchical composition of GBM. Globally, cell death was increased after dual treatment in all the GSC lines, thus VPA enhanced the anticancer action in combination with PTX. Three cell lines (GBM2, G144, G179) showed an increased synergism at lower concentrations of both drugs: using lower doses, toxicity can be minimalized and therapeutic efficacy maintained. This approach is strictly dependent on time-scheduled

administration, as cells should be incubated 24hs with VPA prior to PTX treatment, in order to promote an initial differentiation of cancer stem-like cells. Indeed, reverse treatment didn't display any synergism. The clinical use of PTX is hampered by its reverse side effects (Cavaletti et al., 1995), but it is chiefly dependent upon high dose regimens and on Cremophor EL, which is used as vehicle (Mielke et al., 2006). Therefore, VPA administration may consent to reduce PTX concentration, maintaining the same killing effect and allowing an effective treatment (Catalano et al., 2007). The effectiveness of VPA combined with PTX administration is due to the ability of VPA to enhance the sensitivity to chemotherapeutic agents (Mai and Altucci, 2009). Moreover, VPA induces α tubulin acetylation, which suppresses microtubule dynamics and can positively affect PTX binding to microtubules (Catalano et al., 2007; Yagi et al., 2010). Collectively, the combination of VPA and PTX could be a real potential therapeutic strategy for killing GSCs specifically, and might provide insight in the design of future treatment of GBM.

DIFFERENTIATION CAPACITY IS IMPAIRED IN GSC LINES

In order to characterize the differentiation-inducing ability of VPA, the effect of its administration on GSC lines was assessed, both morphologically and through the evaluation of immunoreactive cells for stem cell and neural differentiation markers. GSCs showed evident morphological changes after VPA treatment compared to untreated cells, from rolling spheres to attached star-shaped cells with neurite-like structures, indicating a sort of differentiation process (Angelucci et al., 2008; Benítez et al., 2008). GSCs cultured in RPMI supplemented with FCS were characterized by a flat morphology with elaborated process and spindle-like structures, as expected (Singh et al., 2003). Immunoreactivity for stem cell or differentiation markers was performed to clearly characterize the differentiation process. Firstly, untreated cells were characterized by highly expression of stemness markers (CD133 and Nestin), anyway they stained positively also for differentiation markers, even if at lower percentages. Within a single sphere, originating from $CD133^+$ GSCs, cells can expressed markers of all three neural lineage (Beier et al., 2007). This is not surprising as brain tumor cells are very heterogeneous and

express phenotype of more than one lineage (Singh et al., 2004). Moreover, culture conditions mirror the cellular hierarchy existing in the original tumor (Singh et al., 2003) and glioma stem cells proliferation and differentiation cannot be completely stopped *in vitro*, so no pure CD133 cultures can be achieved, even in a medium specific for NSC growth (Huang et al., 2008). Importantly, no single definitive immunophenotype can still be attributed to GSCs (Gürsel et al., 2011b). Indeed, the expression of CD133 in GSC and its reliability as a marker for stem like cells remains controversial (Piccirillo et al., 2009b; Wang et al., 2008; Wu and Wu, 2009). Anyway, CD133 effectiveness as glioma stem cell marker should not be neglected until a specific marker for GSCs will be found (Huang et al., 2008). GFAP usually is considered a marker for astrocytic differentiation, but it is also expressed by undifferentiated NSCs and GSCs (Doetsch et al., 1999; Gürsel et al., 2011b; Ignatova et al., 2002), thus strongly expression of GFAP can be detected before differentiation (Gürsel et al., 2011a). Differentiation assay, both with VPA and serum addiction, demonstrated that GSCs did not differentiate terminally and often co-expressed differentiation markers with stem cells progenitor markers, as a sort of retained self-renewal: a 'down-up' trend in the percentage of $CD133^+$ cells is paired with a 'up-down' trend for differentiation markers (Huang et al., 2008). So GSCs show important differences from NSCs, as they are not able to differentiate terminally under conditions that would induce terminal differentiation in NSCs. The aberrant differentiation program reflects the disregulation of developmental features of GSCs (Galli et al., 2004). Enhanced self-renewal and altered differentiation abilities of GSCs are demonstrated by their ability to maintain undifferentiated state and to resist differentiation and even de-differentiate (Huang et al., 2008; Yuan et al., 2004). The aberrant pattern of marker localization is another feature that sustains the aberrant differentiation capability (Asklund et al., 2004; Benítez et al., 2008; Kim et al., 2011). Finally, the cancer-associated differentiation arrest might be caused by a deviant expression of transcription factors (Rosenbauer and Tenen, 2007); this hypothesis is a link between aberrant methylation of important developmental genes found in GSCs and incomplete differentiation. In conclusion the question whether GSCs are able to accomplish neuronal, astrocytic or oligodendroglial development should still be elucidated. The potential use of VPA

for a differentiation inducing therapy has to be considered, even if it can require combination therapy to fulfill its therapeutic potential (Nolan et al., 2008).

FUNCTIONAL METHYLATION PROFILES UNDERLYING VPA-INDUCED DIFFERENTIATION IN GSC LINES

VPA is an HDACi (Gottlicher, 2001; Phiel et al., 2001) and it is potentially able to modify gene expression profile of cancer cells upon treatment (Cameron et al., 1999; De la Cruz-Hernández et al., 2011; Suzuki et al., 2002). VPA is able to regulate the expression of proteins essential for the maintenance of chromatin, such as SMC, DNMT1 and HIP1 (Marchion et al., 2005). Furthermore, Cervoni and Szyf demonstrated that the methylation pattern is determined by local histone acetylation states (Cervoni and Szyf, 2001). Thus, epigenomic processes such as acetylation and methylation are strictly interconnected and we decided to assess an epigenomic screening of GSC treated with VPA, through the evaluation of the genome-wide methylation profiles. The major involvement of promoter regions by VPA treatment in comparison to PTX administration can be considered a marker for a higher specificity of VPA epigenetic action: the number of promoter regions that changed the methylation status after PTX treatment was approximately a half compared to VPA treated cells. The general drug cytotoxic effect could lead to promoter hypermethylation (Bredberg and Bodmer, 2007). PTX treatment induced a heavy methylation of promoter regions in GBM2 cell line, due to its sensitivity to PTX, whereas G144 methylation profile was less influenced. Anyway, the global methylation profiles give only partial information, as changes are also influenced by the starting methylation status. So, the drug effect seems to be cell-specific and may depend on the differentiation level and the underlying genetic alterations (Duenas-Gonzalez et al., 2008). VPA and PTX showed a general anti-cancer activity through the epigenetic modulation of cancer-relevant genes. Methylation of several well known oncogenes, such as *ABL*, *MYC* and *AKT2* (Mure et al., 2010) or the methylation of cyclin-dependent kinases (*CDK4*, *CDK6*) (Michaud et al., 2010), which are key genes in GBM pathogenesis, were accomplished by drug treatment. VPA was also able to

induce the demethylation of *CDKN2B*, a tumor-suppressor gene, which has a main role in GBM pathogenesis (Network, 2008).

Besides the general anti-cancer activity, most importantly, VPA caused a dominant demethylation of genes related to *development* and *neurogenesis* in both cell lines, highlighting the potential differentiation ability of this drug (Mai and Altucci, 2009). In addition, VPA was found to be able to de-methylate (and potentially, re-activate) genes specifically silenced in GSCs. These findings are entirely consistent with the concept that developmentally-regulated genes are aberrantly silenced in cancer and they can be reactivated by an epigenetic treatment (Lee et al., 2008; Widschwendter et al., 2007). This mechanism might allow the unlocking of the perpetual stem cell state of cancer stem-like cells into a pro-differentiation state. The analysis of pathways influenced by drug treatment evidenced a difference between the two cell lines: the (epi)genetic differences impact the specific down-stream effects, after drug treatment (Raponi et al., 2004). The pro-differentiation ability of VPA was further demonstrated by the methylation induction of genes involved in stem cell pathways, such as Wnt/β-catenin signaling. Several *WNT* isoforms (*WNT2*, *WNT2B*, *WNT7A)* were methylated, but also LPR6, which is a co-receptor of *WNT* (Liu et al., 2010a), *TCF4*, specifically involved in astrocytoma malignancies and *MTOR*, implicated in GBM cell growth (Mallon et al., 2011). TGFβ signaling is also implicated in self-renewal of GSCs and VPA caused the methylation of TGFB3 gene (Ikushima et al., 2009; Peñuelas et al., 2009). Anyway, VPA is not entirely able to induce a terminal differentiation of GSCs, so it should be considered as the first step in the disruption of the self-renewal loop of cancer-stem like cells. A second pharmacological agent is necessary to achieve a real depletion of the stem cell pool.

CONCLUSIONS

The most important contribution of this study is the attempt to give an initial insight in the identification of the key molecular landscapes underlying the main features of stem cell counterpart in GBM. Development and nervous system differentiation were the leading

mechanisms, which were affected both at genomic and epigenomic level in GSCs. VPA administration was demonstrated to be the first modulator of the cancer stem-like phenotype, by an initial differentiation-inducing ability and by its ability to unlock the perpetual stem cell state, typical of cancer cells endowed with stem-like properties. Anyway, GSCs are severely de-regulated both at genomic and epigenomic levels and terminal differentiation was impaired. Thus, a dual treatment, combining VPA with a common chemotherapeutic agent, such as PTX, could be an effective treatment to hit specifically the stem-like subpopulation of GBM.

APPENDIX

Table A1. New 'exclusive' CNAs of GSC lines identified through a comparison with literature data.

Cytoband	Position (Mb)		GSC lines			
	from	to	Amplification	Gain	Deletion	Loss
1p36.21-p36.13	14.17	17.27				GBM7
1p36.13	17.31	17.96	GBM7			
1p35.1-p34.3	32.35	38.36				GBM7
1p35.1-p34.3	33.56	34.44			GBM7	
1p34.3	36.84	37.66			GBM7	
1p13.3	109.62	109.68		GliNS2		
1q42.13	228.32	228.44				GBM7
1q44	246.54	247.18		GliNS2		
1q44	247.07	247.18				GBM2
2p23.2	28.64	28.72		GliNS2		
2p22.3	25.61	26.4		GBM7		
2p22.3	32.04	32.81		GBM7		
2p13.1-p11.2	74.97	84.78				GBM2
2p11.2	85.41	85.64		GBM7		
2p11.2	86.11	86.18				GliNS2
2q11.2	96.8	96.91				G179
2q12.1	102.16	102.8				GBM2
2q14.2	119.96	120.15	GBM2			
2q22.1-q23.1	137.1	148.4				GBM2
2q33.3-q35	208.98	216.44				GliNS2
2q37.1	231.63	231.91				G166
3p21.1	52.52	52.56		GliNS2		
3p21.1-p14.3	53.51	56.31				GBM2
3p14.3	57.08	57.17		GliNS2		
3q25.1-q25.33	153.32	160.03				G179
5p14.1-p13.3	26.98	29.94				GliNS2
5p13.3	31.45	32.63		GBM2		
5q11.2	50.71	50.73				GBM2
6p12.1-p11.2	55.22	57.3		G166		
6q16.1	97.17	97.48		G166		
6q21	107.21	108.88		GBM2		
6q21	112.49	112.68		GliNS2		
8q22.3	103.64	104.17		GBM7		
8q22.3-q23.2	104.27	111.73				G166
8q24.23-q24.3	139.22	146.25				GBM2
9q31.1	103.24	103.5				GBM7
10q11.21	43.67	44.42			GBM2	
10q22.1	72.13	73.25				GBM7
10q23.32-q23.33	93.69	94.38		G166		
11p11.2	47.28	47.42		GBM2		
11p11.2-q11	48.04	55.46				GBM2
12q24.11-q24.13	108.8	109.7		GBM7		
14q13.2	34.11	35.08		GBM7		
14q32.31-q32.33	101.41	102.57		GBM7		
16p13.11	15.44	15.87		G166		
16q21-q23.1	67.21	68.04		GBM7		
17p13.3	0.2	1.29		GBM7		
17p13.1	7.4	7.45		GliNS2		
17p11.2	17.76	17.91		GliNS2		
20p13-p12.3	3.04	6.04		GBM7		
20q21.3	61.63	62.13				G179
21q22.2-q22.3	41.37	42.1				G179
Xp22.33-p11.22	2.71	52.71				G179
Xp22.31	7.28	7.84				GBM2
Xp22.11	23.84	24.14		GBM7		
Xp11.21-p11.1	56.28	56.61	G179			

Table A2. Top 10 pathways associated to new 'exclusive' CNA regions. Each pathway is associated with a p-value (calculated by Ingenuity Pathway Analysis, IPA, software), which indicates the probability that such association could have occurred by chance.

Canonical pathway	Genes (↑gain; ↓loss)	p-value
PPAR signaling	RAS↑;HSP90AA1↑;IL18RAP↑;IL1A↑;IL1B↑;IL1F5↑;IL1F6↑;IL1F7↑; IL1F8↑;IL1F9↑;IL1F10↑;IL1R1↑;IL1RAPL1↓;IL1RL1↑;IL1RL2↑; IL1LRN↑;INS↑;MAP4K4↑;NFKBIA↑;NR1H3↑;SOS2↑;TRAF6↑	1.94e-05
IL-6 signaling	ELK1↓;HRAS↑;HSPB7↓;IL18RAP↑;IL1A↑;IL1B↑;IL1F5↑;IL1F6↑;IL1F7↑; IL1F8↑;IL1F9↑;IL1F10↑;IL1R1↑;IL1RAPL1↓;IL1RL1↑;IL1RL2↑;IL1RN↑; MAP4K4↑;NFKBIA↑;RRAS2↑;SOS2↑;TNFAIP6↑;TRAF6↑	3.41e-05
Il-10 signaling	ELK1↓;IL18RAP↑;IL1A↑;IL1B↑;IL1F5↑;IL1F6↑;IL1F7↑;IL1F8↑;IL1F9↑; IL1F10↑;IL1R1↑;IL1RAPL1↓;IL1RL1↑;IL1RL2↑;IL1RN↑;MAP4K4↑; NFKBIA↑;TRAF6↑	7.96e-05
EIF2 signaling	EIF5↑;EIF1AX↓;EIF2C1↓;EIF2C2↓;EIF2C3↓;EIF2C4↓;EIF2S3↑;EIF3E↓; EIF3F↑;EIF3I↓;EIF4A1↑;EIF4G2↑;HRAS↑;INS↑;PIK3C2A↑;PPP1CC↑; RRAS2↑;SOS2↑	9.57e-04
NF-kB signaling	BMPR2↑;CASP8↑;HADAC1↓;HRAS↑;IL1A↑;IL1B↑;IL1F5↑;IL1F6↑; IL1F7↑;IL1F8↑;IL1F9↑;IL1F10↑;IL1R1↑;IL1LRN↑;INS↑;LCK↓; MAP4K4↑;NFKBIA↑;PIK3C2↑;RRAS↑;SIGIRR↑;TAB3↓;TANK↑; TLR7↓;TRAF3↑;TRAF6↑;ZAP70↑	2.76e-03
p38 MAPK signaling	ATF2↑;CREB1↑;ELK1↓;ESPB7↓;IL18RAP↑;IL1A↑;IL1B↑;IL1F5↑; IL1F6↑;IL1F7↑;IL1F8↑;IL1F9↑;IL1F10↑;IL1R1↑;IL1RAPL1↓;IL1RL1↑; IL1RL2↑;IL1RN↑;STAT1↑;TRAF6↑	3.56e-03
LXR/LXR activation	IL18RAP↑;IL1A↑;IL1B↑;IL1F5↑;IL1F6↑;IL1F7↑;IL1F8↑;IL1F9↑;IL1F10↑; IL1R1↑;IL1RAPL1↓;IL1RL1↑;IL1RL2↑;IL1RN↑;NR1H3↑	7.07e-03
Integrin signaling	ACTR3↑;ARF6↑;ARPC2↑;ARPC3↑;CRK↑;HRAS↑;ILK↑;ITGA4↑; ITGA6↑;ITGAV↑;ITGB6↑;LIMS1↑;MYL2↑;NCK2↑;PARVA↑;PIK3C2A↑; PPP1CC↑;PTK2↓;RALB↑;RAP2B↓;RHAOG↑;RND3↑;RRAS2↑;SOS2↑; TSPAN↑;TSPAN7↓;TTN↑;WAS↓;WIPF1↑	1.65e-02
Regulation of eIF4 and p70S6K signaling	EIF1AX↓;EIF2C1↓;EIF2C2↓;EIF2C3↓;EIF2C4↓;EIF2S3↑;EIF3E↓;EIF3F↑; EIF3I↓;EIF4A1↑;EIF4G2↑;HRAS↑;ITGA4↑;PI3KC2A↑;PPP2R5C↑; RRAS2↑;SOS2↑	2.92e-02
Ephrin receptor signaling	ACTR3↑;ANGPT1↓;ARPC2↑;ARPC3↑;ATF2↑;CFL2↑;CREB1↑;CRK↑; CXCL12↓;CXCR4↑;EPHA2↓;EPHA4↑;EPHA10↓;FIGF↓;GRIN3A↓; GRINA↓;HRAS↑;ITGA4↑;MAP4K4↑;NCK2↑;PTK2↓;RRAS2↑;SOS2↑; WAS↓;WIPF1↑	3.14e-02

Table A3. Statistical analysis (p-values, t-test) of the effects of VPA and PTX on cell viability. p-values are referred to each specific treated cultures compared to respective untreated cells

Treatment	**VPA**																	
Dose	**0.5mM**			**1mM**			**3mM**			**6mM**			**10mM**			**20mM**		
Time (hs)	**24**	**48**	**72**	**24**	**48**	**72**	**24**	**48**	**72**	**24**	**48**	**72**	**24**	**48**	**72**	**24**	**48**	**72**
GBM2	n.s.	.01	.0001	.01	.001	.0001	.01	.0001	.0001	.001	.0001	.0001	.001	.0001	.0001	.0001	.0001	.0001
GBM7	n.s.	n.s.	n.s.	n.s.	n.s.	n.s.	n.s.	n.s.	n.s.	n.s.	n.s.	n.s.	n.s.	n.s.	.01	n.s.	n.s.	.001
G144	n.s.	n.s.	n.s.	n.s.	n.s.	.05	n.s.	n.s.	.01	n.s.	n.s.	.01	n.s.	n.s.	.001	.05	n.s.	.001
G166	n.s.	.01	n.s.	.01	.05	.01	.001	.01	.01	.01	.01	.001	.01	.01	.01	.001	.001	.001
G179	n.s.	n.s.	n.s.	n.s.	n.s.	n.s.	n.s.	n.s.	.001	n.s.	n.s.	.0001	n.s.	.01	.0001	n.s.	.01	.0001
GliNS2	n.s.	n.s.	.001	n.s.	n.s.	.001	n.s.	n.s.	.01	n.s.	n.s.	.05	n.s.	n.s.	.001	n.s.	n.s.	.0001

Treatment	**PTX**																	
Dose	**0.01µM**			**0.1µM**			**1µM**			**10µM**			**20µM**			**50µM**		
Time (hs)	**24**	**48**	**72**	**24**	**48**	**72**	**24**	**48**	**72**	**24**	**48**	**72**	**24**	**48**	**72**	**24**	**48**	**72**
GBM2	n.s.	.0001	.0001	n.s.	.0001	.0001	n.s.	.0001	.0001	n.s.	.0001	.0001	n.s.	.0001	.0001	n.s.	.0001	.0001
GBM7	n.s.	n.s.	n.s.	n.s.	.05	n.s.	n.s.	.05	n.s.	n.s.	.01	n.s.	n.s.	.01	n.s.	n.s.	.05	.05
G144	n.s.	n.s.	n.s.	n.s.	.01	.01	n.s.	.01	.01	n.s.	.01	.01	n.s.	.05	n.s.	.001	.001	.001
G166	n.s.	n.s.	n.s.	n.s.	n.s.	n.s.	n.s.	n.s.	.05	n.s.	n.s.	.05	n.s.	n.s.	.01	n.s.	n.s.	.01
G179	n.s.	n.s.	n.s.	n.s.	.05	.001	n.s.	.01	.0001	n.s.	.01	.0001	n.s.	.0001	.0001	n.s.	.0001	.0001
GliNS2	n.s.	n.s.	n.s.	n.s.	n.s.	n.s.	n.s.	n.s.	n.s.	n.s.	n.s.	n.s.	n.s.	n.s.	n.s.	n.s.	.0001	.0001

n.s.= not statistically significant

Table A4. The Cooperative Index (CI) for viability assays of VPA and PTX treatments. CI was calculated to determine the synergistic (CI<1), additive (CI=1) or antagonistic (CI>1) effects of the combined treatment.

Cell line	VPA\PTX	0.1µM	1µM	10µM	20µM	50µM
GBM2	10mM	1.4	1.4	1.3	1.2	1.3
	6mM	1.4	1.4	1.3	1.2	1.3
	1mM	0.87	0.83	0.79	0.95	0.95
	0.5mM	0.85	0.78	0.73	0.93	0.97
GBM7	10mM	1.3	1.1	1.2	1.1	0.53
	6mM	1.3	1.3	1	1	0.6
G144	10mM	1.08	1.2	1	0.85	0.63
	6mM	1.9	1.4	1.1	0.9	0.64
	1mM	1.1	0.86	0.94	0.79	0.73
	0.5mM	0.77	0.63	0.63	0.56	0.63
G166	10mM	1.3	1.1	0.9	0.7	0.7
	6mM	>2	>2	1.7	0.8	1.4
G179	10mM	1.1	1.1	1.1	1.3	1.2
	6mM	0.9	1	1	0.8	0.53
	1mM	0.47	0.40	0.49	0.49	0.56
	0.5mM	0.38	0.41	0.48	0.66	0.47
GliNS2	10mM	>2	>2	1	1	0.9
	6mM	>2	>2	>2	1.2	1.4
Cell line	**PTX\VPA**	**1mM**	**3mM**	**6mM**	**10mM**	**20mM**
GBM2	1µM	>2	>2	>2	>2	>2
G144	1µM	>2	>2	>2	1,4	1,14

Figure A1. Morphological changes induced by VPA treatment at different concentrations (2-3-6-10mM) for 24, 48 and 72hs in GSC lines. (A). GBM7; (B). G166; (C). G179; (D). GliNS2 cell lines.

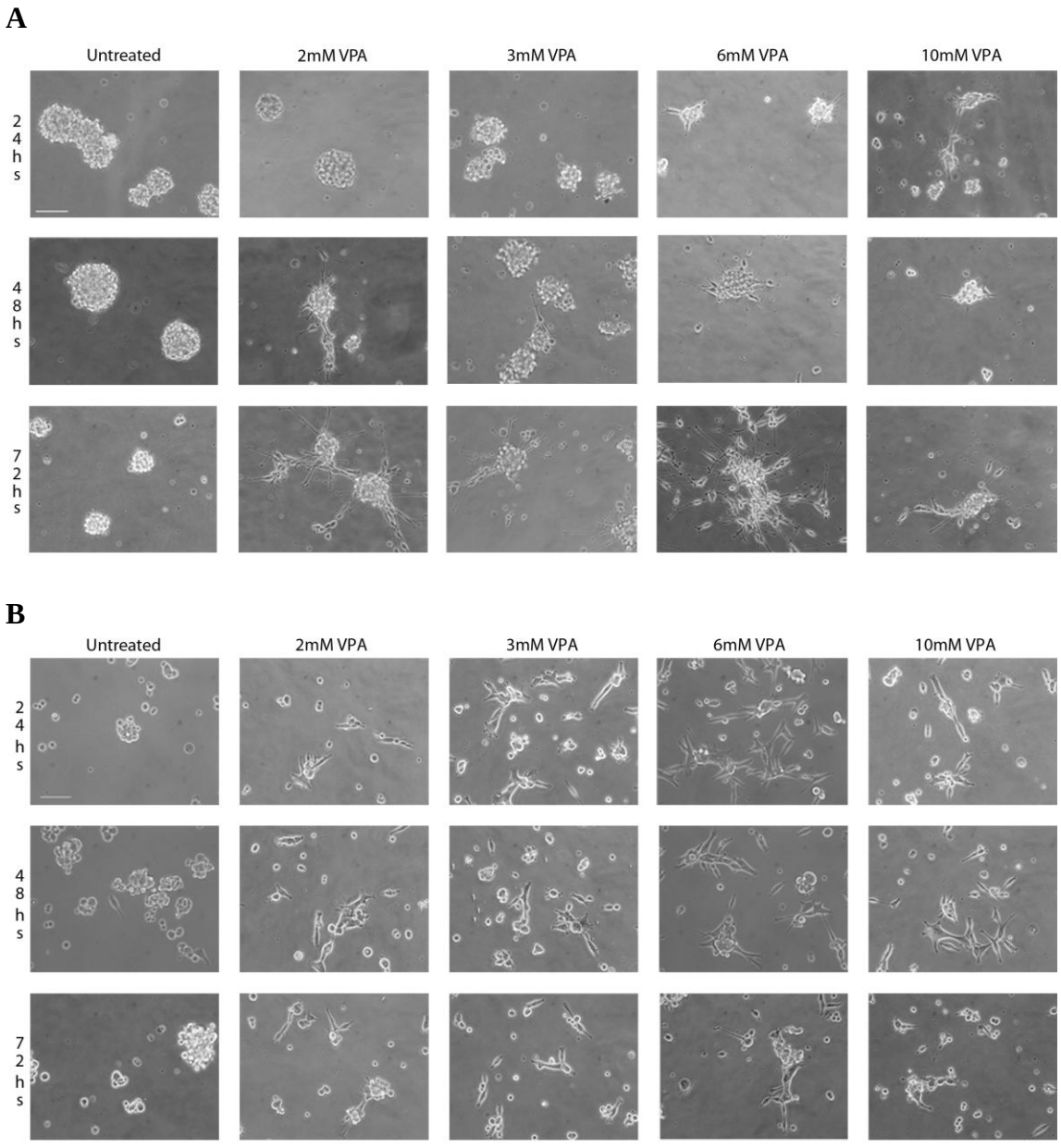

C

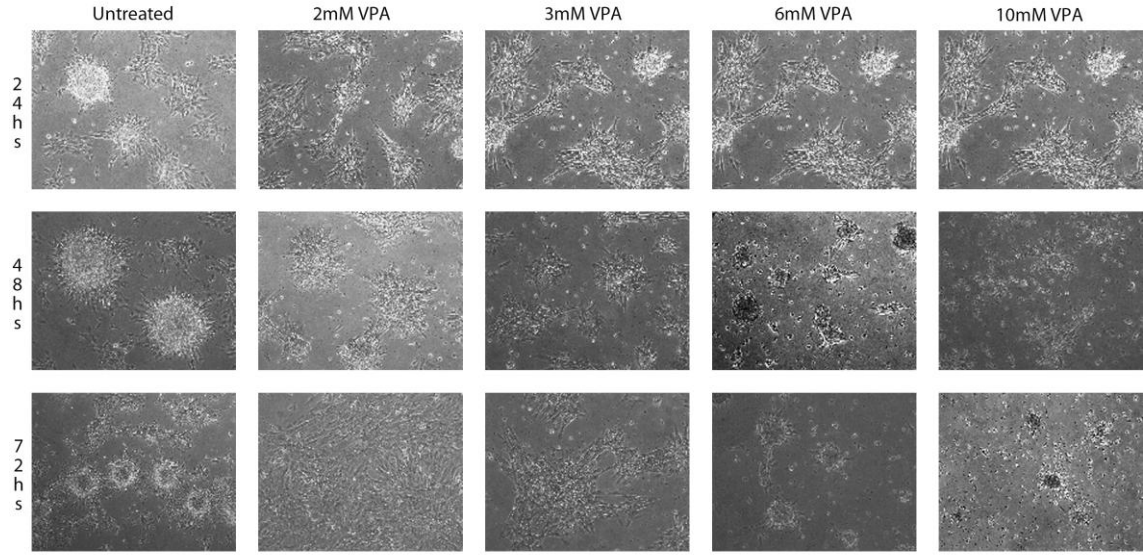
Untreated
2mM VPA
3mM VPA
6mM VPA
10mM VPA
24hs
48hs
72hs

D

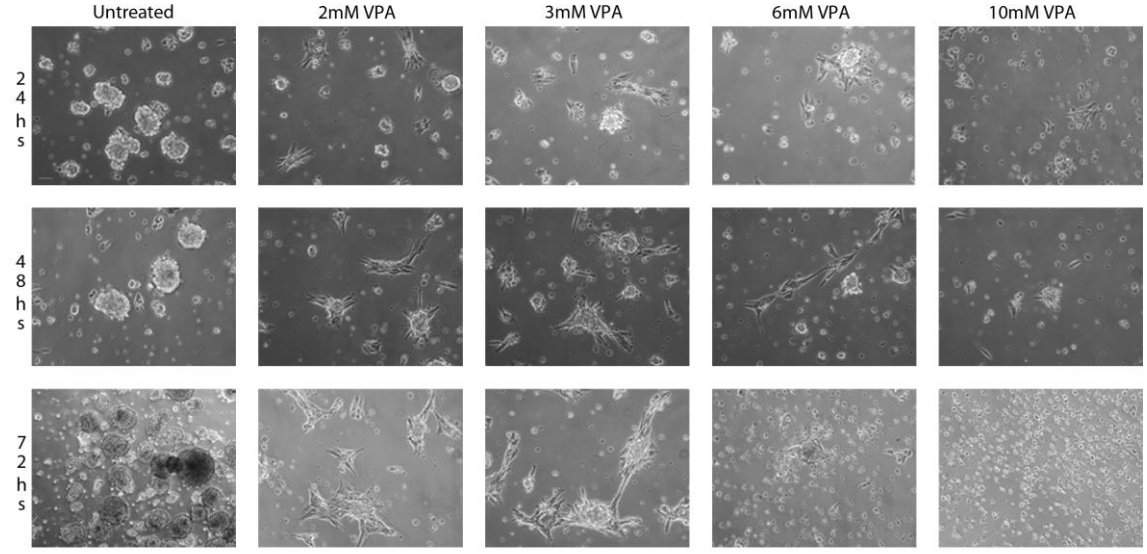
Untreated
2mM VPA
3mM VPA
6mM VPA
10mM VPA
24hs
48hs
72hs

Table A5. Methylation percentages of GSC lines (GBM2, G144 and G166), foetal NSC lines (CB660SP and CB660) and PBL pool for each specific chromosome. Global genomic percentages of methylation are expressed as the mean values of all chromosome-specific values.

	GBM2		G144		G166		CB660SP		CB660		PBL pool	
Percentages	**Met**	**Unmet**	**Met**	**Unmet**	**Met**	**Unmet**	**Met**	**Unmet**	**Met**	**Unmet**	**Met**	**Unmet**
Chr1	34.2	65.8	41.9	58.1	17.1	82.9	57.3	42.7	26.7	73.3	20.1	79.9
Chr2	37.4	62.6	44.2	55.8	28.6	71.4	56.3	43.7	29.6	70.4	18.1	81.9
Chr3	25.2	74.8	35.2	64.8	15.7	84.3	48.8	51.2	21.3	78.7	12.6	87.4
Chr4	38.8	61.2	42.4	57.6	30.8	69.2	55.7	44.3	30.1	69.9	24.9	75.1
Chr5	36.9	63.1	40.4	59.6	26.5	73.5	52.7	47.3	31.8	68.2	20.1	79.9
Chr6	34.5	65.5	39.3	60.7	21.9	78.1	48.6	51.4	25.0	75.0	19.3	80.7
Chr7	45.3	54.7	46.5	53.5	30.6	69.4	62.7	37.3	37.8	62.2	28.3	71.7
Chr8	40.1	59.9	46.3	53.7	28.5	71.5	64.4	35.6	34.8	65.2	25.7	74.3
Chr9	40.2	59.8	46.1	53.9	21.4	78.6	63.6	36.4	33.7	66.3	25.5	74.5
Chr10	36.0	64.0	44.0	56.0	24.1	75.9	58.2	41.8	30.9	69.1	23.2	76.8
Chr11	35.1	64.9	43.8	56.2	17.4	82.6	59.6	40.4	32.1	67.9	22.0	78.0
Chr12	31.2	68.8	39.9	60.1	19.3	80.7	55.3	44.7	25.3	74.7	21.2	78.8
Chr13	47.9	52.1	45.3	54.7	34.8	65.2	63.4	36.6	41.8	58.2	29.5	70.5
Chr14	35.0	65.0	42.1	57.9	24.2	75.8	55.1	44.9	27.6	72.4	19.2	80.8
Chr15	33.3	66.7	40.8	59.2	22.9	77.1	57.9	42.1	24.9	75.1	15.9	84.1
Chr16	48.7	51.3	50.1	49.9	32.3	67.7	68.3	31.7	44.1	55.9	34.2	65.8
Chr17	40.1	59.9	45.7	54.3	20.4	79.6	63.5	36.5	32.7	67.3	22.3	77.7
Chr18	50.0	50.0	52.9	47.1	36.4	63.6	65.0	35.0	47.8	56.2	35.1	64.9
Chr19	50.8	49.2	52.0	48.0	26.2	73.8	70.0	30.0	42.6	57.4	22.9	66.1
Chr20	36.5	63.5	49.5	50.5	11.6	88.4	62.3	37.7	36.8	63.2	24.5	75.5
Chr21	57.9	42.1	47.8	55.2	35.4	64.6	69.6	30.4	49.7	50.3	38.6	61.4
Chr22	46.5	53.5	49.9	50.1	23.5	76.5	71.8	28.2	40.0	60.0	27.5	72.5
ChrX	33.3	66.7	37.1	62.9	19.5	80.5	75.9	24.1	45.5	54.5	20.8	79.2
ChrY	63.8	36.2	63.6	36.4	11.3	88.7	N.D.	N.D.	N.D.	N.D.	69.4	30.6
Mean	40.8	59.2	45.3	54.7	24.2	75.8	61.1	38.9	34.5	65.7	26.3	73.7

Abbreviations: Met, methylation ; Unmet, unmethylation; N.D., not determined as CB660SP and CB660 are female cell lines (46,XX).

Table A6. List of Top 10 pathways influenced by DNA methylation pattern in GSCs. Each pathway is associated with a p-value (calculated by Ingenuity Pathway Analysis, IPA, software), which indicates the probability that such association could have occurred by chance.

Canonical pathway	Genes (↑unmethylated; ↓methylated gene promoters)	p-value
Molecular mechanism of cancer	ABL1↑;ADCY3↓;ADCY6↑;ADCY8↑;AKT1↑;AKT2↑;AKT3↑;APH1A↑; ARHGEF2↑;ARHGEF3↑;ARHGEF4↓;ARHGEF10↓;ARHGEF11↑; ARHGEF12↑;ATR↑;BCL2L1↑;BMP4↑;BMP7↑;BMP8B↑;CASP6↑; CASP9↑;CCND3↑;CCNE2↑;DCD25A↑;CDC25C↑;CDK4↑;CDK6↑; CDKN2C↑;CDKN2D↑;CHEK1↑;CREBBP↓;CTNND1↓;CYSC↑;DAXX↑; DIABLO↑;E2F1↑;E2F2↑;E2F5↑;E2F6↑;ELK1↑;FOXO1↑;FZD4↑;FZD5↓; FZD9↑;GAB2↑;GNA12↑;GNA13↑;GNA14↓;GNAQ↑;GRB2↑	2.48e-08
Cyclins and cell cycle regulation	ABL1↑;ATR↑;CCNA2↑;CCNB3↓;CCND3↑;CCNE2↑;CDC25A↑;CDC2↑; CDK4↑;CDK6↑;CDKN2C↑;CDKN2D↑;E2F1↑;E2F2↑;E2F5↑;E2F6↑; GSK3B↑;HDAC2↑;HDAC5↑;HDAC7↑;HDAC11↑;SKP1↑;PPP2CA↑; PPP2CB↑;PPP2R1B↑;PPP2R2B↑;PPP2R5E↑;RAF1↑;SIN3A↑;TGFB1↑; TGFB2↑;TGFB3↑	3.9e-06
Chronic myeloid leukemia signaling	ABL1↑;AKT1↑;AKT2↑;AKT3↑;BCL2L1↑;CDK4↑;CDK6↑;CHUK↑; E2F1↑;E2F2↑;E2F5↑;E2F6↑;GAB2↑;GRB2↑;HDAC2↑;HDAC5↑; HDAC7↑;HDAC11↑;MAP2K2↑;MAPK1↑;EVI1↑;MYC↑;PIK3C2B↑; PIK3R3↑;RAF1↑;RBL1↑;RELA↑;RRAS↑;SIN3A↑;SOS1↑;SOS2↑; STAT5B↑;TGFB1↑;TGFB2↑;TGFB3↑	1.48e-05
Cell cycle: G1/S checkpoint regulation	ABL1↑;ATR↑;CCND3↑;CCNE2↑;CDC25A↑;CDK4↑;CDK6↑;E2F1↑; E2F2↑;E2F5↑;E2F6↑;GSK3B↑;HDAC2↑;HDAC5↑;HDAC7↑;HDAC11↑; SKP1↑;MAX↑;MYC↑;RBL1↑;SIN3A↑;TGFB1↑;TGFB2↑;TGFB3↑	1.61e-05
Breast cancer regulation by stathmin1	ADCY3↓;ADCY6↑;ADCY8↑;ARHGEF2↑;ARHGEF3↑;ARHGEF4↓; ARHGEF10↓;ARHGEF11↑;ARHGEF12↑;CALM2↑;CCNE2↑;CDC2↑; E2F1↑;E2F2↑;E2F5↑;E2F6↑;GNA13↑;GNAQ↑;GNB1↑;GNB4↑;GNB5↑; GNB1L↑;GNB2L1↑;GNG13↑;GRB2↑;ITPR2↑;MAP2K2↑;MAPK1↑; PAK1↑;PIK3C2B↑;PIK3R3↑;PPP1CC↑;PPP1R12A↑;PPP1R14B↑; PPP1R3C↑;PPP2CA↑;PPP2CB↑;PPP2R2B↑;PPP2R5E↑;PRKAG2↑; PRKCZ↑;PRKD1↑;PRKD3↑;RAF1↑;RB1CC1↑;ROCK1ROCK2↑; RRAS↑;SHC1↑	2.41e-05
PI3K/AKT signaling	AKT1↑;AKT2↑;AKT3↑;BCL2L1↑;CDC37↑;CHUK↑;FOXO1↑;GAB2↑; GRB2↑;GSK3A↑;GSK3B↑;GYS1↑;HSP90AA1↑;ITGA↑;JAK1↑; MAP2K2↑;MAP3K5↑;MAPK1↑;PIK3R3↑;PPP2CA↑;PPP2CB↑; PPP2R1B↑;PPP2R2B↑;PPP2R5E↑;PRKCZ↑;PTGS2↑;RAF1↑;RELA↑; RHEB↑;RRAS↑;SHC1↑;SOS1↑;SOS2↑;TSC1↑;TYK2↑;YWHAE↑; YWHAG↑;YWHAQ↑;YWHAZ↑	1.02e-04
Pancreatic adenocarcinoma signaling	ABL1↑;AKT1↑;AKT2↑;AKT3↑;BCL2L1↑;BRCA2↓;CASP9↑;CDK4↑; E2F1↑;E2F2↑;E2F5↑;E2F6↑;ELK1↑;GRB2↑;HBEGF↑;JAK1↑; MAP2K2↑;MAPK1↑;MAPK12↑;NOTCH1↑;PIK3C2B↑;PIK3R3↑; PTGS2↑;RAF1↑;RALGDS↑;RELA↑;SIN3A↑;SMAD2↑;STAT1↑;STAT3 ↑;TGFA↑;TGFB1↑;TGFB2↑;TGFB3↑;TYK2↑;VEGFC↓	1.44e-04
Regulation of eIF4 and p70S6K signaling	AKT1↑;AKT2↑;AKT3↑;EIF1AX↑;EIF2A↑;EIF2S2↑;EIF2S3↑;EIF3D↑; EIF3E↑;EIF3H↑;EIF4A3↑;EIF4G2↑;EIF4G3↑;GRB2↑;IRS1↓;ITGA5↑; MAP2K2↑;MAPK1↑;MAPK11↑;MAPK12↑;PABPC1↑;PAIP1↑; PIK3C2B↑;PIK3R3↑;PPP2CA↑;PPP2CB↑;PPP2R1B↑;PPP2R2B↑; PPP2R5E↑; PRKCZ↑;RAF1↑;RPS6↑;RRAS↑;SHC1↑;SOS1↑;SOS2↑	1.44e-04
Role of BRCA1 in DNA damage response	ATR1↑;BARD1↑;BRCA2↓;BRIP1↑;C17Orf70↑;CHEK1↑;E2F1↑;E2F2↑; E2F5↑;E2F6↑;FANCA↑;FANCC↑;FANCF↑;FANCG↑;FANCL↑;HLTF↑; NBN↑;RBBP8↑;RBL1↑;RFC2↑;RFC4↑;STAT1↑	3.25e-04

Table A6. Cont'd

Canonical pathway	Genes (↑unmethylated; ↓methylated gene promoters)	p-value
Ephrin receptor signaling	ABI1↑;ABL1↑;ADAM10↑;AKT1↑;AKT2↑;AKT3↑;ARPC3↑;ATF2↑; CREB5↑;CXCR4↑;EFNA5↑;EFNB2↑;EPHA2↑;EPHA4↑;EPHA5↑; EPHB4↑;GNA12↑;GNA13↑;GNA14↓;GNAQ↑;GNB1↑;GNB4↑;GNB5↑; GNB1L↑;GNB2L1↑;GNG13↑;GRB2↑;ITGA5↑;MAP2K2↑;MAP3K14↑; MAPK1↑;PAK1↑;PAK6↑;PAK7↑;PTK2↑;PTPN13↑;RAF1↑;RGS3↓; ROCK1↑;ROCK2↑;RRAS↑;SH2D3C↑;SHC1↑;SORBS1↑;SOS1↑;SOS2↑; STAT3↑;VEGFC↓;WAS↑;WASL↑	3.92e-04

Table A7. Methylation percentages of GBM2 and G144 cell lines, untreated and 2mM VPA or 10μM PTX treated cells for 96hs, specific for each specific chromosome. Global genomic percentages of methylation are expressed as the mean values of all chromosome-specific values.

	GBM2 CTRL		GBM2+VPA		GBM2+PTX		G144 CTRL		G144+VPA		G144+PTX	
Percentage	**Met**	**Unmet**	**Met**	**Unmet**	**Met**	**Unmet**	**Met**	**Unmet**	**Met**	**Unmet**	**Met**	**Unmet**
Chr1	34.2	65.8	50.9	49.1	60	40	41.9	58.1	36.0	64.0	30.7	69.3
Chr2	37.4	62.6	50.7	49.3	62.4	37.6	44.2	55.8	34.2	65.8	30.7	69.3
Chr3	25.2	74.8	49.5	50.5	51.9	48.1	35.2	64.8	29.2	70.8	24.2	75.8
Chr4	38.8	61.2	49.3	50.7	61.6	38.4	42.4	57.6	34.6	65.4	30.9	69.1
Chr5	36.9	63.1	55.3	44.7	57.2	42.8	40.4	59.6	35.4	64.6	31.9	68.1
Chr6	34.5	65.5	56.5	43.5	54.9	45.1	39.3	60.7	36.2	63.8	32.2	67.8
Chr7	45.3	54.7	68.2	31.8	67.6	32.4	46.5	53.5	34.1	65.9	34.2	65.8
Chr8	40.1	59.9	46.3	57.3	67.1	32.9	46.3	53.7	40.8	59.2	37.0	63.0
Chr9	40.2	59.8	63.6	36.4	67.3	32.7	46.1	53.9	37.8	62.2	33.7	66.3
Chr10	36.0	64.0	59.8	50.2	59.0	41.0	44.0	56.0	32.7	67.3	32.5	67.5
Chr11	35.1	64.9	43.4	56.6	62.6	37.4	43.8	56.2	35.9	64.1	25.2	74.8
Chr12	31.2	68.8	56.7	43.3	56.0	44.0	39.9	60.1	35.8	64.2	30.3	69.7
Chr13	47.9	52.1	31.6	68.4	64.0	36.0	45.3	54.7	39.9	60.1	37.6	62.4
Chr14	35.0	65.0	61.7	38.3	59.9	40.1	42.1	57.9	34.5	65.5	30.1	69.9
Chr15	33.3	66.7	56.8	43.2	60.8	39.2	40.8	59.2	34.4	65.6	28.1	71.9
Chr16	48.7	51.3	49.8	50.2	69.9	30.1	50.1	49.9	44.1	55.9	42.3	57.7
Chr17	40.1	59.9	54.3	45.7	65.8	34.2	45.7	54.3	34.9	65.1	32.7	67.3
Chr18	50.0	50.0	48.4	51.6	70.5	29.5	52.9	47.1	42.1	57.9	30.1	69.9
Chr19	50.8	49.2	56.0	44.0	71.3	28.7	52.0	48.0	43.6	56.4	39.4	60.6
Chr20	36.5	63.5	51.1	48.9	66.5	33.5	49.5	50.5	41.6	58.4	35.3	64.7
Chr21	57.9	42.1	60.6	39.4	73.1	26.9	47.8	55.2	40.5	59.5	39.8	60.2
Chr22	46.5	53.5	59.9	40.1	70.6	29.4	49.9	50.1	36.8	63.2	33.6	66.4
ChrX	33.3	66.7	35.4	64.6	55.0	45.0	37.1	62.9	42.6	57.4	31.0	69.0
ChrY	63.8	36.2	29.0	71.0	64.7	35.3	63.6	36.4	57.1	42.9	53.1	46.9
Mean	40.8	59.2	51.9	48.1	63.3	36.7	45.3	54.7	38.1	61.9	33.6	66.4

Abbreviations: Met, methylation ; Unmet, unmethylation; N.D., not determined as CB660SP and CB660 are female cell lines (46,XX).

Table A8. Percentages of methylated and unmethylated CGIs in untreated and 2mM VPA or 10µM PTX treated GSCs for 96hs.

Cell line and treatment	% of unmethylated CGIs (expected values)*					% of methylated CGIs (expected values)*				
	Promoter	Inside	Downstream	Divergent Promoter	Unknown	Promoter	Inside	Downstream	Divergent Promoter	Unknown
G144+PTX	6.3 (7.5)	20.4 (19.7)	2.5 (2.3)	0.6 (0.4)	5.5 (4.7)	20.8 (20.5)	33.7 (35.3)	2.8 (2.3)	2.2 (2.0)	5.2 (4.8)
G144+VPA	7.4 (8.1)	21.7 (21.4)	2.4 (2.5)	0.4 (0.5)	5.3 (5.1)	19.4 (19.8)	32.6 (34.1)	3.6 (2.2)	2.5 (2.0)	4.7 (4.7)
G144	9.8	25.7	3.0	0.6	6.2	17.2	29.7	2.0	1.7	4.1
GBM2+PTX	15.2 (10.9)	36.5 (38.5)	3.8 (4.6)	1.1 (0.9)	7.2 (8.5)	11.8 (12.4)	18.6 (19.1)	1.4 (1.3)	1.3 (0.8)	3.1 (1.9)
GBM2+VPA	13.3 (8.8)	29.6 (31.2)	2.7 (3.7)	1.3 (0.8)	4.6 (6.9)	13.2 (16.5)	25.9 (25.5)	2.4 (1.6)	1.2 (1.4)	5.8 (4.0)
GBM2	7.0	24.7	3.0	0.6	5.5	19.9	30.7	2.0	1.7	4.9

*expected values were calculated, based on the percentages of variation regarding the global genomic changes in the methylation status after drug treatment

Table A9. List of Top 10 pathways influenced by VPA treatment in changing the gene promoter methylation status in GBM2 cell line. Each pathway is associated with a p-value (calculated by Ingenuity Pathway Analysis, IPA, software), which indicates the probability that such association could have occurred by chance.

Canonical pathway	Genes (↑demethylated; ↓methylated gene promoters)	p-value
Dopamine Receptor Signaling	ADCY3↑;ADCY5↑;ADCY8↓;CALY↓;DRD4↑;GCH1↓;MAOA↓;NCS1↑; PPP1R12A↓;PPP2CA↓;PPP2R1B↓;PPP2R2B↓;PPP2R5E↓;PRKAG1↓; PRKAG2↓	1.25e-03
Cyclins and Cell Cycle Regulation	ABL1↓;CCNE2↓;CDK1↓;CDKN2B↑;CDKN2C↓;HDAC2↓;PPP2CA↓; PPP2RB1↓; PPP2R2B↓;PPP2R5E↓;SIN3A↓;TGFB3↓	5.1e-03
Cell Cycle: G1/S Checkpoint Regulation	ABL1↓;CCNE2↓;CDK4↓;CDK6↓;CDKN2B↑;HDAC2↓;MAX↓;MYC↓; RBL1↓; SIN3A↓;TGFB3↓	5.16e-03
Small Cell Lung Cancer Signaling	ABL1↓;AKT2↓;BCL2L1↓;CCNE2↓;CDK4↓;CDK6↓;CDKN2B↑;CYCS↓; MAX↓; MYC↓;PIK3C2B↓;PTGS2↓;SIN3A↓	6.43e-03
Molecular Mechanisms of Cancer	ABL1↓;ADCY3↑;ADCY5↑;ADCY8↓;AKT2↓;APH1A↓;ARHGEF2↓; ARHGEF4↑;ARHGEF19↑;BCL2L1↓;BMP4↓;CCNE2↓;CDK4↓;CDK6↓; CDKN2B↑;CDKN2C↓;CYCS↓;DAXX↓;DVL1↑;ELK1↓;GRB2↓;LRP6↓; MAP3K7↓;MAX↓;MYC↓;PAK1↓;PAK7↓;PIK3C2B↓;PRKAG1↓; PRKAG2↓;PTCH2↑;RASA1↓;RASGRF1↓;RBL1↓;SHH↓;SIN3A↓; TCF4↓;TGFB3↓;TYK2↓;XIAP↓	1.11e-02
Wnt/β-catenin Signaling	AKT2↓;DVL1↑;DVL2↓;KREMEN2↓;LRP6↓;MAP3K7↓;MYC↓; PPP2CA↓;PPP2R1B↓;PPP2R2B↓;PPP2R5E↓;SOX1↑;SOX4↓;SOX7↓;SO X14↓;SOX18↑;TCF4↓;TGFB3↓;TLE1↓;UBC↓;WNT2↓;WNT2B↓; WNT7A↓	1.47e-02
Pancreatic Adenocarcinoma Signaling	ABL1↓;AKT2↓;BCL2L1↓;BRCA2↓;CDKN2B↑;CYP2E1↑;ELK1↓; GRB2↓;PIK3C2B↓;PTGS2↓;SIN3A↓;STAT1↓;TGFA↓;TGFB3↓; TYK2↓	1.59e-02
Regulation of eIF4 and p70S6K Signaling	AKT2↓;EIF2A↓;EIF2S2↓;EIF3D↓;EIF3E↓;EIF3H↓;EIF4G2↓;GRB2↓; MKNK1↓;MTOR↓;PIK3C2B↓;PPP2CA↓;PPP2R1B↓;PPP2R2B↓; PPP2R5E↓;RPS6↓	1.59e-02
Cell Cycle Control of Chromosomal Replication	CDK4↓;CDK6↓;MCM3↓;MCM6↓;MCM7↓;ORC2↓	2.36e-02
CDK5 Signaling	ABL1↓;ADCY3↑;ADCY5↑;ADCY8↓;LAMB1↓;NGF↓;PPP1R12A↓; PPP2CA↓; PPP2R1B↓;PPP2R2B↓;PPP2R5E↓;PRKAG1↓;PRKAG2↓	3.23e-02

Table A10. List of Top 10 pathways influenced by PTX treatment in changing the gene promoter methylation status in GBM2 cell line. Each pathway is associated with a p-value (calculated by Ingenuity Pathway Analysis, IPA, software), which indicates the probability that such association could have occurred by chance.

Canonical pathway	Genes (↑demethylated; ↓methylated gene promoters)	p-value
PPAR signaling	CHUK↓;CITED2↓;HSP90AA1↓;INSR↓;JUN↑;MAP3K14↓;NFKBIE↓; PDGFB↓;PDGFC↓;PDGFD↓;RELA↓;RRAS↓; SOS2↓;STAT5B↓	1.95e-04
Phospholipase C signaling	ADCY4↓;ARHGEF11↓;FNBP1↓;GNAQ↓;GNB1↓;GNB4↓;HDAC4↓; HDAC5↓;HDAC7↓;HDAC11↓;NAPEPLD↓;PLA2G12A↓;PPP1R14A↑; PPP3CA↓;PPP3CB↓;PRKCZ↓;PRKD1↓	2.21e-04
IL-8 signaling	BRAF↓;CHUK↓;FNBP1↓;GNB1↓;GNB4↓;HBEGF↓;IRAK1↓;MAPK12↓; NAPEPLD↓;PDGFC↓;PRKCZ↓PRKD1↓;PTK2↓;RELA↓;RHOC↓; RHOF↓;RND2↓;ROCK2↓;RRAS↓;SRC↓	2.21e-04
Molecular mechanism of cancer	ADCY4↓;ARHGEF11↓;BBC3↓;BMP8B↓;BRAF↓;CASP9↓;CCNE1↓; CDC25A↓;CDKN2D↓;CTNNA2↓;FNBP1↓;FOXO1↓;GAB2↓;GNAQ↓; JAK1↓;JUN↑;MAPK12↓;NFKBIE↓;PRKCZ↓;PRKD1↓;PTK2↓; RALGDS↓;RASGRP1↓;RELA↓;RHOC↓;RHOF↓;RND2↓;SMAD2↓; SOS2↓;SRC↓	4.46e-04
mTOR signaling	EIF4A3↓;EIF4G1↓;FNBP1↓;INSR↓;NAPEPLD↓;PDGFC↓;PPP2R2C↓; PRKCZ↓;PRKD1↓;PRR5↓;RHEB↓;RHOC↓;RHOF↓;RND2↓;RPS6KA2↓; RPS6KA5↓; RRAS2↓	7.62e-04
Semaphorin signaling in neurons	CFL2↓;FNBP1↓;PLXNA1↓;PTK2↓;RHOC↓;RHOF↓;RND2↓;ROCK2↓; SEMA7A↓	1.13e-03
PI3K/AKT signaling	CHUK↓;FOXO1↓;GAB2↓;HLA-B↓;HSP90AA1↓;JAK1↓;MCL1↑; NFKBIE↓; PPP2R2C↓;PRKCZ↓;RELA↓;RHEB↓;RRAS2↓;SOS2↓	2.11e-02
DNA methylation and transcriptional repression signaling	CDH3↓;CDH4↓;DNMT3A↓;RBBP7↓;SAP130↓	2.77e-03
IL-3 signaling	FOXO1↓;GAB2↓;JAK1↓;JUN↑;PPP3CA↓;PPP3CB↓;PRKCZ↓;PRKD1↓ ;RRAS2↓; STAT5B↓	3.06e-03
Colorectal cancer metastasis signaling	ADCY4↓;BRAF↓;CASP9↓;FNBP1↓;GNB1↓;GNB4↓;JAK1↓;JUN↑;LEF1 ↓;MAPK12↓;MMP15↓;PDGFC↓;RALGDS↓;RELA↓;RHOC↓;RHOF↓; RND2↓;RRAS2↓;SMAD2↓;SOS2↓;SRC↓; WNT9A↓	3.96e-03

Table A11. List of pathways influenced by VPA treatment in changing the gene promoter methylation status in G144 cell line. Each pathway is associated with a p-value (calculated by Ingenuity Pathway Analysis, IPA, software), which indicates the probability that such association could have occurred by chance.

Canonical pathway	Genes (↑demethylated; ↓methylated gene promoters)	p-value
Glutammate receptor signaling	GNG7↑;GRIK2↓;GRIN3A↑;GRM2↑;SLC1A2↑	2.77e-03
IL-8 signaling	ANGPT2↓;CCND2↑;GNG7↑;PRKCE↑;RHOV↑;ROCK1↓;RRAS↑; TRAF6↑	9.86e-03
CXCR4 signaling	CXCL12↑;ELMO2↓;GNG7↑;PRKCE↑;RHOV↑;ROCK1↓;RRAS2↑	1.66e-02
G-protein coupled receptor signaling	BAI1↑;DRD4↓;FZD5↑;GPR123↑;GPR148↓;GRM2↑;LPHN1↑; MC1R↑;NMUR1↑;PRKCE↑;PTGER3↑;RASGRP1↓;RRAS2↑; S1PR1↓;SCTR↑	3.31e-02

Table A12. List of pathways influenced by PTX treatment in changing the gene promoter methylation status in G144 cell line. Each pathway is associated with a p-value (calculated by Ingenuity Pathway Analysis, IPA, software), which indicates the probability that such association could have occurred by chance.

Canonical pathway	Genes (↑demethylated; ↓methylated gene promoters)	p-value
Dopamine receptor signaling	ADCY3↑;ADCY5↑;CALY↑;PPP1R14A↑;PPP2R2C↑;SLC18A3↑	5.0e-04
Colorectal cancer metastasis	ADCY3↑;ADCY5↑;BRAF↑;FZD8↑;MMP16↓;RHOG↑;SIAH1↑; TGFB2↑; VEGFC↑	4.6e-03
Molecular mechanism of cancer	AP1M2↑;AP1S3↑;AP2A2↑;FYN↑;PPP2R2C↑	1.6e-02
Wnt/β-Catenin signaling	APC2↑;DKK3↑;FZD8↑;KREMEN1↑;PPP2R2C↑;TGFB2↑	2.65e-02
TR/RXR activation	RXRA↑;SLC16A2↓;THRB↑;UCP2↑	2.85e-02
CDK5 signaling	ADCY3↑;ADCY5↑;PPP1R14A↑;PPP2R2C↑;TGFB2↑	3.07e-02
ILK signaling	FLNA↑;PARVB↓;PPP2R2C↑;RHOG↑;SNAI2↓;VEGFC↑	3.47e-02
Phosphol ipase C signaling	ADCY3↑;ADCY5↑;FYN↑;NFATC4↑;PLA2G6↑;PPP1R14A↑;RHOG↑	3.48e-02
p53 signaling	PLAGL1↑;PPP1R13B↑;RRM2B↑;SNAI2↓	3.78e-02
ERK/MAPK signaling	BRAF↑;DUSP2↑;FYN↑;PLA2G6↑;PPP1R14A↑;PPP2R2C↑	3.97e-02

Table A13. Commonly VPA modified gene promoters between GBM2 and G144 cell lines.

Gene	Chromosome position	Description	GBM2+VPA	G144+VPA
HES3*	1p36.31	hairy and enhancer of split 3 (Drosophila)	unmet	unmet
FLJ37453	1p36.21	uncharacterized LOC729614	unmet	unmet
TRAPPC3	1p34.3	trafficking protein particle complex 3	met	met
KANK4	1p31.3	KN motif and ankyrin repeat domains 4	unmet	unmet
CYP2J2	1p31.3-p31.2	cytochrome P450, family 2, subfamily J, polypeptide	met	met
CGN	1q21	cingulin	met	met
C1orf43	1q21.2	chromosome 1 open reading frame 43	met	met
DPM3	1q22	dolichyl-phosphate mannosyltransferase polypeptide 3	met	met
KRTCAP2	1q22	keratinocyte associated protein 2	met	met
BC047397	1q23.3	Homo sapiens cDNA clone IMAGE:5267529	unmet	unmet
LAD1	1q25.1-q32.3	ladinin 1	met	unmet
SH3BP5L	1q44	SH3-binding domain protein 5-lik	met	met
FLJ14126	2p24.1	hypothetical protein FLJ14126	met	met
PRKCE	2p21	protein kinase C, epsilon	met	unmet
AK027226	2p11.2	Homo sapiens cDNA: FLJ23573 fis, clone LNG12520	unmet	unmet
AK097347	2q11.1	Homo sapiens cDNA FLJ40028 fis, clone STOMA2008638	unmet	unmet
SCTR	2q14.1	secretin receptor	unmet	unmet
ERCC3	2q21	excision repair cross-complementing rodent repair deficiency, complementation group 3	met	met
LOC401010	2q21.1	nucleolar complex associated 2 homolog (S. cerevisiae) pseudogene	unmet	unmet
C3orf62	3p21.31	chromosome 3 open reading frame 62	unmet	unmet
CCDC13	3p22.1	coiled-coil domain containing 13	met	unmet
CYP8B1	3p22.1	cytochrome P450, family 8, subfamily B, polypeptide 1	met	met
KBTBD8	3p14	kelch repeat and BTB (POZ) domain containing 8	met	met
CPNE4	3q22.1	copine IV	met	met
OTP*	5q13.3	orthopedia homeobox	unmet	met
KCTD16	5q31.3	potassium channel tetramerisation domain containing 16	met	met
ZNF300	5q33.1	zinc finger protein 300	met	met
LOC153752	5q34	hypothetical gene supported by AK055284	unmet	unmet
ZNF322	6p22.1	zinc finger protein 322	met	met
ETV7*	6p21	ets variant 7	unmet	unmet
LYRM2	6q15	LYR motif containing 2	met	met
SFT2D1	6q27	SFT2 domain containing 1	met	met
ZNF680	7q11.21	zinc finger protein 680	unmet	unmet
CEP41	7q32	centrosomal protein 41kDa	met	unmet
WHSC1L1	8p11.2	Wolf-Hirschhorn syndrome candidate 1-like 1	met	met
LOC286189	8q13.1	uncharacterized LOC286189	met	unmet
RPL30	8q22	ribosomal protein L30	met	met
OSR2*	8q22.2	odd-skipped related 2 (Drosophila)	unmet	unmet
FAM49B	8q24.21	family with sequence similarity 49, member B	unmet	unmet

Table A13. Cont'd

Gene	Chromosome position	Description	GBM2+VPA	G144+VPA
NAPRT1	8q24.3	nicotinate phosphoribosyltransferase domain containing 1	unmet	unmet
PIGO	9p13.3	phosphatidylinositol glycan anchor biosynthesis, class O	met	met
GRIN3A	9q31.1	glutamate receptor, ionotropic, N-methyl-D-aspartate 3A	met	unmet
FAM125B	9q33.3	family with sequence similarity 125, member B	unmet	unmet
CD151	11p15.5	CD151 molecule (Raph blood group)	unmet	met
DBX1	11p15.1	developing brain homeobox 1	met	unmet
DRD4	11p15.5	dopamine receptor D4	met	met
LOC100129826	11p15.5	uncharacterized LOC100129826	unmet	unmet
PTPN5	11p15.1	protein tyrosine phosphatase, non-receptor type 5 (striatum-enriched)	met	unmet
SAAL1	11p15.1	serum amyloid A-like 1	met	unmet
TOLLIP	11p15.5	toll interacting protein	unmet	met
UEVLD	11p15.1	UEV and lactate/malate dehyrogenase domains	met	unmet
PRKCDBP	11p15.4	protein kinase C, delta binding protein	met	met
CSTF3	11p13	cleavage stimulation factor, 3' pre-RNA, subunit 3, 77kDa	unmet	unmet
ARFGAP2	11p11.2-p11.12	ADP-ribosylation factor GTPase activating protein 2	met	unmet
TP53I11	11p11.2	tumor protein p53 inducible protein 11	unmet	unmet
LOC441601	11p11.12	septin 7 pseudogene	unmet	met
TCIRG1	11q13.2	T-cell, immune regulator 1, ATPase, H+ transporting, lysosomal V0 subunit A3	unmet	met
AK124882	11q13.3	Homo sapiens cDNA FLJ42892 fis, clone BRHIP3008565	unmet	met
P2rx6	11q23	purinergic receptor P2X, ligand-gated ion channel, 6	met	met
CCDC77	12p13.33	coiled-coil domain containing 77	met	met
KIF5A	12q13.13	kinesin family member 5A	met	unmet
PAN2	12q13.2	PAN2 poly(A) specific ribonuclease subunit homolog (S. cerevisiae)	met	met
OBFC2B	12q13.3	oligonucleotide/oligosaccharide-binding fold containing 2B	met	met
STAT2	12q13.3	signal transducer and activator of transcription 2	met	met
LINC00485	12q23.2	long intergenic non-protein coding RNA 485	met	met
DHX37	12q24.31	DEAH (Asp-Glu-Ala-His) box polypeptide 37	met	met
POP5	12q24.31	processing of precursor 5, ribonuclease P/MRP subunit (S. cerevisiae)	met	unmet
SUGT1P3	13q14.11	suppressor of G2 allele of SKP1 (S. cerevisiae) pseudogene 3	unmet	met
RCBTB2	13q14.3	regulator of chromosome condensation (RCC1) and BTB (POZ) domain containing protein 2	met	met

Table A13. Cont'd

Gene	Chromosome position	Description	GBM2+VPA	G144+VPA
C13orf27	13q33.1	chromosome 13 open reading frame 27	unmet	unmet
TMEM55B	14q11.2	transmembrane protein 55B	met	met
SDR39U1	14q12	short chain dehydrogenase/reductase family 39U, member 1	met	met
STXBP6	14q12	syntaxin binding protein 6	met	met
NEK9	14q24.3	NIMA (never in mitosis gene a)-related kinase 9	unmet	unmet
ITPKA	15q15.1	inositol-trisphosphate 3-kinase A	unmet	unmet
SCAPER	15q24	S-phase cyclin A-associated protein in the ER	met	met
STOML1	15q24-q25	stomatin (EPB72)-like 1	met	met
POLG	15q25	polymerase (DNA directed), gamma	met	met
CLDN6	16p13.3	claudin 6	unmet	met
MYH11	16p13.11	myosin, heavy chain 11, smooth muscle	met	unmet
SRCAP	16p11.2	Snf2-related CREBBP activator protein	met	met
HOXB5	17q21.3	homeobox B5	met	unmet
C17orf64	17q23.2	chromosome 17 open reading frame 64	unmet	unmet
ZNF160	19q13.42	zinc finger protein 160	unmet	met
ZNF610	19q13.41	zinc finger protein 610	met	met
C19orf20	19p13.3	chromosome 19 open reading frame 20	unmet	met
WDR18	19p13.3	WD repeat domain 18	unmet	met
PIGU	20q11.2	phosphatidylinositol glycan anchor biosynthesis, class U	met	met
DDRGK1	20p13	DDRGK domain containing 1	met	met
ELMO2	20q13	engulfment and cell motility 2	met	met
TTPAL	20q13.12	tocopherol (alpha) transfer protein-like	met	unmet
C20orf166-AS1	20q13.33	C20orf166 antisense RNA 1 (non-protein coding)	met	unmet
MX1	21q22.3	myxovirus (influenza virus) resistance 1, interferon-inducible protein p78 (mouse)	met	met
DQ656048	22q12.2	Homo sapiens clone UGL074-A-H6, mRNA sequence	met	met
VENTXP1	Xp21.3	VENT homeobox pseudogene 1	unmet	met
PIM2	Xp11.23	pim-2 oncogene	met	met
DLG3	Xq13.1	discs, large homolog 3 (Drosophila)	met	met
MIR542	Xq26.3	microRNA 542	unmet	unmet

*genes targeted by Suz12 in ES cells (Lee et al., 2006b). Abbreviation: met, methylated; unmet, unmethylated gene promoters.

REFERENCES

Alaminos, M., Dávalos, V., Ropero, S., Setién, F., Paz, M.F., Herranz, M., Fraga, M.F., Mora, J., Cheung, N.K., Gerald, W.L., *et al.* (2005). EMP3, a myelin-related gene located in the critical 19q13.3 region, is epigenetically silenced and exhibits features of a candidate tumor suppressor in glioma and neuroblastoma. Cancer Res *65*, 2565-2571.

Angelucci, A., Muzi, P., Cristiano, L., Millimaggi, D., Cimini, A., Dolo, V., Miano, R., Vicentini, C., Cerù, M.P., and Bologna, M. (2008). Neuroendocrine transdifferentiation induced by VPA is mediated by PPARgamma activation and confers resistance to antiblastic therapy in prostate carcinoma. Prostate *68*, 588-598.

Aouali, N., Palissot, V., El-Khoury, V., Moussay, E., Janji, B., Pierson, S., Brons, N.H., Kellner, L., Bosseler, M., Van Moer, K., *et al.* (2009). Peroxisome proliferator-activated receptor gamma agonists potentiate the cytotoxic effect of valproic acid in multiple myeloma cells. Br J Haematol *147*, 662-671.

Aronica, E., Boer, K., Becker, A., Redeker, S., Spliet, W.G., van Rijen, P.C., Wittink, F., Breit, T., Wadman, W.J., Lopes da Silva, F.H., *et al.* (2008). Gene expression profile analysis of epilepsy-associated gangliogliomas. Neuroscience *151*, 272-292.

Artavanis-Tsakonas, S., Rand, M.D., and Lake, R.J. (1999). Notch signaling: cell fate control and signal integration in development. Science *284*, 770-776.

Asklund, T., Appelskog, I.B., Ammerpohl, O., Ekström, T.J., and Almqvist, P.M. (2004). Histone deacetylase inhibitor 4-phenylbutyrate modulates glial fibrillary acidic protein and connexin 43 expression, and enhances gap-junction communication, in human glioblastoma cells. Eur J Cancer *40*, 1073-1081.

Baeza, N., Weller, M., Yonekawa, Y., Kleihues, P., and Ohgaki, H. (2003). PTEN methylation and expression in glioblastomas. Acta Neuropathol *106*, 479-485.

Bao, S., Wu, Q., McLendon, R.E., Hao, Y., Shi, Q., Hjelmeland, A.B., Dewhirst, M.W., Bigner, D.D., and Rich, J.N. (2006). Glioma stem cells promote radioresistance by preferential activation of the DNA damage response. Nature *444*, 756-760.

Barbashina, V., Salazar, P., Holland, E.C., Rosenblum, M.K., and Ladanyi, M. (2005). Allelic losses at 1p36 and 19q13 in gliomas: correlation with histologic classification, definition of a 150-kb minimal deleted region on 1p36, and evaluation of CAMTA1 as a candidate tumor suppressor gene. Clin Cancer Res *11*, 1119-1128.

Bayani, J., Pandita, A., and Squire, J.A. (2005). Molecular cytogenetic analysis in the study of brain tumors: findings and applications. Neurosurg Focus *19*, E1.

Behin, A., Hoang-Xuan, K., Carpentier, A.F., and Delattre, J.Y. (2003). Primary brain tumours in adults. Lancet *361*, 323-331.

Beier, D., Hau, P., Proescholdt, M., Lohmeier, A., Wischhusen, J., Oefner, P.J., Aigner, L., Brawanski, A., Bogdahn, U., and Beier, C.P. (2007). CD133(+) and CD133(-) glioblastoma-derived cancer stem cells show differential growth characteristics and molecular profiles. Cancer Res *67*, 4010-4015.

Beissbarth, T., and Speed, T.P. (2004). GOstat: find statistically overrepresented Gene Ontologies within a group of genes. Bioinformatics *20*, 1464-1465.

Ben-Porath, I., Thomson, M.W., Carey, V.J., Ge, R., Bell, G.W., Regev, A., and Weinberg, R.A. (2008). An embryonic stem cell-like gene expression signature in poorly differentiated aggressive human tumors. Nat Genet *40*, 499-507.

Bentivegna, A., Conconi, D., Panzeri, E., Sala, E., Bovo, G., Viganò, P., Brunelli, S., Bossi, M., Tredici, G., Strada, G., *et al.* (2010). Biological heterogeneity of putative bladder cancer stem-like cell populations from human bladder transitional cell carcinoma samples. Cancer Sci *101*, 416-424.

Benítez, J.A., Arregui, L., Cabrera, G., and Segovia, J. (2008). Valproic acid induces polarization, neuronal-like differentiation of a subpopulation of C6 glioma cells and selectively regulates transgene expression. Neuroscience *156*, 911-920.

Berger, S.L., Kouzarides, T., Shiekhattar, R., and Shilatifard, A. (2009). An operational definition of epigenetics. Genes Dev *23*, 781-783.

Bernstein, B.E., Meissner, A., and Lander, E.S. (2007). The mammalian epigenome. Cell *128*, 669-681.

Bernstein, B.E., Mikkelsen, T.S., Xie, X., Kamal, M., Huebert, D.J., Cuff, J., Fry, B., Meissner, A., Wernig, M., Plath, K., *et al.* (2006). A bivalent chromatin structure marks key developmental genes in embryonic stem cells. Cell *125*, 315-326.

Bhattacharya, S., Das, A., Mallya, K., and Ahmad, I. (2007). Maintenance of retinal stem cells by Abcg2 is regulated by notch signaling. J Cell Sci *120*, 2652-2662.

Bird, A. (2002). DNA methylation patterns and epigenetic memory. Genes Dev *16*, 6-21.

Blaheta, R.A., Michaelis, M., Driever, P.H., and Cinatl, J. (2005). Evolving anticancer drug valproic acid: insights into the mechanism and clinical studies. Med Res Rev *25*, 383-397.

Bonavia, R., Inda, M.M., Cavenee, W.K., and Furnari, F.B. (2011). Heterogeneity maintenance in glioblastoma: a social network. Cancer Res *71*, 4055-4060.

Bonnet, D., and Dick, J.E. (1997). Human acute myeloid leukemia is organized as a hierarchy that originates from a primitive hematopoietic cell. Nat Med *3*, 730-737.

Botrugno, O.A., Santoro, F., and Minucci, S. (2009). Histone deacetylase inhibitors as a new weapon in the arsenal of differentiation therapies of cancer. Cancer Lett *280*, 134-144.

Brandes, A.A., Franceschi, E., Tosoni, A., Blatt, V., Pession, A., Tallini, G., Bertorelle, R., Bartolini, S., Calbucci, F., Andreoli, A., *et al.* (2008). MGMT promoter methylation status can predict the incidence and outcome of pseudoprogression after concomitant radiochemotherapy in newly diagnosed glioblastoma patients. J Clin Oncol *26*, 2192-2197.

Bredberg, A., and Bodmer, W. (2007). Cytostatic drug treatment causes seeding of gene promoter methylation. Eur J Cancer *43*, 947-954.

Buckner, J.C., Brown, P.D., O'Neill, B.P., Meyer, F.B., Wetmore, C.J., and Uhm, J.H. (2007). Central nervous system tumors. Mayo Clin Proc *82*, 1271-1286.

Büschges, R., Weber, R.G., Actor, B., Lichter, P., Collins, V.P., and Reifenberger, G. (1999). Amplification and expression of cyclin D genes (CCND1, CCND2 and CCND3) in human malignant gliomas. Brain Pathol *9*, 435-442; discussion 432-433.

Cadieux, B., Ching, T.T., VandenBerg, S.R., and Costello, J.F. (2006). Genome-wide hypomethylation in human glioblastomas associated with specific copy number alteration, methylenetetrahydrofolate reductase allele status, and increased proliferation. Cancer Res *66*, 8469-8476.

Cahan, M.A., Walter, K.A., Colvin, O.M., and Brem, H. (1994). Cytotoxicity of taxol in vitro against human and rat malignant brain tumors. Cancer Chemother Pharmacol *33*, 441-444.

Cairncross, G., Berkey, B., Shaw, E., Jenkins, R., Scheithauer, B., Brachman, D., Buckner, J., Fink, K., Souhami, L., Laperierre, N., *et al.* (2006). Phase III trial of chemotherapy plus radiotherapy compared with radiotherapy alone for pure and mixed anaplastic oligodendroglioma: Intergroup Radiation Therapy Oncology Group Trial 9402. J Clin Oncol *24*, 2707-2714.

Cameron, E.E., Bachman, K.E., Myohanen, S., Herman, J.G., and Baylin, S.B. (1999). Synergy of demethylation and histone deacetylase inhibition in the re-expression of genes silenced in cancer. Nature Genet *21*, 103-107.

Campbell, T.N., and Robbins, S.M. (2008). The Eph receptor/ephrin system: an emerging player in the invasion game. Curr Issues Mol Biol *10*, 61-66.

Camphausen, K., Cerna, D., Scott, T., Sproull, M., Burgan, W.E., Cerra, M.A., Fine, H., and Tofilon, P.J. (2005). Enhancement of in vitro and in vivo tumor cell radiosensitivity by valproic acid. Int J Cancer *114*, 380-386.

Catalano, M.G., Fortunati, N., Pugliese, M., Costantino, L., Poli, R., Bosco, O., and Boccuzzi, G. (2005). Valproic acid induces apoptosis and cell cycle arrest in poorly differentiated thyroid cancer cells. J Clin Endocrinol Metab *90*, 1383-1389.

Catalano, M.G., Poli, R., Pugliese, M., Fortunati, N., and Boccuzzi, G. (2007). Valproic acid enhances tubulin acetylation and apoptotic activity of paclitaxel on anaplastic thyroid cancer cell lines. Endocr Relat Cancer *14*, 839-845.

Cavaletti, G., Tredici, G., Braga, M., and Tazzari, S. (1995). Experimental peripheral neuropathy induced in adult rats by repeated intraperitoneal administration of taxol. Exp Neurol *133*, 64-72.

Cervoni, N., and Szyf, M. (2001). Demethylase activity is directed by histone acetylation. J Biol Chem *276*, 40778-40787.

Chaffanet, M., Chauvin, C., Lainé, M., Berger, F., Chédin, M., Rost, N., Nissou, M.F., and Benabid, A.L. (1992). EGF receptor amplification and expression in human brain tumours. Eur J Cancer *28*, 11-17.

Chakravarthy, A.B., Kelley, M.C., McLaren, B., Truica, C.I., Billheimer, D., Mayer, I.A., Grau, A.M., Johnson, D.H., Simpson, J.F., Beauchamp, R.D., *et al.* (2006). Neoadjuvant concurrent paclitaxel and radiation in stage II/III breast cancer. Clin Cancer Res *12*, 1570-1576.

Chamberlain, M.C., and Kormanik, P. (1995). Salvage chemotherapy with paclitaxel for recurrent primary brain tumors. J Clin Oncol *13*, 2066-2071.

Chan, T.A., Glockner, S., Yi, J.M., Chen, W., Van Neste, L., Cope, L., Herman, J.G., Velculescu, V., Schuebel, K.E., Ahuja, N., *et al.* (2008). Convergence of mutation and epigenetic alterations identifies common genes in cancer that predict for poor prognosis. PLoS Med *5*, e114.

Chari, R., Thu, K.L., Wilson, I.M., Lockwood, W.W., Lonergan, K.M., Coe, B.P., Malloff, C.A., Gazdar, A.F., Lam, S., Garnis, C., *et al.* (2010). Integrating the multiple dimensions of genomic and epigenomic landscapes of cancer. Cancer Metastasis Rev *29*, 73-93.

Chateauvieux, S., Morceau, F., Dicato, M., and Diederich, M. (2010). Molecular and therapeutic potential and toxicity of valproic acid. J Biomed Biotechnol *2010*.

Chen, C.H., Chang, Y.J., Ku, M.S., Chung, K.T., and Yang, J.T. (2011). Enhancement of temozolomide-induced apoptosis by valproic acid in human glioma cell lines through redox regulation. J Mol Med (Berl) *89*, 303-315.

Chen, J.G., and Horwitz, S.B. (2002). Differential mitotic responses to microtubule-stabilizing and -destabilizing drugs. Cancer Res *62*, 1935-1938.

Cheng, Y.C., Lin, H., Huang, M.J., Chow, J.M., Lin, S., and Liu, H.E. (2007). Downregulation of c-Myc is critical for valproic acid-induced growth arrest and myeloid differentiation of acute myeloid leukemia. Leuk Res *31*, 1403-1411.

Cheung, S.W., Shaw, C.A., Scott, D.A., Patel, A., Sahoo, T., Bacino, C.A., Pursley, A., Li, J., Erickson, R., Gropman, A.L., *et al.* (2007). Microarray-based CGH detects chromosomal mosaicism not revealed by conventional cytogenetics. Am J Med Genet A *143A*, 1679-1686.

Cinatl, J., Driever, P.H., Kotchetkov, R., Pouckova, P., Kornhuber, B., and Schwabe, D. (1997). Sodium valproate inhibits in vivo growth of human neuroblastoma cells. Anticancer Drugs *8*, 958-963.

Cinatl, J., Scholz, M., Driever, P.H., Henrich, D., Kabickova, H., Vogel, J.U., Doerr, H.W., and Kornhuber, B. (1996). Antitumor activity of sodium valproate in cultures of human neuroblastoma cells. Anticancer Drugs *7*, 766-773.

Clarke, M.F., Dick, J.E., Dirks, P.B., Eaves, C.J., Jamieson, C.H., Jones, D.L., Visvader, J., Weissman, I.L., and Wahl, G.M. (2006). Cancer stem cells--perspectives on current status and future directions: AACR Workshop on cancer stem cells. Cancer Res *66*, 9339-9344.

Coomber, B.L., Stewart, P.A., Hayakawa, K., Farrell, C.L., and Del Maestro, R.F. (1987). Quantitative morphology of human glioblastoma multiforme microvessels: structural basis of blood-brain barrier defect. J Neurooncol *5*, 299-307.

Costello, J.F. (2000). Aberrant CpG-island methylation has non-random and tumour-type-specific patterns. Nature Genet *24*, 132-138.

Costello, J.F., Berger, M.S., Huang, H.S., and Cavenee, W.K. (1996). Silencing of p16/CDKN2 expression in human gliomas by methylation and chromatin condensation. Cancer Res *56*, 2405-2410.

Costello, J.F., Plass, C., Arap, W., Chapman, V.M., Held, W.A., Berger, M.S., Su Huang, H.J., and Cavenee, W.K. (1997). Cyclin-dependent kinase 6 (CDK6) amplification in human gliomas identified using two-dimensional separation of genomic DNA. Cancer Res *57*, 1250-1254.

Costello, J.F., Plass, C., and Cavenee, W.K. (2000). Aberrant methylation of genes in low-grade astrocytomas. Brain Tumor Pathol *17*, 49-56.

Crown, J., and O'Leary, M. (2000). The taxanes: an update. Lancet *355*, 1176-1178.

Dahlback, H.S., Brandal, P., Meling, T.R., Gorunova, L., Scheie, D., and Heim, S. (2009). Genomic aberrations in 80 cases of primary glioblastoma multiforme: Pathogenetic heterogeneity and putative cytogenetic pathways. Genes Chromosomes Cancer *48*, 908-924.

Dalerba, P., Cho, R.W., and Clarke, M.F. (2007). Cancer stem cells: models and concepts. Annu Rev Med *58*, 267-284.

De la Cruz-Hernández, E., Perez-Plasencia, C., Pérez-Cardenas, E., Gonzalez-Fierro, A., Trejo-Becerril, C., Chávez-Blanco, A., Taja-Chayeb, L., Vidal, S., Gutiérrez, O., Dominguez, G.I., *et al.* (2011).

Transcriptional changes induced by epigenetic therapy with hydralazine and magnesium valproate in cervical carcinoma. Oncol Rep *25*, 399-407.

De Smet, C., De Backer, O., Faraoni, I., Lurquin, C., Brasseur, F., and Boon, T. (1996). The activation of human gene MAGE-1 in tumor cells is correlated with genome-wide demethylation. Proc Natl Acad Sci U S A *93*, 7149-7153.

De Smet, C., Loriot, A., and Boon, T. (2004). Promoter-dependent mechanism leading to selective hypomethylation within the 5' region of gene MAGE-A1 in tumor cells. Mol Cell Biol *24*, 4781-4790.

de Tayrac, M., Etcheverry, A., Aubry, M., Saïkali, S., Hamlat, A., Quillien, V., Le Treut, A., Galibert, M.D., and Mosser, J. (2009). Integrative genome-wide analysis reveals a robust genomic glioblastoma signature associated with copy number driving changes in gene expression. Genes Chromosomes Cancer *48*, 55-68.

De Witt Hamer, P.C., Van Tilborg, A.A., Eijk, P.P., Sminia, P., Troost, D., Van Noorden, C.J., Ylstra, B., and Leenstra, S. (2008). The genomic profile of human malignant glioma is altered early in primary cell culture and preserved in spheroids. Oncogene *27*, 2091-2096.

DeAngelis, L.M. (2001). Brain tumors. N Engl J Med *344*, 114-123.

Denysenko, T., Gennero, L., Roos, M.A., Melcarne, A., Juenemann, C., Faccani, G., Morra, I., Cavallo, G., Reguzzi, S., Pescarmona, G., *et al.* (2010). Glioblastoma cancer stem cells: heterogeneity, microenvironment and related therapeutic strategies. Cell Biochem Funct *28*, 343-351.

Dirks, P.B. (2008). Brain tumour stem cells: the undercurrents of human brain cancer and their relationship to neural stem cells. Philos Trans R Soc Lond B Biol Sci *363*, 139-152.

Doetsch, F., Caillé, I., Lim, D.A., García-Verdugo, J.M., and Alvarez-Buylla, A. (1999). Subventricular zone astrocytes are neural stem cells in the adult mammalian brain. Cell *97*, 703-716.

Dropcho, E.J., and Soong, S.J. (1996). The prognostic impact of prior low grade histology in patients with anaplastic gliomas: a case-control study. Neurology *47*, 684-690.

Ducray, F., Idbaih, A., de Reyniès, A., Bièche, I., Thillet, J., Mokhtari, K., Lair, S., Marie, Y., Paris, S., Vidaud, M., *et al.* (2008). Anaplastic oligodendrogliomas with 1p19q codeletion have a proneural gene expression profile. Mol Cancer *7*, 41.

Duenas-Gonzalez, A., Candelaria, M., Perez-Plascencia, C., Perez-Cardenas, E., de la Cruz-Hernandez, E., and Herrera, L.A. (2008). Valproic acid as epigenetic cancer drug: preclinical, clinical and transcriptional effects on solid tumors. Cancer Treat Rev *34*, 206-222.

Eden, A., Gaudet, F., Waghmare, A., and Jaenisch, R. (2003). Chromosomal instability and tumors promoted by DNA hypomethylation. Science *300*, 455.

Ehrich, M., Turner, J., Gibbs, P., Lipton, L., Giovanneti, M., Cantor, C., and van den Boom, D. (2008). Cytosine methylation profiling of cancer cell lines. Proc Natl Acad Sci U S A *105*, 4844-4849.

Ehrlich, M. (2002). DNA methylation in cancer: too much, but also too little. Oncogene *21*, 5400-5413.

Elhajouji, A., Cunha, M., and Kirsch-Volders, M. (1998). Spindle poisons can induce polyploidy by mitotic slippage and micronucleate mononucleates in the cytokinesis-block assay. Mutagenesis *13*, 193-198.

Erenpreisa, J.E., Ivanov, A., Dekena, G., Vitina, A., Krampe, R., Freivalds, T., Selivanova, G., and Roach, H.I. (2000). Arrest in metaphase and anatomy of mitotic catastrophe: mild heat shock in two human osteosarcoma cell lines. Cell Biol Int *24*, 61-70.

Ernst, A., Hofmann, S., Ahmadi, R., Becker, N., Korshunov, A., Engel, F., Hartmann, C., Felsberg, J., Sabel, M., Peterziel, H., *et al.* (2009). Genomic and expression profiling of glioblastoma stem cell-like spheroid cultures identifies novel tumor-relevant genes associated with survival. Clin Cancer Res *15*, 6541-6550.

Esteller, M. (2002). CpG island hypermethylation and tumor suppressor genes: a booming present, a brighter future. Oncogene *21*, 5427-5440.

Esteller, M. (2005). Aberrant DNA methylation as a cancer-inducing mechanism. Annu Rev Pharmacol Toxicol *45*, 629-656.

Esteller, M. (2007a). Cancer epigenomics: DNA methylomes and histone-modification maps. Nat Rev Genet *8*, 286-298.

Esteller, M. (2007b). Epigenetic gene silencing in cancer: the DNA hypermethylome. Hum Mol Genet *16 Spec No 1*, R50-59.

Esteller, M. (2008). Epigenetics in cancer. N Engl J Med *358*, 1148-1159.

Esteller, M., Hamilton, S.R., Burger, P.C., Baylin, S.B., and Herman, J.G. (1999). Inactivation of the DNA repair gene O6-methylguanine-DNA methyltransferase by promoter hypermethylation is a common event in primary human neoplasia. Cancer Res *59*, 793-797.

Eyler, C.E., and Rich, J.N. (2008). Survival of the fittest: cancer stem cells in therapeutic resistance and angiogenesis. J Clin Oncol *26*, 2839-2845.

Fan, X., Salford, L.G., and Widegren, B. (2007). Glioma stem cells: evidence and limitation. Semin Cancer Biol *17*, 214-218.

Fanelli, M., Caprodossi, S., Ricci-Vitiani, L., Porcellini, A., Tomassoni-Ardori, F., Amatori, S., Andreoni, F., Magnani, M., De Maria, R., Santoni, A., *et al.* (2008). Loss of pericentromeric DNA methylation pattern in human glioblastoma is associated with altered DNA methyltransferases expression and involves the stem cell compartment. Oncogene *27*, 358-365.

Farrell, C.J., and Plotkin, S.R. (2007). Genetic causes of brain tumors: neurofibromatosis, tuberous sclerosis, von Hippel-Lindau, and other syndromes. Neurol Clin *25*, 925-946, viii.

Feinberg, A.P., Ohlsson, R., and Henikoff, S. (2006). The epigenetic progenitor origin of human cancer. Nat Rev Genet *7*, 21-33.

Fellner, S., Bauer, B., Miller, D.S., Schaffrik, M., Fankhänel, M., Spruss, T., Bernhardt, G., Graeff, C., Färber, L., Gschaidmeier, H., *et al.* (2002). Transport of paclitaxel (Taxol) across the blood-brain barrier in vitro and in vivo. J Clin Invest *110*, 1309-1318.

Fisher, J.L., Schwartzbaum, J.A., Wrensch, M., and Wiemels, J.L. (2007). Epidemiology of brain tumors. Neurol Clin *25*, 867-890, vii.

Foltz, G., Yoon, J.G., Lee, H., Ryken, T.C., Sibenaller, Z., Ehrich, M., Hood, L., and Madan, A. (2009). DNA methyltransferase-mediated transcriptional silencing in malignant glioma: a combined whole-genome microarray and promoter array analysis. Oncogene *28*, 2667-2677.

Fraga, M.F., Ballestar, E., Villar-Garea, A., Boix-Chornet, M., Espada, J., Schotta, G., Bonaldi, T., Haydon, C., Ropero, S., Petrie, K., *et al.* (2005). Loss of acetylation at Lys16 and trimethylation at Lys20 of histone H4 is a common hallmark of human cancer. Nat Genet *37*, 391-400.

Frankel, R.H., Bayona, W., Koslow, M., and Newcomb, E.W. (1992). p53 mutations in human malignant gliomas: comparison of loss of heterozygosity with mutation frequency. Cancer Res *52*, 1427-1433.

Frederick, L., Wang, X.Y., Eley, G., and James, C.D. (2000). Diversity and frequency of epidermal growth factor receptor mutations in human glioblastomas. Cancer Res *60*, 1383-1387.

Frew, A.J., Johnstone, R.W., and Bolden, J.E. (2009). Enhancing the apoptotic and therapeutic effects of HDAC inhibitors. Cancer Lett *280*, 125-133.

Fuks, F., Hurd, P.J., Wolf, D., Nan, X., Bird, A.P., and Kouzarides, T. (2003). The methyl-CpG-binding protein MeCP2 links DNA methylation to histone methylation. J Biol Chem *278*, 4035-4040.

Furnari, F.B., Fenton, T., Bachoo, R.M., Mukasa, A., Stommel, J.M., Stegh, A., Hahn, W.C., Ligon, K.L., Louis, D.N., Brennan, C., *et al.* (2007). Malignant astrocytic glioma: genetics, biology, and paths to treatment. Genes Dev *21*, 2683-2710.

Galli, R., Binda, E., Orfanelli, U., Cipelletti, B., Gritti, A., De Vitis, S., Fiocco, R., Foroni, C., Dimeco, F., and Vescovi, A. (2004). Isolation and characterization of tumorigenic, stem-like neural precursors from human glioblastoma. Cancer Res *64*, 7011-7021.

Gardiner-Garden, M., and Frommer, M. (1987). CpG islands in vertebrate genomes. J Mol Biol *196*, 261-282.

Gaymes, T.J., Padua, R.A., Pla, M., Orr, S., Omidvar, N., Chomienne, C., Mufti, G.J., and Rassool, F.V. (2006). Histone deacetylase inhibitors (HDI) cause DNA damage in leukemia cells: a mechanism for leukemia-specific HDI-dependent apoptosis? Mol Cancer Res *4*, 563-573.

Giannakakou, P., Sackett, D.L., Kang, Y.K., Zhan, Z., Buters, J.T., Fojo, T., and Poruchynsky, M.S. (1997). Paclitaxel-resistant human ovarian cancer cells have mutant beta-tubulins that exhibit impaired paclitaxel-driven polymerization. J Biol Chem *272*, 17118-17125.

Giannini, C., Burger, P.C., Berkey, B.A., Cairncross, J.G., Jenkins, R.B., Mehta, M., Curran, W.J., and Aldape, K. (2008). Anaplastic oligodendroglial tumors: refining the correlation among histopathology, 1p 19q deletion and clinical outcome in Intergroup Radiation Therapy Oncology Group Trial 9402. Brain Pathol *18*, 360-369.

Gottesman, M.M. (2002). Mechanisms of cancer drug resistance. Annu Rev Med *53*, 615-627.

Gottlicher, M. (2001). Valproic acid defines a novel class of HDAC inhibitors inducing differentiation of transformed cells. EMBO J *20*, 6969-6978.

Greger, V., Passarge, E., Höpping, W., Messmer, E., and Horsthemke, B. (1989). Epigenetic changes may contribute to the formation and spontaneous regression of retinoblastoma. Hum Genet *83*, 155-158.

Gregory, P.D., Wagner, K., and Hörz, W. (2001). Histone acetylation and chromatin remodeling. Exp Cell Res *265*, 195-202.

Griffero, F., Daga, A., Marubbi, D., Capra, M.C., Melotti, A., Pattarozzi, A., Gatti, M., Bajetto, A., Porcile, C., Barbieri, F., *et al.* (2009). Different response of human glioma tumor-initiating cells to epidermal growth factor receptor kinase inhibitors. J Biol Chem *284*, 7138-7148.

Gu, J., Kawai, H., Nie, L., Kitao, H., Wiederschain, D., Jochemsen, A.G., Parant, J., Lozano, G., and Yuan, Z.M. (2002). Mutual dependence of MDM2 and MDMX in their functional inactivation of p53. J Biol Chem *277*, 19251-19254.

Göttlicher, M., Minucci, S., Zhu, P., Krämer, O.H., Schimpf, A., Giavara, S., Sleeman, J.P., Lo Coco, F., Nervi, C., Pelicci, P.G., *et al.* (2001). Valproic acid defines a novel class of HDAC inhibitors inducing differentiation of transformed cells. EMBO J *20*, 6969-6978.

Günther, H.S., Schmidt, N.O., Phillips, H.S., Kemming, D., Kharbanda, S., Soriano, R., Modrusan, Z., Meissner, H., Westphal, M., and Lamszus, K. (2008). Glioblastoma-derived stem cell-enriched cultures form distinct subgroups according to molecular and phenotypic criteria. Oncogene *27*, 2897-2909.

Gürsel, D.B., Beyene, R.T., Hofstetter, C., Greenfield, J.P., Souweidane, M.M., Kaplitt, M., Arango-Lievano, M., Howard, B., and Boockvar, J.A. (2011a). Optimization of glioblastoma multiforme stem cell isolation, transfection, and transduction. J Neurooncol *104*, 509-522.

Gürsel, D.B., Shin, B.J., Burkhardt, J.K., Kesavabhotla, K., Schlaff, C.D., and Boockvar, J.A. (2011b). Glioblastoma Stem-Like Cells-Biology and Therapeutic Implications. Cancers (Basel) *3*, 2655-2666.

Hadjipanayis, C.G., and Van Meir, E.G. (2009). Brain cancer propagating cells: biology, genetics and targeted therapies. Trends Mol Med *15*, 519-530.

Hastings, P.J., Ira, G., and Lupski, J.R. (2009). A microhomology-mediated break-induced replication model for the origin of human copy number variation. PLoS Genet *5*, e1000327.

Hatziapostolou, M., and Iliopoulos, D. (2011). Epigenetic aberrations during oncogenesis. Cell Mol Life Sci *68*, 1681-1702.

Hegi, M.E., Diserens, A.C., Gorlia, T., Hamou, M.F., de Tribolet, N., Weller, M., Kros, J.M., Hainfellner, J.A., Mason, W., Mariani, L., *et al.* (2005). MGMT gene silencing and benefit from temozolomide in glioblastoma. N Engl J Med *352*, 997-1003.

Heimans, J.J., Vermorken, J.B., Wolbers, J.G., Eeltink, C.M., Meijer, O.W., Taphoorn, M.J., and Beijnen, J.H. (1994). Paclitaxel (Taxol) concentrations in brain tumor tissue. Ann Oncol *5*, 951-953.

Hemmati, H.D., Nakano, I., Lazareff, J.A., Masterman-Smith, M., Geschwind, D.H., Bronner-Fraser, M., and Kornblum, H.I. (2003). Cancerous stem cells can arise from pediatric brain tumors. Proc Natl Acad Sci U S A *100*, 15178-15183.

Heng, H.H., Stevens, J.B., Liu, G., Bremer, S.W., and Ye, C.J. (2004). Imaging genome abnormalities in cancer research. Cell Chromosome *3*, 1.

Hermanson, M., Funa, K., Hartman, M., Claesson-Welsh, L., Heldin, C.H., Westermark, B., and Nistér, M. (1992). Platelet-derived growth factor and its receptors in human glioma tissue: expression of messenger RNA and protein suggests the presence of autocrine and paracrine loops. Cancer Res *52*, 3213-3219.

Hicklin, D.J., and Ellis, L.M. (2005). Role of the vascular endothelial growth factor pathway in tumor growth and angiogenesis. J Clin Oncol *23*, 1011-1027.

Hirschmann-Jax, C., Foster, A.E., Wulf, G.G., Nuchtern, J.G., Jax, T.W., Gobel, U., Goodell, M.A., and Brenner, M.K. (2004). A distinct "side population" of cells with high drug efflux capacity in human tumor cells. Proc Natl Acad Sci U S A *101*, 14228-14233.

Horwitz, S.B. (1992). Mechanism of action of taxol. Trends Pharmacol Sci *13*, 134-136.

Howard, G., Eiges, R., Gaudet, F., Jaenisch, R., and Eden, A. (2008). Activation and transposition of endogenous retroviral elements in hypomethylation induced tumors in mice. Oncogene *27*, 404-408.

Hrzenjak, A., Moinfar, F., Kremser, M.L., Strohmeier, B., Staber, P.B., Zatloukal, K., and Denk, H. (2006). Valproate inhibition of histone deacetylase 2 affects differentiation and decreases proliferation of endometrial stromal sarcoma cells. Mol Cancer Ther *5*, 2203-2210.

Hsu, P.P., and Sabatini, D.M. (2008). Cancer cell metabolism: Warburg and beyond. Cell *134*, 703-707.

Huang, Q., Zhang, Q.B., Dong, J., Wu, Y.Y., Shen, Y.T., Zhao, Y.D., Zhu, Y.D., Diao, Y., Wang, A.D., and Lan, Q. (2008). Glioma stem cells are more aggressive in recurrent tumors with malignant progression than in the primary tumor, and both can be maintained long-term in vitro. BMC Cancer *8*, 304.

Huang, Z., Cheng, L., Guryanova, O.A., Wu, Q., and Bao, S. (2010). Cancer stem cells in glioblastoma--molecular signaling and therapeutic targeting. Protein Cell *1*, 638-655.

Huse, J.T., and Holland, E.C. (2010). Targeting brain cancer: advances in the molecular pathology of malignant glioma and medulloblastoma. Nat Rev Cancer *10*, 319-331.

Huse, J.T., Phillips, H.S., and Brennan, C.W. (2011). Molecular subclassification of diffuse gliomas: seeing order in the chaos. Glia *59*, 1190-1199.

Ichimura, K., Bolin, M.B., Goike, H.M., Schmidt, E.E., Moshref, A., and Collins, V.P. (2000). Deregulation of the p14ARF/MDM2/p53 pathway is a prerequisite for human astrocytic gliomas with G1-S transition control gene abnormalities. Cancer Res *60*, 417-424.

Ichimura, K., Ohgaki, H., Kleihues, P., and Collins, V.P. (2004). Molecular pathogenesis of astrocytic tumours. J Neurooncol *70*, 137-160.

Ichimura, K., Schmidt, E.E., Goike, H.M., and Collins, V.P. (1996). Human glioblastomas with no alterations of the CDKN2A (p16INK4A, MTS1) and CDK4 genes have frequent mutations of the retinoblastoma gene. Oncogene *13*, 1065-1072.

Ichimura, K., Vogazianou, A.P., Liu, L., Pearson, D.M., Bäcklund, L.M., Plant, K., Baird, K., Langford, C.F., Gregory, S.G., and Collins, V.P. (2008). 1p36 is a preferential target of chromosome 1 deletions in astrocytic tumours and homozygously deleted in a subset of glioblastomas. Oncogene *27*, 2097-2108.

Idbaih, A., Crinière, E., Ligon, K.L., Delattre, O., and Delattre, J.Y. (2010). Array-based genomics in glioma research. Brain Pathol *20*, 28-38.

Idbaih, A., Marie, Y., Pierron, G., Brennetot, C., Hoang-Xuan, K., Kujas, M., Mokhtari, K., Sanson, M., Lejeune, J., Aurias, A., *et al.* (2005). Two types of chromosome 1p losses with opposite significance in gliomas. Ann Neurol *58*, 483-487.

Ignatova, T.N., Kukekov, V.G., Laywell, E.D., Suslov, O.N., Vrionis, F.D., and Steindler, D.A. (2002). Human cortical glial tumors contain neural stem-like cells expressing astroglial and neuronal markers in vitro. Glia *39*, 193-206.

Ikushima, H., Todo, T., Ino, Y., Takahashi, M., Miyazawa, K., and Miyazono, K. (2009). Autocrine TGF-beta signaling maintains tumorigenicity of glioma-initiating cells through Sry-related HMG-box factors. Cell Stem Cell *5*, 504-514.

Iourov, I.Y., Vorsanova, S.G., and Yurov, Y.B. (2008). Molecular cytogenetics and cytogenomics of brain diseases. Curr Genomics *9*, 452-465.

Ishii, H., Iwatsuki, M., Ieta, K., Ohta, D., Haraguchi, N., Mimori, K., and Mori, M. (2008). Cancer stem cells and chemoradiation resistance. Cancer Sci *99*, 1871-1877.

Izumoto, S., Arita, N., Ohnishi, T., Hiraga, S., Taki, T., and Hayakawa, T. (1995). Homozygous deletions of p16INK4A/MTS1 and p15INK4B/MTS2 genes in glioma cells and primary glioma tissues. Cancer Lett *97*, 241-247.

Jemal, A., Siegel, R., Ward, E., Murray, T., Xu, J., and Thun, M.J. (2007). Cancer statistics, 2007. CA Cancer J Clin *57*, 43-66.

Jen, J., Harper, J.W., Bigner, S.H., Bigner, D.D., Papadopoulos, N., Markowitz, S., Willson, J.K., Kinzler, K.W., and Vogelstein, B. (1994). Deletion of p16 and p15 genes in brain tumors. Cancer Res *54*, 6353-6358.

Jeon, H.M., Jin, X., Lee, J.S., Oh, S.Y., Sohn, Y.W., Park, H.J., Joo, K.M., Park, W.Y., Nam, D.H., DePinho, R.A., *et al.* (2008). Inhibitor of differentiation 4 drives brain tumor-initiating cell genesis through cyclin E and notch signaling. Genes Dev *22*, 2028-2033.

Jones, P.A., and Baylin, S.B. (2002). The fundamental role of epigenetic events in cancer. Nat Rev Genet *3*, 415-428.

Jones, P.A., and Baylin, S.B. (2007). The epigenomics of cancer. Cell *128*, 683-692.

Joo, K.M., Kim, S.Y., Jin, X., Song, S.Y., Kong, D.S., Lee, J.I., Jeon, J.W., Kim, M.H., Kang, B.G., Jung, Y., *et al.* (2008). Clinical and biological implications of CD133-positive and CD133-negative cells in glioblastomas. Lab Invest *88*, 808-815.

Jordan, M.A., Wendell, K., Gardiner, S., Derry, W.B., Copp, H., and Wilson, L. (1996). Mitotic block induced in HeLa cells by low concentrations of paclitaxel (Taxol) results in abnormal mitotic exit and apoptotic cell death. Cancer Res *56*, 816-825.

Jordan, M.A., and Wilson, L. (1998). Microtubules and actin filaments: dynamic targets for cancer chemotherapy. Curr Opin Cell Biol *10*, 123-130.

Kamath, K., Wilson, L., Cabral, F., and Jordan, M.A. (2005). BetaIII-tubulin induces paclitaxel resistance in association with reduced effects on microtubule dynamic instability. J Biol Chem *280*, 12902-12907.

Karmakar, S., Banik, N.L., Patel, S.J., and Ray, S.K. (2007). Combination of all-trans retinoic acid and taxol regressed glioblastoma T98G xenografts in nude mice. Apoptosis *12*, 2077-2087.

Karmakar, S., Banik, N.L., and Ray, S.K. (2008). Combination of all-trans retinoic acid and paclitaxel-induced differentiation and apoptosis in human glioblastoma U87MG xenografts in nude mice. Cancer *112*, 596-607.

Kaus, A., Widera, D., Kassmer, S., Peter, J., Zaenker, K., Kaltschmidt, C., and Kaltschmidt, B. (2010). Neural stem cells adopt tumorigenic properties by constitutively activated NF-kappaB and subsequent VEGF up-regulation. Stem Cells Dev *19*, 999-1015.

Keshet, I., Schlesinger, Y., Farkash, S., Rand, E., Hecht, M., Segal, E., Pikarski, E., Young, R.A., Niveleau, A., Cedar, H., *et al.* (2006). Evidence for an instructive mechanism of de novo methylation in cancer cells. Nat Genet *38*, 149-153.

Kim, B., Kim, H., Song, B.J., Cha, S.H., Lee, M.O., and Park, S.H. (2006a). Oligonucleotide DNA chips are useful adjuncts in epigenetic studies of glioblastomas. Neuropathology *26*, 409-416.

Kim, G.D., Ni, J., Kelesoglu, N., Roberts, R.J., and Pradhan, S. (2002). Co-operation and communication between the human maintenance and de novo DNA (cytosine-5) methyltransferases. EMBO J *21*, 4183-4195.

Kim, J.K., Samaranayake, M., and Pradhan, S. (2009). Epigenetic mechanisms in mammals. Cell Mol Life Sci *66*, 596-612.

Kim, K.J., Lee, K.H., Kim, H.S., Moon, K.S., Jung, T.Y., Jung, S., and Lee, M.C. (2011). The presence of stem cell marker-expressing cells is not prognostically significant in glioblastomas. Neuropathology *31*, 494-502.

Kim, T.Y., Zhong, S., Fields, C.R., Kim, J.H., and Robertson, K.D. (2006b). Epigenomic profiling reveals novel and frequent targets of aberrant DNA methylation-mediated silencing in malignant glioma. Cancer Res *66*, 7490-7501.

Kleihues, P., and Ohgaki, H. (1999). Primary and secondary glioblastomas: from concept to clinical diagnosis. Neuro Oncol *1*, 44-51.

Klink, B., Schlingelhof, B., Klink, M., Stout-Weider, K., Patt, S., and Schrock, E. (2011). Glioblastomas with oligodendroglial component-common origin of the different histological parts and genetic subclassification. Cell Oncol (Dordr) *34*, 261-275.

Korkaya, H., Liu, S., and Wicha, M.S. (2011). Regulation of cancer stem cells by cytokine networks: attacking cancer's inflammatory roots. Clin Cancer Res *17*, 6125-6129.

Kortenhorst, M.S., Isharwal, S., van Diest, P.J., Chowdhury, W.H., Marlow, C., Carducci, M.A., Rodriguez, R., and Veltri, R.W. (2009). Valproic acid causes dose- and time-dependent changes in nuclear structure in prostate cancer cells in vitro and in vivo. Mol Cancer Ther *8*, 802-808.

Kouzarides, T. (2007). Chromatin modifications and their function. Cell *128*, 693-705.

Kramar, F., Zemanova, Z., Michalova, K., Babicka, L., Ransdorfova, S., Hrabal, P., and Kozler, P. (2007). Cytogenetic analyses in 81 patients with brain gliomas: correlation with clinical outcome and morphological data. J Neurooncol *84*, 201-211.

Kristensen, L.S., Nielsen, H.M., and Hansen, L.L. (2009). Epigenetics and cancer treatment. Eur J Pharmacol *625*, 131-142.

Kubota, H., Nishizaki, T., Harada, K., Oga, A., Ito, H., Suzuki, M., and Sasaki, K. (2001). Identification of recurrent chromosomal rearrangements and the unique relationship between low-level amplification and translocation in glioblastoma. Genes Chromosomes Cancer *31*, 125-133.

Kuendgen, A., Strupp, C., Aivado, M., Bernhardt, A., Hildebrandt, B., Haas, R., Germing, U., and Gattermann, N. (2004). Treatment of myelodysplastic syndromes with valproic acid alone or in combination with all-trans retinoic acid. Blood *104*, 1266-1269.

Kunitz, A., Wolter, M., van den Boom, J., Felsberg, J., Tews, B., Hahn, M., Benner, A., Sabel, M., Lichter, P., Reifenberger, G., *et al.* (2007). DNA hypermethylation and aberrant expression of the EMP3 gene at 19q13.3 in Human Gliomas. Brain Pathol *17*, 363-370.

Laffaire, J., Everhard, S., Idbaih, A., Crinière, E., Marie, Y., de Reyniès, A., Schiappa, R., Mokhtari, K., Hoang-Xuan, K., Sanson, M., *et al.* (2011). Methylation profiling identifies 2 groups of gliomas according to their tumorigenesis. Neuro Oncol *13*, 84-98.

Lagneaux, L., Gillet, N., Stamatopoulos, B., Delforge, A., Dejeneffe, M., Massy, M., Meuleman, N., Kentos, A., Martiat, P., Willems, L., *et al.* (2007). Valproic acid induces apoptosis in chronic lymphocytic leukemia cells through activation of the death receptor pathway and potentiates TRAIL response. Exp Hematol *35*, 1527-1537.

Laird, P.W. (2010). Principles and challenges of genomewide DNA methylation analysis. Nat Rev Genet *11*, 191-203.

Lanzi, C., Cassinelli, G., Cuccuru, G., Supino, R., Zuco, V., Ferlini, C., Scambia, G., and Zunino, F. (2001). Cell cycle checkpoint efficiency and cellular response to paclitaxel in prostate cancer cells. Prostate *48*, 254-264.

Lapidot, T., Sirard, C., Vormoor, J., Murdoch, B., Hoang, T., Caceres-Cortes, J., Minden, M., Paterson, B., Caligiuri, M.A., and Dick, J.E. (1994). A cell initiating human acute myeloid leukaemia after transplantation into SCID mice. Nature *367*, 645-648.

Lee, J., Kotliarova, S., Kotliarov, Y., Li, A., Su, Q., Donin, N.M., Pastorino, S., Purow, B.W., Christopher, N., Zhang, W., *et al.* (2006a). Tumor stem cells derived from glioblastomas cultured in bFGF and EGF more closely mirror the phenotype and genotype of primary tumors than do serum-cultured cell lines. Cancer Cell *9*, 391-403.

Lee, J., Son, M.J., Woolard, K., Donin, N.M., Li, A., Cheng, C.H., Kotliarova, S., Kotliarov, Y., Walling, J., Ahn, S., *et al.* (2008). Epigenetic-mediated dysfunction of the bone morphogenetic protein pathway inhibits differentiation of glioblastoma-initiating cells. Cancer Cell *13*, 69-80.

Lee, T.I., Jenner, R.G., Boyer, L.A., Guenther, M.G., Levine, S.S., Kumar, R.M., Chevalier, B., Johnstone, S.E., Cole, M.F., Isono, K., *et al.* (2006b). Control of developmental regulators by Polycomb in human embryonic stem cells. Cell *125*, 301-313.

Lengauer, C., Kinzler, K.W., and Vogelstein, B. (1998). Genetic instabilities in human cancers. Nature *396*, 643-649.

Leonard, G.D., Fojo, T., and Bates, S.E. (2003). The role of ABC transporters in clinical practice. Oncologist *8*, 411-424.

Li, A., Walling, J., Kotliarov, Y., Center, A., Steed, M.E., Ahn, S.J., Rosenblum, M., Mikkelsen, T., Zenklusen, J.C., and Fine, H.A. (2008). Genomic changes and gene expression profiles reveal that established glioma cell lines are poorly representative of primary human gliomas. Mol Cancer Res *6*, 21-30.

Li, X.N., Shu, Q., Su, J.M., Perlaky, L., Blaney, S.M., and Lau, C.C. (2005). Valproic acid induces growth arrest, apoptosis, and senescence in medulloblastomas by increasing histone hyperacetylation and regulating expression of p21Cip1, CDK4, and CMYC. Mol Cancer Ther *4*, 1912-1922.

Libermann, T.A., Nusbaum, H.R., Razon, N., Kris, R., Lax, I., Soreq, H., Whittle, N., Waterfield, M.D., Ullrich, A., and Schlessinger, J. (1985). Amplification, enhanced expression and possible rearrangement of EGF receptor gene in primary human brain tumours of glial origin. Nature *313*, 144-147.

Liebmann, J., Cook, J.A., Lipschultz, C., Teague, D., Fisher, J., and Mitchell, J.B. (1994). The influence of Cremophor EL on the cell cycle effects of paclitaxel (Taxol) in human tumor cell lines. Cancer Chemother Pharmacol *33*, 331-339.

Liu, C.C., Prior, J., Piwnica-Worms, D., and Bu, G. (2010a). LRP6 overexpression defines a class of breast cancer subtype and is a target for therapy. Proc Natl Acad Sci U S A *107*, 5136-5141.

Liu, F., Park, P.J., Lai, W., Maher, E., Chakravarti, A., Durso, L., Jiang, X., Yu, Y., Brosius, A., Thomas, M., *et al.* (2006a). A genome-wide screen reveals functional gene clusters in the cancer genome and identifies EphA2 as a mitogen in glioblastoma. Cancer Res *66*, 10815-10823.

Liu, G., Yuan, X., Zeng, Z., Tunici, P., Ng, H., Abdulkadir, I.R., Lu, L., Irvin, D., Black, K.L., and Yu, J.S. (2006b). Analysis of gene expression and chemoresistance of CD133+ cancer stem cells in glioblastoma. Mol Cancer *5*, 67.

Liu, L., Ichimura, K., Pettersson, E.H., and Collins, V.P. (1998). Chromosome 7 rearrangements in glioblastomas; loci adjacent to EGFR are independently amplified. J Neuropathol Exp Neurol *57*, 1138-1145.

Liu, L., Ichimura, K., Pettersson, E.H., Goike, H.M., and Collins, V.P. (2000). The complexity of the 7p12 amplicon in human astrocytic gliomas: detailed mapping of 246 tumors. J Neuropathol Exp Neurol *59*, 1087-1093.

Liu, W.M., Laux, H., Henry, J.Y., Bolton, T.B., Dalgleish, A.G., and Galustian, C. (2010b). A microarray study of altered gene expression in colorectal cancer cells after treatment with immunomodulatory drugs: differences in action in vivo and in vitro. Mol Biol Rep *37*, 1801-1814.

Lo, K.C., Rossi, M.R., LaDuca, J., Hicks, D.G., Turpaz, Y., Hawthorn, L., and Cowell, J.K. (2007). Candidate glioblastoma development gene identification using concordance between copy number abnormalities and gene expression level changes. Genes Chromosomes Cancer *46*, 875-894.

Lobo, N.A., Shimono, Y., Qian, D., and Clarke, M.F. (2007). The biology of cancer stem cells. Annu Rev Cell Dev Biol *23*, 675-699.

Lottaz, C., Beier, D., Meyer, K., Kumar, P., Hermann, A., Schwarz, J., Junker, M., Oefner, P.J., Bogdahn, U., Wischhusen, J., *et al.* (2010). Transcriptional profiles of CD133+ and CD133- glioblastoma-derived cancer stem cell lines suggest different cells of origin. Cancer Res *70*, 2030-2040.

Louis, D.N., Ohgaki, H., Wiestler, O.D., Cavenee, W.K., Burger, P.C., Jouvet, A., Scheithauer, B.W., and Kleihues, P. (2007). The 2007 WHO classification of tumours of the central nervous system. Acta Neuropathol *114*, 97-109.

Löscher, W. (1999). Valproate: a reappraisal of its pharmacodynamic properties and mechanisms of action. Prog Neurobiol *58*, 31-59.

Maher, E.A., Brennan, C., Wen, P.Y., Durso, L., Ligon, K.L., Richardson, A., Khatry, D., Feng, B., Sinha, R., Louis, D.N., *et al.* (2006). Marked genomic differences characterize primary and secondary glioblastoma subtypes and identify two distinct molecular and clinical secondary glioblastoma entities. Cancer Res *66*, 11502-11513.

Maher, E.A., Furnari, F.B., Bachoo, R.M., Rowitch, D.H., Louis, D.N., Cavenee, W.K., and DePinho, R.A. (2001). Malignant glioma: genetics and biology of a grave matter. Genes Dev *15*, 1311-1333.

Mahlknecht, U., and Hoelzer, D. (2000). Histone acetylation modifiers in the pathogenesis of malignant disease. Mol Med *6*, 623-644.

Mai, A., and Altucci, L. (2009). Epi-drugs to fight cancer: from chemistry to cancer treatment, the road ahead. Int J Biochem Cell Biol *41*, 199-213.

Mallon, R., Feldberg, L.R., Lucas, J., Chaudhary, I., Dehnhardt, C., Santos, E.D., Chen, Z., dos Santos, O., Ayral-Kaloustian, S., Venkatesan, A., *et al.* (2011). Antitumor efficacy of PKI-587, a highly potent dual PI3K/mTOR kinase inhibitor. Clin Cancer Res *17*, 3193-3203.

Marchion, D.C., Bicaku, E., Daud, A.I., Sullivan, D.M., and Munster, P.N. (2005). Valproic acid alters chromatin structure by regulation of chromatin modulation proteins. Cancer Res *65*, 3815-3822.

Markman, M. (2003). Managing taxane toxicities. Support Care Cancer *11*, 144-147.

Marks, P.A., and Xu, W.S. (2009). Histone deacetylase inhibitors: Potential in cancer therapy. J Cell Biochem *107*, 600-608.

Martin, M.L., Breen, K.C., and Regan, C.M. (1988). Perturbations of cellular functions integral to neural tube formation by the putative teratogen sodium valproate. Toxicol In Vitro *2*, 43-48.

Martinez, R., and Esteller, M. (2010). The DNA methylome of glioblastoma multiforme. Neurobiol Dis *39*, 40-46.

Martín-Subero, J.I., Kreuz, M., Bibikova, M., Bentink, S., Ammerpohl, O., Wickham-Garcia, E., Rosolowski, M., Richter, J., Lopez-Serra, L., Ballestar, E., *et al.* (2009). New insights into the biology and origin of mature aggressive B-cell lymphomas by combined epigenomic, genomic, and transcriptional profiling. Blood *113*, 2488-2497.

McCarroll, S.A. (2010). Copy number variation and human genome maps. Nat Genet *42*, 365-366.

Mellinghoff, I.K., Wang, M.Y., Vivanco, I., Haas-Kogan, D.A., Zhu, S., Dia, E.Q., Lu, K.V., Yoshimoto, K., Huang, J.H., Chute, D.J., *et al.* (2005). Molecular determinants of the response of glioblastomas to EGFR kinase inhibitors. N Engl J Med *353*, 2012-2024.

Mesdjian, E., Ciesielski, L., Valli, M., Bruguerolle, B., Jadot, G., Bouyard, P., and Mandel, P. (1982). Sodium valproate: kinetic profile and effects on GABA levels in various brain areas of the rat. Prog Neuropsychopharmacol Biol Psychiatry *6*, 223-233.

Michaud, K., Solomon, D.A., Oermann, E., Kim, J.S., Zhong, W.Z., Prados, M.D., Ozawa, T., James, C.D., and Waldman, T. (2010). Pharmacologic inhibition of cyclin-dependent kinases 4 and 6 arrests the growth of glioblastoma multiforme intracranial xenografts. Cancer Res *70*, 3228-3238.

Mielke, S., Sparreboom, A., and Mross, K. (2006). Peripheral neuropathy: a persisting challenge in paclitaxel-based regimes. Eur J Cancer *42*, 24-30.

Mikkelsen, T.S., Ku, M., Jaffe, D.B., Issac, B., Lieberman, E., Giannoukos, G., Alvarez, P., Brockman, W., Kim, T.K., Koche, R.P., *et al.* (2007). Genome-wide maps of chromatin state in pluripotent and lineage-committed cells. Nature *448*, 553-560.

Miller, C.R., and Perry, A. (2007). Glioblastoma. Arch Pathol Lab Med *131*, 397-406.

Mischel, P.S., Nelson, S.F., and Cloughesy, T.F. (2003). Molecular analysis of glioblastoma: pathway profiling and its implications for patient therapy. Cancer Biol Ther *2*, 242-247.

Mizoguchi, M., Kuga, D., Guan, Y., Hata, N., Nakamizo, A., Yoshimoto, K., and Sasaki, T. (2011). Loss of heterozygosity analysis in malignant gliomas. Brain Tumor Pathol *28*, 191-196.

Mollenhauer, J., Wiemann, S., Scheurlen, W., Korn, B., Hayashi, Y., Wilgenbus, K.K., von Deimling, A., and Poustka, A. (1997). DMBT1, a new member of the SRCR superfamily, on chromosome 10q25.3-26.1 is deleted in malignant brain tumours. Nat Genet *17*, 32-39.

Molofsky, A.V., Slutsky, S.G., Joseph, N.M., He, S., Pardal, R., Krishnamurthy, J., Sharpless, N.E., and Morrison, S.J. (2006). Increasing p16INK4a expression decreases forebrain progenitors and neurogenesis during ageing. Nature *443*, 448-452.

Mueller, W., Hartmann, C., Hoffmann, A., Lanksch, W., Kiwit, J., Tonn, J., Veelken, J., Schramm, J., Weller, M., Wiestler, O.D., *et al.* (2002). Genetic signature of oligoastrocytomas correlates with tumor location and denotes distinct molecular subsets. Am J Pathol *161*, 313-319.

Mulholland, P.J., Fiegler, H., Mazzanti, C., Gorman, P., Sasieni, P., Adams, J., Jones, T.A., Babbage, J.W., Vatcheva, R., Ichimura, K., *et al.* (2006). Genomic profiling identifies discrete deletions associated with translocations in glioblastoma multiforme. Cell Cycle *5*, 783-791.

Munshi, A., Kurland, J.F., Nishikawa, T., Tanaka, T., Hobbs, M.L., Tucker, S.L., Ismail, S., Stevens, C., and Meyn, R.E. (2005). Histone deacetylase inhibitors radiosensitize human melanoma cells by suppressing DNA repair activity. Clin Cancer Res *11*, 4912-4922.

Mure, H., Matsuzaki, K., Kitazato, K.T., Mizobuchi, Y., Kuwayama, K., Kageji, T., and Nagahiro, S. (2010). Akt2 and Akt3 play a pivotal role in malignant gliomas. Neuro Oncol *12*, 221-232.

Nagane, M., Coufal, F., Lin, H., Bögler, O., Cavenee, W.K., and Huang, H.J. (1996). A common mutant epidermal growth factor receptor confers enhanced tumorigenicity on human glioblastoma cells by increasing proliferation and reducing apoptosis. Cancer Res *56*, 5079-5086.

Nagarajan, R.P., and Costello, J.F. (2009). Molecular epigenetics and genetics in neuro-oncology. Neurotherapeutics *6*, 436-446.

Nakada, M., Nakada, S., Demuth, T., Tran, N.L., Hoelzinger, D.B., and Berens, M.E. (2007). Molecular targets of glioma invasion. Cell Mol Life Sci *64*, 458-478.

Nakamura, M., Yonekawa, Y., Kleihues, P., and Ohgaki, H. (2001). Promoter hypermethylation of the RB1 gene in glioblastomas. Lab Invest *81*, 77-82.

Network, C.G.A.R. (2008). Comprehensive genomic characterization defines human glioblastoma genes and core pathways. Nature *455*, 1061-1068.

Nikanjam, M., Gibbs, A.R., Hunt, C.A., Budinger, T.F., and Forte, T.M. (2007). Synthetic nano-LDL with paclitaxel oleate as a targeted drug delivery vehicle for glioblastoma multiforme. J Control Release *124*, 163-171.

Nogales, E. (2000). Structural insights into microtubule function. Annu Rev Biochem *69*, 277-302.

Nogales, E., Wolf, S.G., Khan, I.A., Ludueña, R.F., and Downing, K.H. (1995). Structure of tubulin at 6.5 A and location of the taxol-binding site. Nature *375*, 424-427.

Nolan, L., Johnson, P.W., Ganesan, A., Packham, G., and Crabb, S.J. (2008). Will histone deacetylase inhibitors require combination with other agents to fulfil their therapeutic potential? Br J Cancer *99*, 689-694.

Nord, H., Hartmann, C., Andersson, R., Menzel, U., Pfeifer, S., Piotrowski, A., Bogdan, A., Kloc, W., Sandgren, J., Olofsson, T., *et al.* (2009). Characterization of novel and complex genomic aberrations in glioblastoma using a 32K BAC array. Neuro Oncol *11*, 803-818.

Noushmehr, H., Weisenberger, D.J., Diefes, K., Phillips, H.S., Pujara, K., Berman, B.P., Pan, F., Pelloski, C.E., Sulman, E.P., Bhat, K.P., *et al.* (2010). Identification of a CpG island methylator phenotype that defines a distinct subgroup of glioma. Cancer Cell *17*, 510-522.

Ogawa, O., Eccles, M.R., Szeto, J., McNoe, L.A., Yun, K., Maw, M.A., Smith, P.J., and Reeve, A.E. (1993). Relaxation of insulin-like growth factor II gene imprinting implicated in Wilms' tumour. Nature *362*, 749-751.

Ohgaki, H., Dessen, P., Jourde, B., Horstmann, S., Nishikawa, T., Di Patre, P.L., Burkhard, C., Schüler, D., Probst-Hensch, N.M., Maiorka, P.C., *et al.* (2004). Genetic pathways to glioblastoma: a population-based study. Cancer Res *64*, 6892-6899.

Ohgaki, H., and Kleihues, P. (2005). Population-based studies on incidence, survival rates, and genetic alterations in astrocytic and oligodendroglial gliomas. J Neuropathol Exp Neurol *64*, 479-489.

Ohgaki, H., and Kleihues, P. (2007). Genetic pathways to primary and secondary glioblastoma. Am J Pathol *170*, 1445-1453.

Ohm, J.E., McGarvey, K.M., Yu, X., Cheng, L., Schuebel, K.E., Cope, L., Mohammad, H.P., Chen, W., Daniel, V.C., Yu, W., *et al.* (2007). A stem cell-like chromatin pattern may predispose tumor suppressor genes to DNA hypermethylation and heritable silencing. Nat Genet *39*, 237-242.

Pallini, R., Ricci-Vitiani, L., Banna, G.L., Signore, M., Lombardi, D., Todaro, M., Stassi, G., Martini, M., Maira, G., Larocca, L.M., *et al.* (2008). Cancer stem cell analysis and clinical outcome in patients with glioblastoma multiforme. Clin Cancer Res *14*, 8205-8212.

Panzeri, E., Conconi, D., Antolini, L., Redaelli, S., Valsecchi, M.G., Bovo, G., Pallotti, F., Viganò, P., Strada, G., Dalprà, L., *et al.* (2011). Chromosomal aberrations in bladder cancer: fresh versus formalin fixed paraffin embedded tissue and targeted FISH versus wide microarray-based CGH analysis. PLoS One *6*, e24237.

Pardal, R., Clarke, M.F., and Morrison, S.J. (2003). Applying the principles of stem-cell biology to cancer. Nat Rev Cancer *3*, 895-902.

Parsons, D.W., Jones, S., Zhang, X., Lin, J.C., Leary, R.J., Angenendt, P., Mankoo, P., Carter, H., Siu, I.M., Gallia, G.L., *et al.* (2008). An integrated genomic analysis of human glioblastoma multiforme. Science *321*, 1807-1812.

Passegué, E., Jamieson, C.H., Ailles, L.E., and Weissman, I.L. (2003). Normal and leukemic hematopoiesis: are leukemias a stem cell disorder or a reacquisition of stem cell characteristics? Proc Natl Acad Sci U S A *100 Suppl 1*, 11842-11849.

Perez, E.A. (2009). Microtubule inhibitors: Differentiating tubulin-inhibiting agents based on mechanisms of action, clinical activity, and resistance. Mol Cancer Ther *8*, 2086-2095.

Perez-Plasencia, C., and Duenas-Gonzalez, A. (2006). Can the state of cancer chemotherapy resistance be reverted by epigenetic therapy? Mol Cancer *5*, 27.

Perucca, E. (2002). Pharmacological and therapeutic properties of valproate: a summary after 35 years of clinical experience. CNS Drugs *16*, 695-714.

Peñuelas, S., Anido, J., Prieto-Sánchez, R.M., Folch, G., Barba, I., Cuartas, I., García-Dorado, D., Poca, M.A., Sahuquillo, J., Baselga, J., *et al.* (2009). TGF-beta increases glioma-initiating cell self-renewal through the induction of LIF in human glioblastoma. Cancer Cell *15*, 315-327.

Phiel, C.J., Zhang, F., Huang, E.Y., Guenther, M.G., Lazar, M.A., and Klein, P.S. (2001). Histone deacetylase is a direct target of valproic acid, a potent anticonvulsant, mood stabilizer, and teratogen. J Biol Chem *276*, 36734-36741.

Phillips, H.S., Kharbanda, S., Chen, R., Forrest, W.F., Soriano, R.H., Wu, T.D., Misra, A., Nigro, J.M., Colman, H., Soroceanu, L., *et al.* (2006). Molecular subclasses of high-grade glioma predict prognosis, delineate a pattern of disease progression, and resemble stages in neurogenesis. Cancer Cell *9*, 157-173.

Piccirillo, S.G., Binda, E., Fiocco, R., Vescovi, A.L., and Shah, K. (2009a). Brain cancer stem cells. J Mol Med (Berl) *87*, 1087-1095.

Piccirillo, S.G., Combi, R., Cajola, L., Patrizi, A., Redaelli, S., Bentivegna, A., Baronchelli, S., Maira, G., Pollo, B., Mangiola, A., *et al.* (2009b). Distinct pools of cancer stem-like cells coexist within human glioblastomas and display different tumorigenicity and independent genomic evolution. Oncogene *28*, 1807-1811.

Piccirillo, S.G., and Vescovi, A.L. (2006). Bone morphogenetic proteins regulate tumorigenicity in human glioblastoma stem cells. Ernst Schering Found Symp Proc, 59-81.

Pinder, R.M., Brogden, R.N., Speight, T.M., and Avery, G.S. (1977). Sodium valproate: a review of its pharmacological properties and therapeutic efficacy in epilepsy. Drugs *13*, 81-123.

Pinkel, D., Segraves, R., Sudar, D., Clark, S., Poole, I., Kowbel, D., Collins, C., Kuo, W.L., Chen, C., Zhai, Y., *et al.* (1998). High resolution analysis of DNA copy number variation using comparative genomic hybridization to microarrays. Nat Genet *20*, 207-211.

Pollard, S.M., Yoshikawa, K., Clarke, I.D., Danovi, D., Stricker, S., Russell, R., Bayani, J., Head, R., Lee, M., Bernstein, M., *et al.* (2009). Glioma stem cell lines expanded in adherent culture have tumor-specific phenotypes and are suitable for chemical and genetic screens. Cell Stem Cell *4*, 568-580.

Rakovitch, E., Mellado, W., Hall, E.J., Pandita, T.K., Sawant, S., and Geard, C.R. (1999). Paclitaxel sensitivity correlates with p53 status and DNA fragmentation, but not G2/M accumulation. Int J Radiat Oncol Biol Phys *44*, 1119-1124.

Raponi, M., Belly, R.T., Karp, J.E., Lancet, J.E., Atkins, D., and Wang, Y. (2004). Microarray analysis reveals genetic pathways modulated by tipifarnib in acute myeloid leukemia. BMC Cancer *4*, 56.

Rasheed, B.K., McLendon, R.E., Friedman, H.S., Friedman, A.H., Fuchs, H.E., Bigner, D.D., and Bigner, S.H. (1995). Chromosome 10 deletion mapping in human gliomas: a common deletion region in 10q25. Oncogene *10*, 2243-2246.

Rebetz, J., Tian, D., Persson, A., Widegren, B., Salford, L.G., Englund, E., Gisselsson, D., and Fan, X. (2008). Glial progenitor-like phenotype in low-grade glioma and enhanced CD133-expression and neuronal lineage differentiation potential in high-grade glioma. PLoS One *3*, e1936.

Redon, R., Ishikawa, S., Fitch, K.R., Feuk, L., Perry, G.H., Andrews, T.D., Fiegler, H., Shapero, M.H., Carson, A.R., Chen, W., *et al.* (2006). Global variation in copy number in the human genome. Nature *444*, 444-454.

Regan, C.M. (1985). Therapeutic levels of sodium valproate inhibit mitotic indices in cells of neural origin. Brain Res *347*, 394-398.

Regenbrecht, C.R., Lehrach, H., and Adjaye, J. (2008). Stemming cancer: functional genomics of cancer stem cells in solid tumors. Stem Cell Rev *4*, 319-328.

Reguart, N., He, B., Taron, M., You, L., Jablons, D.M., and Rosell, R. (2005). The role of Wnt signaling in cancer and stem cells. Future Oncol *1*, 787-797.

Reifenberger, G., and Collins, V.P. (2004). Pathology and molecular genetics of astrocytic gliomas. J Mol Med (Berl) *82*, 656-670.

Reifenberger, G., Reifenberger, J., Ichimura, K., Meltzer, P.S., and Collins, V.P. (1994). Amplification of multiple genes from chromosomal region 12q13-14 in human malignant gliomas: preliminary mapping of the amplicons shows preferential involvement of CDK4, SAS, and MDM2. Cancer Res *54*, 4299-4303.

Reya, T., Morrison, S.J., Clarke, M.F., and Weissman, I.L. (2001). Stem cells, cancer, and cancer stem cells. Nature *414*, 105-111.

Riffell, J.L., Zimmerman, C., Khong, A., McHardy, L.M., and Roberge, M. (2009). Effects of chemical manipulation of mitotic arrest and slippage on cancer cell survival and proliferation. Cell Cycle *8*, 3025-3038.

Ringrose, L., and Paro, R. (2004). Epigenetic regulation of cellular memory by the Polycomb and Trithorax group proteins. Annu Rev Genet *38*, 413-443.

Ringrose, L., and Paro, R. (2007). Polycomb/Trithorax response elements and epigenetic memory of cell identity. Development *134*, 223-232.

Rodríguez-Paredes, M., and Esteller, M. (2011). Cancer epigenetics reaches mainstream oncology. Nat Med *17*, 330-339.

Rosato, R.R., Almenara, J.A., Dai, Y., and Grant, S. (2003). Simultaneous activation of the intrinsic and extrinsic pathways by histone deacetylase (HDAC) inhibitors and tumor necrosis factor-related apoptosis-inducing ligand (TRAIL) synergistically induces mitochondrial damage and apoptosis in human leukemia cells. Mol Cancer Ther *2*, 1273-1284.

Rosenbauer, F., and Tenen, D.G. (2007). Transcription factors in myeloid development: balancing differentiation with transformation. Nat Rev Immunol *7*, 105-117.

Rowinsky, E.K., Wright, M., Monsarrat, B., Lesser, G.J., and Donehower, R.C. (1993). Taxol: pharmacology, metabolism and clinical implications. Cancer Surv *17*, 283-304.

Roy Choudhury, S., Karmakar, S., Banik, N.L., and Ray, S.K. (2011). Valproic Acid Induced Differentiation and Potentiated Efficacy of Taxol and Nanotaxol for Controlling Growth of Human Glioblastoma LN18 and T98G Cells. Neurochem Res.

Régina, A., Demeule, M., Ché, C., Lavallée, I., Poirier, J., Gabathuler, R., Béliveau, R., and Castaigne, J.P. (2008). Antitumour activity of ANG1005, a conjugate between paclitaxel and the new brain delivery vector Angiopep-2. Br J Pharmacol *155*, 185-197.

Sadikovic, B., Al-Romaih, K., Squire, J.A., and Zielenska, M. (2008). Cause and consequences of genetic and epigenetic alterations in human cancer. Curr Genomics *9*, 394-408.

Sakai, T., Toguchida, J., Ohtani, N., Yandell, D.W., Rapaport, J.M., and Dryja, T.P. (1991). Allele-specific hypermethylation of the retinoblastoma tumor-suppressor gene. Am J Hum Genet *48*, 880-888.

Salven, P., Mustjoki, S., Alitalo, R., Alitalo, K., and Rafii, S. (2003). VEGFR-3 and CD133 identify a population of CD34+ lymphatic/vascular endothelial precursor cells. Blood *101*, 168-172.

Sanai, N., Alvarez-Buylla, A., and Berger, M.S. (2005). Neural stem cells and the origin of gliomas. N Engl J Med *353*, 811-822.

Sarkar, B., Dosch, J., and Simeone, D.M. (2009). Cancer stem cells: a new theory regarding a timeless disease. Chem Rev *109*, 3200-3208.

Savickiene, J., Borutinskaite, V.V., Treigyte, G., Magnusson, K.E., and Navakauskiene, R. (2006). The novel histone deacetylase inhibitor BML-210 exerts growth inhibitory, proapoptotic and differentiation stimulating effects on the human leukemia cell lines. Eur J Pharmacol *549*, 9-18.

Schiff, P.B., and Horwitz, S.B. (1980). Taxol stabilizes microtubules in mouse fibroblast cells. Proc Natl Acad Sci U S A *77*, 1561-1565.

Schlegel, J., Merdes, A., Stumm, G., Albert, F.K., Forsting, M., Hynes, N., and Kiessling, M. (1994). Amplification of the epidermal-growth-factor-receptor gene correlates with different growth behaviour in human glioblastoma. Int J Cancer *56*, 72-77.

Schlesinger, Y., Straussman, R., Keshet, I., Farkash, S., Hecht, M., Zimmerman, J., Eden, E., Yakhini, Z., Ben-Shushan, E., Reubinoff, B.E., *et al.* (2007). Polycomb-mediated methylation on Lys27 of histone H3 pre-marks genes for de novo methylation in cancer. Nat Genet *39*, 232-236.

Schmidt, E.E., Ichimura, K., Reifenberger, G., and Collins, V.P. (1994). CDKN2 (p16/MTS1) gene deletion or CDK4 amplification occurs in the majority of glioblastomas. Cancer Res *54*, 6321-6324.

Schmidt, M.C., Antweiler, S., Urban, N., Mueller, W., Kuklik, A., Meyer-Puttlitz, B., Wiestler, O.D., Louis, D.N., Fimmers, R., and von Deimling, A. (2002). Impact of genotype and morphology on the prognosis of glioblastoma. J Neuropathol Exp Neurol *61*, 321-328.

Schraivogel, D., Weinmann, L., Beier, D., Tabatabai, G., Eichner, A., Zhu, J.Y., Anton, M., Sixt, M., Weller, M., Beier, C.P., *et al.* (2011). CAMTA1 is a novel tumour suppressor regulated by miR-9/9(*) in glioblastoma stem cells. EMBO J *30*, 4309-4322.

Schuebel, K., Chen, W., and Baylin, S.B. (2006). CIMPle origin for promoter hypermethylation in colorectal cancer? Nat Genet *38*, 738-740.

Schwechheimer, K., Huang, S., and Cavenee, W.K. (1995). EGFR gene amplification--rearrangement in human glioblastomas. Int J Cancer *62*, 145-148.

Scolnick, D.M., and Halazonetis, T.D. (2000). Chfr defines a mitotic stress checkpoint that delays entry into metaphase. Nature *406*, 430-435.

Sebat, J., Lakshmi, B., Troge, J., Alexander, J., Young, J., Lundin, P., Månér, S., Massa, H., Walker, M., Chi, M., *et al.* (2004). Large-scale copy number polymorphism in the human genome. Science *305*, 525-528.

Shapiro, J.R., Yung, W.K., and Shapiro, W.R. (1981). Isolation, karyotype, and clonal growth of heterogeneous subpopulations of human malignant gliomas. Cancer Res *41*, 2349-2359.

Sharma, S., Kelly, T.K., and Jones, P.A. (2010). Epigenetics in cancer. Carcinogenesis *31*, 27-36.

Shen, W.H., Balajee, A.S., Wang, J., Wu, H., Eng, C., Pandolfi, P.P., and Yin, Y. (2007). Essential role for nuclear PTEN in maintaining chromosomal integrity. Cell *128*, 157-170.

Shen, W.T., Wong, T.S., Chung, W.Y., Wong, M.G., Kebebew, E., Duh, Q.Y., and Clark, O.H. (2005). Valproic acid inhibits growth, induces apoptosis, and modulates apoptosis-regulatory and differentiation gene expression in human thyroid cancer cells. Surgery *138*, 979-984; discussion 984-975.

Shih, A.H., and Holland, E.C. (2006). Notch signaling enhances nestin expression in gliomas. Neoplasia *8*, 1072-1082.

Singh, S.K., Clarke, I.D., Hide, T., and Dirks, P.B. (2004). Cancer stem cells in nervous system tumors. Oncogene *23*, 7267-7273.

Singh, S.K., Clarke, I.D., Terasaki, M., Bonn, V.E., Hawkins, C., Squire, J., and Dirks, P.B. (2003). Identification of a cancer stem cell in human brain tumors. Cancer Res *63*, 5821-5828.

Smith, J.S., Alderete, B., Minn, Y., Borell, T.J., Perry, A., Mohapatra, G., Hosek, S.M., Kimmel, D., O'Fallon, J., Yates, A., *et al.* (1999). Localization of common deletion regions on 1p and 19q in human gliomas and their association with histological subtype. Oncogene *18*, 4144-4152.

Smith, J.S., Perry, A., Borell, T.J., Lee, H.K., O'Fallon, J., Hosek, S.M., Kimmel, D., Yates, A., Burger, P.C., Scheithauer, B.W., *et al.* (2000). Alterations of chromosome arms 1p and 19q as predictors of survival in oligodendrogliomas, astrocytomas, and mixed oligoastrocytomas. J Clin Oncol *18*, 636-645.

Stankiewicz, P., and Lupski, J.R. (2010). Structural variation in the human genome and its role in disease. Annu Rev Med *61*, 437-455.

Stanton, R.A., Gernert, K.M., Nettles, J.H., and Aneja, R. (2011). Drugs that target dynamic microtubules: a new molecular perspective. Med Res Rev *31*, 443-481.

Steinbach, J.P., Blaicher, H.P., Herrlinger, U., Wick, W., Nägele, T., Meyermann, R., Tatagiba, M., Bamberg, M., Dichgans, J., Karnath, H.O., *et al.* (2006). Surviving glioblastoma for more than 5 years: the patient's perspective. Neurology *66*, 239-242.

Straussman, R., Nejman, D., Roberts, D., Steinfeld, I., Blum, B., Benvenisty, N., Simon, I., Yakhini, Z., and Cedar, H. (2009). Developmental programming of CpG island methylation profiles in the human genome. Nat Struct Mol Biol *16*, 564-571.

Stupp, R., Mason, W.P., van den Bent, M.J., Weller, M., Fisher, B., Taphoorn, M.J., Belanger, K., Brandes, A.A., Marosi, C., Bogdahn, U., *et al.* (2005). Radiotherapy plus concomitant and adjuvant temozolomide for glioblastoma. N Engl J Med *352*, 987-996.

Sugawa, N., Ekstrand, A.J., James, C.D., and Collins, V.P. (1990). Identical splicing of aberrant epidermal growth factor receptor transcripts from amplified rearranged genes in human glioblastomas. Proc Natl Acad Sci U S A *87*, 8602-8606.

Sun, Y., Pollard, S., Conti, L., Toselli, M., Biella, G., Parkin, G., Willatt, L., Falk, A., Cattaneo, E., and Smith, A. (2008). Long-term tripotent differentiation capacity of human neural stem (NS) cells in adherent culture. Mol Cell Neurosci *38*, 245-258.

Suslov, O.N., Kukekov, V.G., Ignatova, T.N., and Steindler, D.A. (2002). Neural stem cell heterogeneity demonstrated by molecular phenotyping of clonal neurospheres. Proc Natl Acad Sci U S A *99*, 14506-14511.

Suzuki, H., Gabrielson, E., Chen, W., Anbazhagan, R., van Engeland, M., Weijenberg, M.P., Herman, J.G., and Baylin, S.B. (2002). A genomic screen for genes upregulated by demethylation and histone deacetylase inhibition in human colorectal cancer. Nat Genet *31*, 141-149.

Svotelis, A., Gévry, N., and Gaudreau, L. (2009). Regulation of gene expression and cellular proliferation by histone H2A.Z. Biochem Cell Biol *87*, 179-188.

Tabatabai, G., Tonn, J.C., Stupp, R., and Weller, M. (2011). The Role of Integrins in Glioma Biology and Anti-Glioma Therapies. Curr Pharm Des.

Tabatabai, G., and Weller, M. (2011). Glioblastoma stem cells. Cell Tissue Res *343*, 459-465.

Tabu, K., Sasai, K., Kimura, T., Wang, L., Aoyanagi, E., Kohsaka, S., Tanino, M., Nishihara, H., and Tanaka, S. (2008). Promoter hypomethylation regulates CD133 expression in human gliomas. Cell Res *18*, 1037-1046.

Takai, N., Kawamata, N., Gui, D., Said, J.W., Miyakawa, I., and Koeffler, H.P. (2004). Human ovarian carcinoma cells: histone deacetylase inhibitors exhibit antiproliferative activity and potently induce apoptosis. Cancer *101*, 2760-2770.

Thelen, P., Schweyer, S., Hemmerlein, B., Wuttke, W., Seseke, F., and Ringert, R.H. (2004). Expressional changes after histone deacetylase inhibition by valproic acid in LNCaP human prostate cancer cells. Int J Oncol *24*, 25-31.

Tseng, S.H., Bobola, M.S., Berger, M.S., and Silber, J.R. (1999). Characterization of paclitaxel (Taxol) sensitivity in human glioma- and medulloblastoma-derived cell lines. Neuro Oncol *1*, 101-108.

Uchida, N., Buck, D.W., He, D., Reitsma, M.J., Masek, M., Phan, T.V., Tsukamoto, A.S., Gage, F.H., and Weissman, I.L. (2000). Direct isolation of human central nervous system stem cells. Proc Natl Acad Sci U S A *97*, 14720-14725.

Ueki, K., Ono, Y., Henson, J.W., Efird, J.T., von Deimling, A., and Louis, D.N. (1996). CDKN2/p16 or RB alterations occur in the majority of glioblastomas and are inversely correlated. Cancer Res *56*, 150-153.

Uhlmann, K., Rohde, K., Zeller, C., Szymas, J., Vogel, S., Marczinek, K., Thiel, G., Nürnberg, P., and Laird, P.W. (2003). Distinct methylation profiles of glioma subtypes. Int J Cancer *106*, 52-59.

Van Lint, C., Emiliani, S., and Verdin, E. (1996). The expression of a small fraction of cellular genes is changed in response to histone hyperacetylation. Gene Expr *5*, 245-253.

Vaquero, A., Loyola, A., and Reinberg, D. (2003). The constantly changing face of chromatin. Sci Aging Knowledge Environ *2003*, RE4.

Verhaak, R.G., Hoadley, K.A., Purdom, E., Wang, V., Qi, Y., Wilkerson, M.D., Miller, C.R., Ding, L., Golub, T., Mesirov, J.P., *et al.* (2010). Integrated genomic analysis identifies clinically relevant subtypes of glioblastoma characterized by abnormalities in PDGFRA, IDH1, EGFR, and NF1. Cancer Cell *17*, 98-110.

Vescovi, A.L., Galli, R., and Reynolds, B.A. (2006). Brain tumour stem cells. Nat Rev Cancer *6*, 425-436.

Vredenburgh, J.J., Desjardins, A., Herndon, J.E., Dowell, J.M., Reardon, D.A., Quinn, J.A., Rich, J.N., Sathornsumetee, S., Gururangan, S., Wagner, M., *et al.* (2007a). Phase II trial of bevacizumab and irinotecan in recurrent malignant glioma. Clin Cancer Res *13*, 1253-1259.

Vredenburgh, J.J., Desjardins, A., Herndon, J.E., Marcello, J., Reardon, D.A., Quinn, J.A., Rich, J.N., Sathornsumetee, S., Gururangan, S., Sampson, J., *et al.* (2007b). Bevacizumab plus irinotecan in recurrent glioblastoma multiforme. J Clin Oncol *25*, 4722-4729.

Waha, A., Güntner, S., Huang, T.H., Yan, P.S., Arslan, B., Pietsch, T., and Wiestler, O.D. (2005). Epigenetic silencing of the protocadherin family member PCDH-gamma-A11 in astrocytomas. Neoplasia *7*, 193-199.

Wang, J., Sakariassen, P., Tsinkalovsky, O., Immervoll, H., Bøe, S.O., Svendsen, A., Prestegarden, L., Røsland, G., Thorsen, F., Stuhr, L., *et al.* (2008). CD133 negative glioma cells form tumors in nude rats and give rise to CD133 positive cells. Int J Cancer *122*, 761-768.

Wang, J., Wakeman, T.P., Lathia, J.D., Hjelmeland, A.B., Wang, X.F., White, R.R., Rich, J.N., and Sullenger, B.A. (2010). Notch promotes radioresistance of glioma stem cells. Stem Cells *28*, 17-28.

Wang, Y., and Leung, F.C. (2004). An evaluation of new criteria for CpG islands in the human genome as gene markers. Bioinformatics *20*, 1170-1177.

Wani, M.C., Taylor, H.L., Wall, M.E., Coggon, P., and McPhail, A.T. (1971). Plant antitumor agents. VI. The isolation and structure of taxol, a novel antileukemic and antitumor agent from Taxus brevifolia. J Am Chem Soc *93*, 2325-2327.

Weber, M. (2005). Chromosome-wide and promoter-specific analyses identify sites of differential DNA methylation in normal and transformed human cells. Nature Genet *37*, 853-862.

Wechsler, D.S., Shelly, C.A., Petroff, C.A., and Dang, C.V. (1997). MXI1, a putative tumor suppressor gene, suppresses growth of human glioblastoma cells. Cancer Res *57*, 4905-4912.

Wen, P.Y., and Kesari, S. (2008). Malignant gliomas in adults. N Engl J Med *359*, 492-507.

Wen, P.Y., Yung, W.K., Lamborn, K.R., Dahia, P.L., Wang, Y., Peng, B., Abrey, L.E., Raizer, J., Cloughesy, T.F., Fink, K., *et al.* (2006). Phase I/II study of imatinib mesylate for recurrent malignant gliomas: North American Brain Tumor Consortium Study 99-08. Clin Cancer Res *12*, 4899-4907.

Westermark, B., Heldin, C.H., and Nistér, M. (1995). Platelet-derived growth factor in human glioma. Glia *15*, 257-263.

Widera, D., Mikenberg, I., Kaltschmidt, B., and Kaltschmidt, C. (2006). Potential role of NF-kappaB in adult neural stem cells: the underrated steersman? Int J Dev Neurosci *24*, 91-102.

Widschwendter, M., Fiegl, H., Egle, D., Mueller-Holzner, E., Spizzo, G., Marth, C., Weisenberger, D.J., Campan, M., Young, J., Jacobs, I., *et al.* (2007). Epigenetic stem cell signature in cancer. Nat Genet *39*, 157-158.

Wilson, A.S., Power, B.E., and Molloy, P.L. (2007). DNA hypomethylation and human diseases. Biochim Biophys Acta *1775*, 138-162.

Wiltshire, R.N., Herndon, J.E., Lloyd, A., Friedman, H.S., Bigner, D.D., Bigner, S.H., and McLendon, R.E. (2004). Comparative genomic hybridization analysis of astrocytomas: prognostic and diagnostic implications. J Mol Diagn *6*, 166-179.

Wu, X., Rauch, T.A., Zhong, X., Bennett, W.P., Latif, F., Krex, D., and Pfeifer, G.P. (2010). CpG island hypermethylation in human astrocytomas. Cancer Res *70*, 2718-2727.

Wu, Y., and Wu, P.Y. (2009). CD133 as a marker for cancer stem cells: progresses and concerns. Stem Cells Dev *18*, 1127-1134.

Wullich, B., Sattler, H.P., Fischer, U., and Meese, E. (1994). Two independent amplification events on chromosome 7 in glioma: amplification of the epidermal growth factor receptor gene and amplification of the oncogene MET. Anticancer Res *14*, 577-579.

Xu, Q., Yuan, X., Liu, G., Black, K.L., and Yu, J.S. (2008). Hedgehog signaling regulates brain tumor-initiating cell proliferation and portends shorter survival for patients with PTEN-coexpressing glioblastomas. Stem Cells *26*, 3018-3026.

Yagi, Y., Fushida, S., Harada, S., Kinoshita, J., Makino, I., Oyama, K., Tajima, H., Fujita, H., Takamura, H., Ninomiya, I., *et al.* (2010). Effects of valproic acid on the cell cycle and apoptosis through acetylation of histone and tubulin in a scirrhous gastric cancer cell line. J Exp Clin Cancer Res *29*, 149.

Yang, D., Van, S., Jiang, X., and Yu, L. (2011). Novel free paclitaxel-loaded poly(L-γ-glutamylglutamine)-paclitaxel nanoparticles. Int J Nanomedicine *6*, 85-91.

Yang, Z., Kenny, A.E., Brito, D.A., and Rieder, C.L. (2009). Cells satisfy the mitotic checkpoint in Taxol, and do so faster in concentrations that stabilize syntelic attachments. J Cell Biol *186*, 675-684.

Yin, A.H., Miraglia, S., Zanjani, E.D., Almeida-Porada, G., Ogawa, M., Leary, A.G., Olweus, J., Kearney, J., and Buck, D.W. (1997). AC133, a novel marker for human hematopoietic stem and progenitor cells. Blood *90*, 5002-5012.

Yin, D., Ogawa, S., Kawamata, N., Tunici, P., Finocchiaro, G., Eoli, M., Ruckert, C., Huynh, T., Liu, G., Kato, M., *et al.* (2009). High-resolution genomic copy number profiling of glioblastoma multiforme by single nucleotide polymorphism DNA microarray. Mol Cancer Res *7*, 665-677.

Yoo, C.B., and Jones, P.A. (2006). Epigenetic therapy of cancer: past, present and future. Nat Rev Drug Discov *5*, 37-50.

Yu, J., Zhang, H., Gu, J., Lin, S., Li, J., Lu, W., Wang, Y., and Zhu, J. (2004). Methylation profiles of thirty four promoter-CpG islands and concordant methylation behaviours of sixteen genes that may contribute to carcinogenesis of astrocytoma. BMC Cancer *4*, 65.

Yuan, X., Curtin, J., Xiong, Y., Liu, G., Waschsmann-Hogiu, S., Farkas, D.L., Black, K.L., and Yu, J.S. (2004). Isolation of cancer stem cells from adult glioblastoma multiforme. Oncogene *23*, 9392-9400.

Zaidi, H.A., Kosztowski, T., DiMeco, F., and Quiñones-Hinojosa, A. (2009). Origins and clinical implications of the brain tumor stem cell hypothesis. J Neurooncol *93*, 49-60.

Zeppernick, F., Ahmadi, R., Campos, B., Dictus, C., Helmke, B.M., Becker, N., Lichter, P., Unterberg, A., Radlwimmer, B., and Herold-Mende, C.C. (2008). Stem cell marker CD133 affects clinical outcome in glioma patients. Clin Cancer Res *14*, 123-129.

Zhang, R., Banik, N.L., and Ray, S.K. (2008). Differential sensitivity of human glioblastoma LN18 (PTEN-positive) and A172 (PTEN-negative) cells to Taxol for apoptosis. Brain Res *1239*, 216-225.

Zhou, B.B., Zhang, H., Damelin, M., Geles, K.G., Grindley, J.C., and Dirks, P.B. (2009). Tumour-initiating cells: challenges and opportunities for anticancer drug discovery. Nat Rev Drug Discov *8*, 806-823.

Zhu, Y., and Parada, L.F. (2002). The molecular and genetic basis of neurological tumours. Nat Rev Cancer *2*, 616-626.

Ziauddin, M.F., Yeow, W.S., Maxhimer, J.B., Baras, A., Chua, A., Reddy, R.M., Tsai, W., Cole, G.W., Schrump, D.S., and Nguyen, D.M. (2006). Valproic acid, an antiepileptic drug with histone deacetylase inhibitory activity, potentiates the cytotoxic effect of Apo2L/TRAIL on cultured thoracic cancer cells through mitochondria-dependent caspase activation. Neoplasia *8*, 446-457.